Available online at www.sciencedirect.com
SCIENCE DIRECT®
Chemie der Erde 65 (2005) 203–270
CHEMIE der ERDE GEOCHEMISTRY
www.elsevier.de/chemer

INVITED REVIEW

The nakhlite meteorites: Augite-rich igneous rocks from Mars

Allan H. Treiman

Lunar and Planetary Institute, 3600 Bay Area Boulevard, Houston, TX 77058-1113, USA

Received 22 October 2004; accepted 18 January 2005

Abstract

The seven nakhlite meteorites are augite-rich igneous rocks that formed in flows or shallow intrusions of basaltic magma on Mars. They consist of euhedral to subhedral crystals of augite and olivine (to 1 cm long) in fine-grained mesostases. The augite crystals have homogeneous cores of $Mg' = 63\%$ and rims that are normally zoned to iron enrichment. The core–rim zoning is cut by iron-enriched zones along fractures and is replaced locally by ferroan low-Ca pyroxene. The core compositions of the olivines vary inversely with the steepness of their rim zoning – sharp rim zoning goes with the most magnesian cores ($Mg' = 42\%$), homogeneous olivines are the most ferroan. The olivine and augite crystals contain multiphase inclusions representing trapped magma. Among the olivine and augite crystals is mesostasis, composed principally of plagioclase and/or glass, with euhedra of titanomagnetite and many minor minerals. Olivine and mesostasis glass are partially replaced by veinlets and patches of iddingsite, a mixture of smectite clays, iron oxy-hydroxides and carbonate minerals. In the mesostasis are rare patches of a salt alteration assemblage: halite, siderite, and anhydrite/gypsum. The nakhlites are little shocked, but have been affected chemically and biologically by their residence on Earth.

Differences among the chemical compositions of the nakhlites can be ascribed mostly to different proportions of augite, olivine, and mesostasis. Compared to common basalts, they are rich in Ca, strongly depleted in Al, and enriched in magmaphile (incompatible) elements, including the LREE. Nakhlites contain little pre-terrestrial organic matter. Oxygen isotope ratios are not terrestrial, and are different in anhydrous silicates and in iddingsite. The alteration assemblages all have heavy oxygen and heavy carbon, while D/H values are extreme and scattered. Igneous sulfur had a solar-system isotopic ratio, but in most minerals was altered to higher and lower values. High precision analyses show mass-independent

E-mail address: treiman@lpi.usra.edu.

0009-2819/$ - see front matter
doi:10.1016/j.chemer.2005.01.004

fractionations of S isotopes. Nitrogen and noble gases are complex and represent three components: two mantle sources (Chas-E and Chas-S), and fractionated Martian atmosphere.

The nakhlites are igneous cumulate rocks, formed from basaltic magma at ~1.3 Ga, containing excess crystals over what would form from pure magma. After accumulation of their augite and olivine crystals, they were affected (to various degrees) by crystallization of the magma, element diffusion among minerals and magma, chemical reactions among minerals and magma, magma movement among the crystals, and post-igneous chemical equilibration. The extent of these modifications varies, from least to greatest, in the order: MIL03346, NWA817, Y000593, Nakhla = Governador Valadares, Lafayette, and NWA998.

Chemical, isotopic, and chronologic data confirm that the nakhlites formed on Mars, most likely in thick lava flows or shallow intrusions. Their crystallization ages, referenced to crater count chronologies for Mars, suggest that the nakhlites formed on the large volcanic constructs of Tharsis, Elysium, or Syrtis Major. The nakhlites were suffused with liquid water, probably at ~620 ma. This water dissolved olivine and mesostasis glass, and deposited iddingsite and salt minerals in their places. The nakhlites were ejected from Mars at ~10.75 Ma by an asteroid impact and fell to Earth within the last 10,000 years.

Although the nakhlites are enriched in incompatible elements, their source mantle was strongly depleted. This depletion event was ancient, as the nakhlites' source mantle was fractionated while short-lived radionuclides (e.g., $t_{1/2} = 9$ my) were still active. This differentiation event may have been core formation coupled with a magma ocean, as is inferred for the moon.

1. Introduction

Nakhlites are achondrite meteorites rich in clinopyroxene; extra-terrestrial basaltic rocks composed primarily of augite. The nakhlite lavas erupted and cooled on Mars, and so they are important sources of data about Mars, including: mantle composition, surface materials, atmosphere composition, liquid water, and potential environments for life. This paper reviews our knowledge of the seven nakhlite meteorites. From that knowledge, I distill a consistent geological and geochemical history, which emphasizes igneous events, magma compositions, magma sources, and alteration by Martian water. I will try to place the nakhlites in a reasonable geological context and suggest some useful lines for future research.

Seven nakhlites are known (Table 1), but collection circumstances are clear for only three. Nakhla, the meteorite eponym for the group, was observed to fall in northern Egypt in 1911. The three Yamato nakhlites were found near each other on the Antarctic ice, and are considered fragments of a single fall (Misawa et al., 2003a). The MIL03346 nakhlite was also found in Antarctica, but far from the Yamato samples (Antarctic Meteorite Newsletter, 2004).

The histories of the other nakhlites are clouded. Lafayette was recognized as a meteorite in 1931 in the Purdue University geology department, where it supposedly had been kept as a glacially striated stone. By other accounts, it fell near Purdue (IN)

Table 1. The Nakhlites, and samples used here

Name	Where found	*Discovery*	Mass (g)	Source	Thin section
Nakhla	El Nakhla al Baharia, Egypt	*1911*	~10,000	Naturhistorisches Museum Wein	#2
				US National Museum	1911
					5891
				Harvard University	#2
Lafayette	Indiana, USA?	1931	~800	Field Museum	AHT1
Governador Valadares	Minas Gerais, Brazil	1958	158	American Museum Natural History	4957-2
NWA817	Northwest Africa (Morocco?)	2000	104	La Memoire de la Terre	AHT1
Y000593 Y000749 Y000802	Yamato Mts., Antarctica	2000	15,002	National Institute for Polar Research (Japan)	,62-2 ,51-1
NWA998	Northwest Africa	2001	456	Univ. Washington James Strope	No. # AHT1
MIL03346	Miller Range, Antarctica	2003	715	ANSMET, Johnson Space Center	,6 ,93

Italicized date indicates observed fall.
Data from: Grady (2000), Grossman and Zipfel (2001), Russell et al. (2003), Misawa et al. (2003a), Antarctic Meteorite Newsletter (2004).

in the 1920s (Nininger, 1935), but ^{14}C dating gives a terrestrial residence age of ~3000 years (Jull et al., 1999). Governador Valadares was reportedly found in 1958 (Burragato et al., 1975), but little is known of its history. The two nakhlites from Northwest Africa, NWA817 and NWA998, were collected at undisclosed (possibly unknown) locations in Morocco or Algeria.

Perhaps the first indication of the nakhlites' importance was recognition that their REE patterns suggested extensive differentiation (Schmitt and Smith, 1963). In the early 1970s, it became clear that the nakhlites held important clues to the evolution of our solar system. First, earlier age determinations of 1.3 Ga (by K–Ar) were confirmed by Rb–Sr and ascribed to igneous crystallization – the first evidence of relatively recent volcanism off the Earth (Gale et al., 1975; Reid and Bunch, 1975). Second, studies of petrography, mineral chemistry, and trace elements solidified the kinship between the nakhlites and terrestrial gabbroic rocks (Laul et al., 1972; Bunch and Reid, 1975). Third, the clay-rich alteration product iddingsite was recognized in the nakhlites, and inferred to be pre-terrestrial (Ashworth and Hutchison, 1975; Bunch and Reid, 1975). From these data, Reid and Bunch (1975) inferred that the

nakhlites came from a highly differentiated planetary body, capable of volcanism as late as 1.3 Ga, and with liquid water near its surface. The nakhlites' parent body could not have been the Moon, the source of the eucrite basaltic meteorites, nor any chondritic or primitive body; in fact '…it, apparently, in some respects, resembles the Earth.' Reid and Bunch (1975) did not specifically suggest that the nakhlites came from Mars, although that idea was in their minds (A. Reid, pers. comm.).

Studies of the nakhlites burgeoned in the 1980s, partly from recognition of the Governador Valadares meteorite (Berkley et al., 1980), but mostly because of strong evidence that the nakhlites (and other meteorites) had formed on Mars (Bogard and Johnson, 1983). In the mid-1990s, the controversy about the ALH84001 Martian meteorite revived interest in (and funding for) studies of Martian meteorites, and that wave of interest continues today. New analytical methods have been developed and applied, new chemical and isotopic systems have been explored, four more nakhlites have been found, and studies of the other Martian meteorites have provided a rich geochemical context. It is in this environment that I have tried to provide a critical review of the nakhlite meteorites and their place in the rapidly growing study of Mars and its meteorites.

2. Petrography and mineral chemistry

The nakhlites are clinopyroxenites, composed mostly of subcalcic augite (Table 2, Fig. 3a), and are fundamentally similar. However, they span a continuum of

Table 2. Modal phase proportions (vol%) of Nakhlites and standard deviations (s.d.)

	Nakhla	Lafayette	Governador Valadares	Y000593	NWA817	NWA998	MIL03346
	s.d.	s.d.	s.d.				s.d.
Augite[a]	80.8±4.3	73.5±6.7	81.2±5.1	76.7	69	68	75.5±4.4
Orthopyroxene	0 –	0 –	0 –	0	0	2	0 –
Olivine[b]	10.8±4.7	16.7±5.7	8.9±3.1	12.2	12.5	10	2.9±1.7
Mesostasis[c]	8.4±2.1	9.8±1.2	9.8±2.2	11.1	18.5	19[d]	21.4±5.7

Data sources: Nakhla, Lafayette: Governador Valadares from Friedman-Lentz et al. (1999); standard deviations are among different thin sections. Y000593: including Y000749 from Imae et al. (2003). NWA817 from Gillet et al. (2002) and Sautter et al. (2002). NWA998 is a new here (1000 points). MIL 03346 is average and standard deviation of values from McKay and Schwandt (2005), Anand et al. (2005a, b), Mikouchi et al. (2005) and Treiman (unpublished).

[a]Includes low-Ca pyroxene as overgrowths on, and replacements of, augites.

[b]Includes poikilitic olivine among pyroxenes and iddingsite replacing it; but not olivine grains in mesostasis.

[c]Finer-grained material among larger pyroxene and olivine grains. Includes discrete oxide crystals (Y000593, 0.6%; NWA817, 1%; MIL03346, 0.9%), quench olivine in MIL03346, and the following: plagioclase and alkali feldspars, silicic and basaltic glass, glass, pigeonite, Fe–Ti oxides, olivine, minor phases, and alteration materials.

[d]NWA998 does not contain mesostasis as defined above. Cited value includes modal abundances of minerals other than augite, orthopyroxene and olivine: i.e., oxides, feldspar, phosphates, sulfides, etc.

petrographic and mineralogic properties (Fig. 1) from MIL03346 and NWA817 (strong chemical zoning in minerals; glassy mesostasis) through NWA998 (little mineral zoning; coarse, fully crystalline mesostasis).

The nakhlites are '…pyroxenites with augite as the most abundant mineral and less abundant olivine, plagioclase, K-feldspar, Fe–Ti oxides, FeS [actually $Fe_{1-x}S$, pyrrhotite], pyrite, chalcopyrite, and a hydrated alteration phase that resembles iddingsite. [The nakhlites] are unbrecciated, and their texture is dominated by elongate subhedral to euhedral prisms of clinopyroxene. Pyroxene prisms are approximately $1 \times 0.3\,mm^2$ and show a preferred alignment' (Fig. 1; Bunch and Reid, 1975). Olivine euhedra and subhedra are less abundant, and commonly larger than the augite grains (to ~5 mm across). Olivine is common between and among the augite grains, and commonly encloses augite. Among these large pyroxene and olivine grains is a finer-grained matrix or mesostasis, marked in most nakhlites (except MIL03346, Figs. 1(h) and 10) by equant crystals of titanomagnetite and by plagioclase laths in sprays or parallel sheaves. Among the plagioclase laths lie the other anhydrous minerals. These two textural settings, *large crystals* and *mesostasis*, encompass nearly all the volume of the nakhlites. Two other settings, *inclusions* in large euhedra and *alteration materials*, are volumetrically minor but significant.

The nakhlites are dominated by their large crystals, euhedra and subhedra of augite and olivine (Table 2). These crystals are commonly interpreted as cumulus grains, settled out of basaltic magma and augmented by post-cumulus overgrowths. NWA998 also contains orthopyroxene crystals as large as some augites. Distinct titanomagnetite crystals, some euhedral, are present among the large augite and olivine grains, and are discussed with the mesostasis.

2.1. Augite

The larger augite crystals are euhedral to subhedral prisms (Figs. 1 and 2), with typical pseudo-octagonal cross-sections. Augite grains average $1 \times 0.2\,mm^2$ (Fig. 1), with more smaller grains than larger – grain width is inversely proportional to the logarithm of grain abundance (Friedman-Lentz et al., 1999; Lentz and McSween, 2003; Stopar et al., 2005). This pattern is characteristic of systems where crystals nucleate and grow continuously. All nakhlites are deficient in the smallest grains (<0.15 mm long), which is consistent with cessation of nucleation or resorption of the smallest grains. The large augite grains tend to be aligned and clustered (Berkley et al., 1980; Friedman-Lentz et al., 1999).

Many large augites are twinned, most commonly with a single twin plane parallel to {1 0 0} through the grain center (e.g., Figs. 1b, d and f; Berkley et al., 1980). Lamellar twins parallel to {0 0 1} are moderately common, especially near sheared or granulated zones (Fig. 10c). Where {0 0 1} twins occur on both sides of a {1 0 0} twin, they appear (in crossed polarized light) as chevrons with the {1 0 0} twin trace forming the chevrons' apices (Fig. 10c; Berkley et al., 1980).

Chemically, the large augites can be divided into cores, rims, replacements, and transgressive zones. The cores are relatively homogeneous and magnesian, and are surrounded (in most samples) by rims of increasingly ferroan augite (Figs. 2

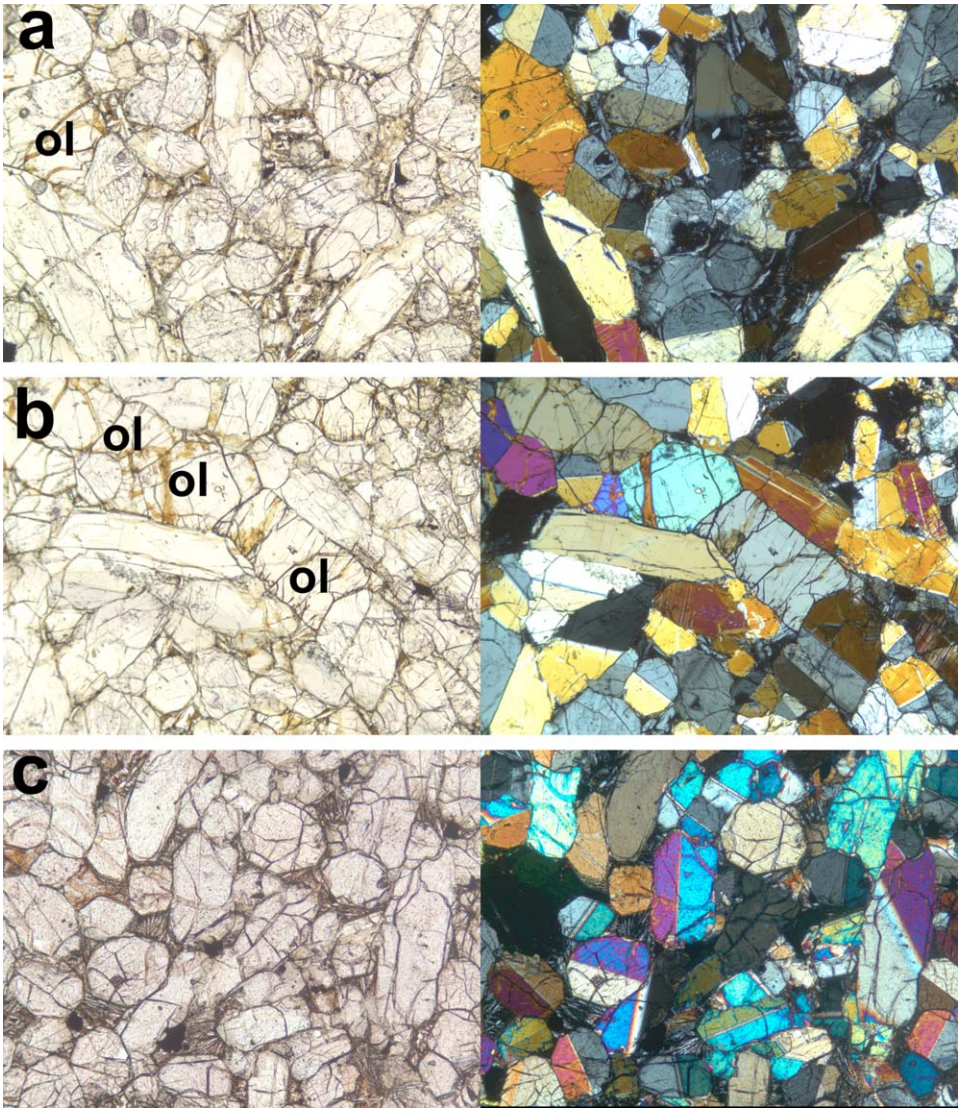

Fig. 1. Nakhlite textures. Image pairs, 2.3 mm across, left in plane polarized light (pl), right in crossed polarizers (xp). Subhedral augites (Fig. 2) and olivines (ol; Fig. 4), with interstitial mesostasis (Fig. 7). Opaques are titanomagnetite and pyrrhotite. Intereference colors (xp) vary. (a) Nakhla, ~10% volume mesostasis. (b) Nakhla, nearly no mesostasis. (c) Governador Valadares. Long augite crystals aligned up-down. (d) Lafayette. In xp, augite colors to blue. (e) NWA817. Euhedral augites and olivine; mesostasis dark, fine-grained. (f) Y000593. Large olivine with symplectites at upper right; in xp, color zoning reflects iron-enriched rim. (g) NWA998. Pyroxene and olivine are subhedral. Mesostasis (white) is entirely plagioclase. (h) MIL03346. Euhedral augites and olivine; mesostasis dark, fine-grained.

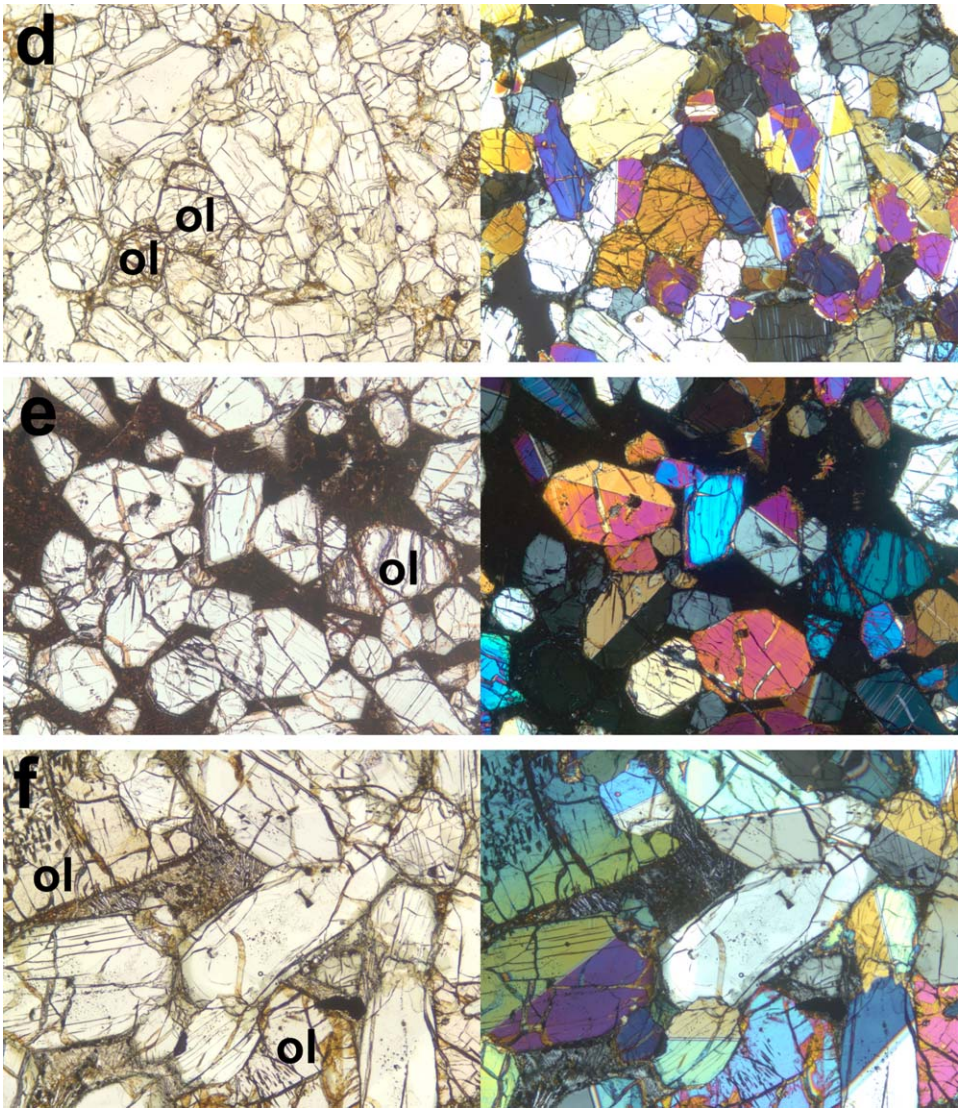

Fig. 1. (*Continued*)

and 3a,b; Table 3). In most samples, one can find zones of ferroan augite cutting across (transgressing) magnesian cores, commonly following fractures (Fig. 2b). Both cores and rims may be replaced by more ferroan pyroxene, both high and low calcium (Fig. 2c). Outside the rim zones, the large augites are decorated with serrated overgrowths and prongs of ferroan pigeonite, which are identical to and continuous with pigeonite of the mesostasis.

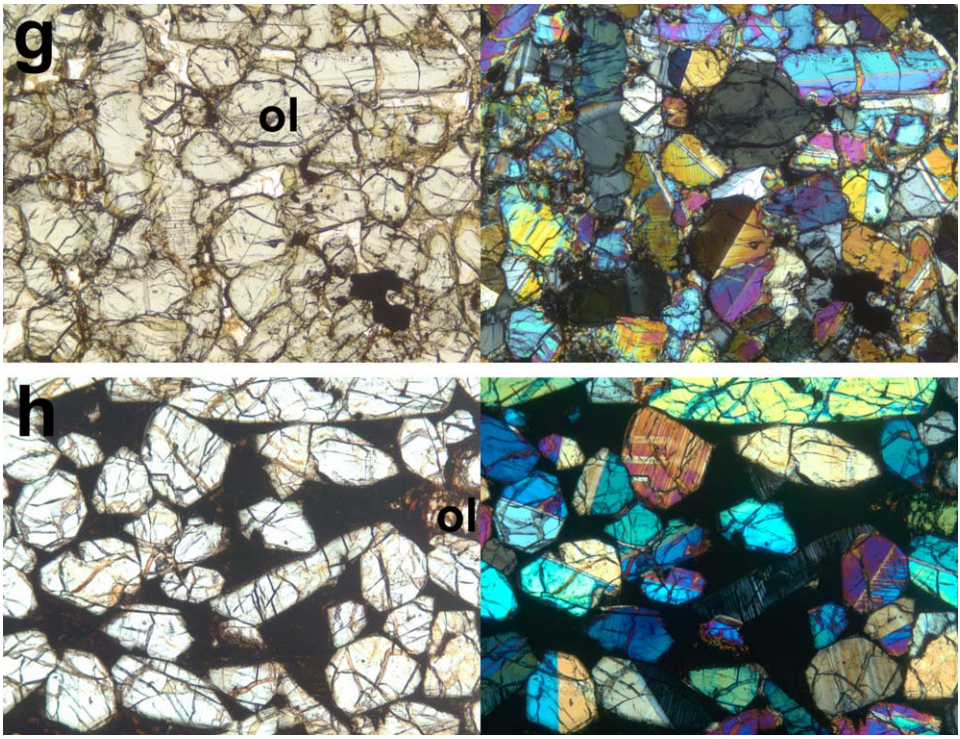

Fig. 1. (*Continued*)

Cores constitute most of the volume of nakhlite augites, and are relatively homogeneous and magnesian at $\sim Wo_{38}En_{39}Fs_{23}$ and molar Mg/(Mg + Fe), $Mg' \approx 63\%$ (Table 3; Figs. 2 and 3a,b; Berkley et al., 1980; Harvey and McSween, 1992a; Friedman-Lentz et al., 1999; Sautter et al., 2002; Imae et al., 2003; Mikouchi et al., 2003; McKay and Schwandt, 2005). In Lafayette and NWA998, these magnesian zones can encompass the whole of the pyroxene, except for replacements and overgrowths of low-Ca pyroxene (Berkley et al., 1980; Harvey and McSween, 1992a; new data). In the other nakhlites, the magnesian areas are the grains' cores, covering ~85–95% of a grain's width (Fig. 3b) or ~60–85% of its volume.

The Mg′ of the cores is essentially constant (Figs. 3a and b; Treiman, 1990), with slight variations that may represent magmatic inclusions. In a few grains, Mg′ decreases toward the grain center; this could be ascribed to original growth as a hollow crystal (Treiman and Sutton, 1992). Other grains have slightly different Mg′ on either side of the grain center (e.g., Fig. 5 of Sautter et al., 2002), which could represent mild sector zoning. In most grains, abundances of minor elements decrease slightly from the center to the edge of the core (Figs. 3c–e), be the elements compatible or incompatible in augite/basalt partitioning (e.g., Cr vs. Ti). The one exception is Cr in MIL03346, which increases slightly from the center to the edge of

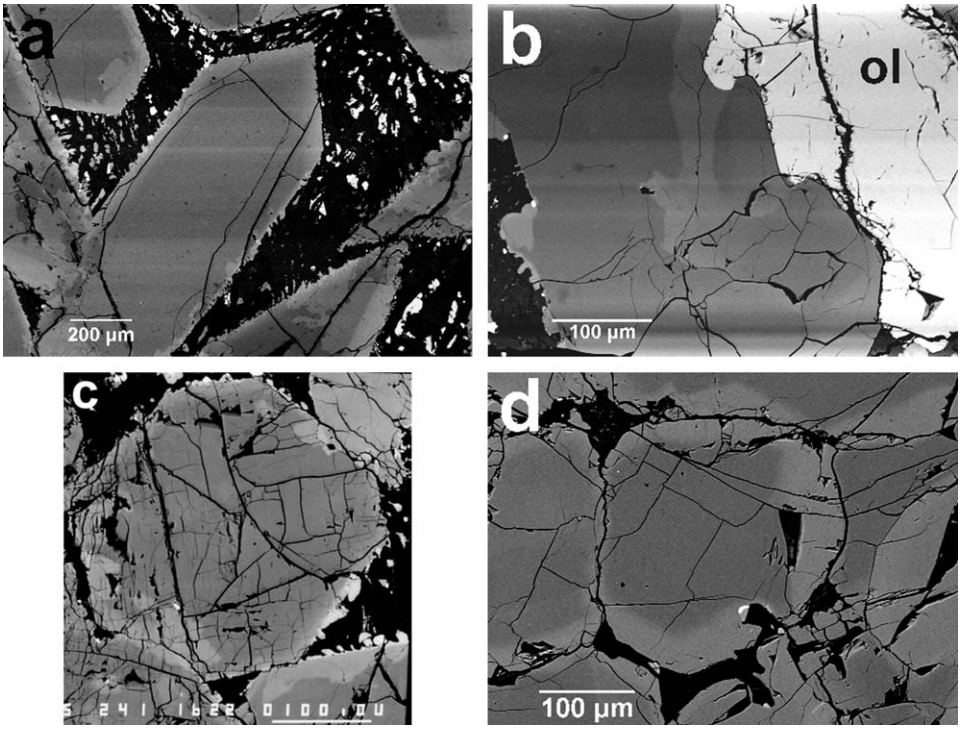

Fig. 2. Large augite grains. BSE images, horizontal bands are artifacts. Lighter tone means greater Fe content. (a) Normal chemical zoning in central grain (Y000593), which has homogeneous core and ferroan rim (see Fig. 3). (b) Fe enrichment along crack (Nakhla). Adjacent olivine is 'ol'. (c) Complex zoning (Nakhla). Edges of center grain are normally zoned at upper left, top, right, and lower right; stepped/replacement zoning at the other edges. Chemical profile in Figs. 3b–d is core to right margin. Augite at lower right has large replacement area, partially associated with cracks. (d) NWA998. Ferroan rim finely exsolved to orthopyroxene and augite.

the core (Fig. 3e). Veinlets of ferroan augite cut the core regions, and 'point' enrichments in Fe, Al and Na (Treiman, 1990) likely represent magmatic inclusions.

Minor element abundances can vary significantly within an augite core, and among cores in a given nakhlite. TiO_2 abundances can vary from 0.15% to 0.26% in the core of an augite grain in Nakhla (new data), from 0.07% to 0.45% in different cores in Nakhla (Table 3; Bunch and Reid, 1975; Berkley et al., 1980; Treiman, 1990; Friedman-Lentz et al., 1999; Lentz et al., 2001), and from 0.09% to 0.3% in Y000593 and its pairs (Table 3; Mikouchi et al., 2003; Wadhwa and Crozaz, 2003). Thus, proposed systematic differences between compositions of nakhlites' augites cores (Wadhwa and Crozaz, 2003) may be within the variability of a single nakhlite.

Augite cores in most nakhlites are surrounded by distinct rim zones of continuously increasing Fe content (decreasing Mg′), which appear optically as

increasingly yellow-greenish color and in BSE imagery as increasing brightness (Figs. 1e, f and 2; Harvey and McSween, 1992a; Friedman-Lentz et al., 1999). The transitions from core to rim zones are abrupt in NWA817. Y000593, and MIL03346, and are more gradual in Nakhla and Governador Valadares (Fig. 3; Harvey and McSween, 1992a; Friedman-Lentz et al., 1999; Szymanski et al., 2003). Rim zones are thickest where augite abuts mesostasis, and may be absent where augite grains abuts augite or olivine (Harvey and McSween, 1992a; Sautter et al., 2002). Where present, rim zones are 10–20 μm thick. The rims' chemical compositions are marked

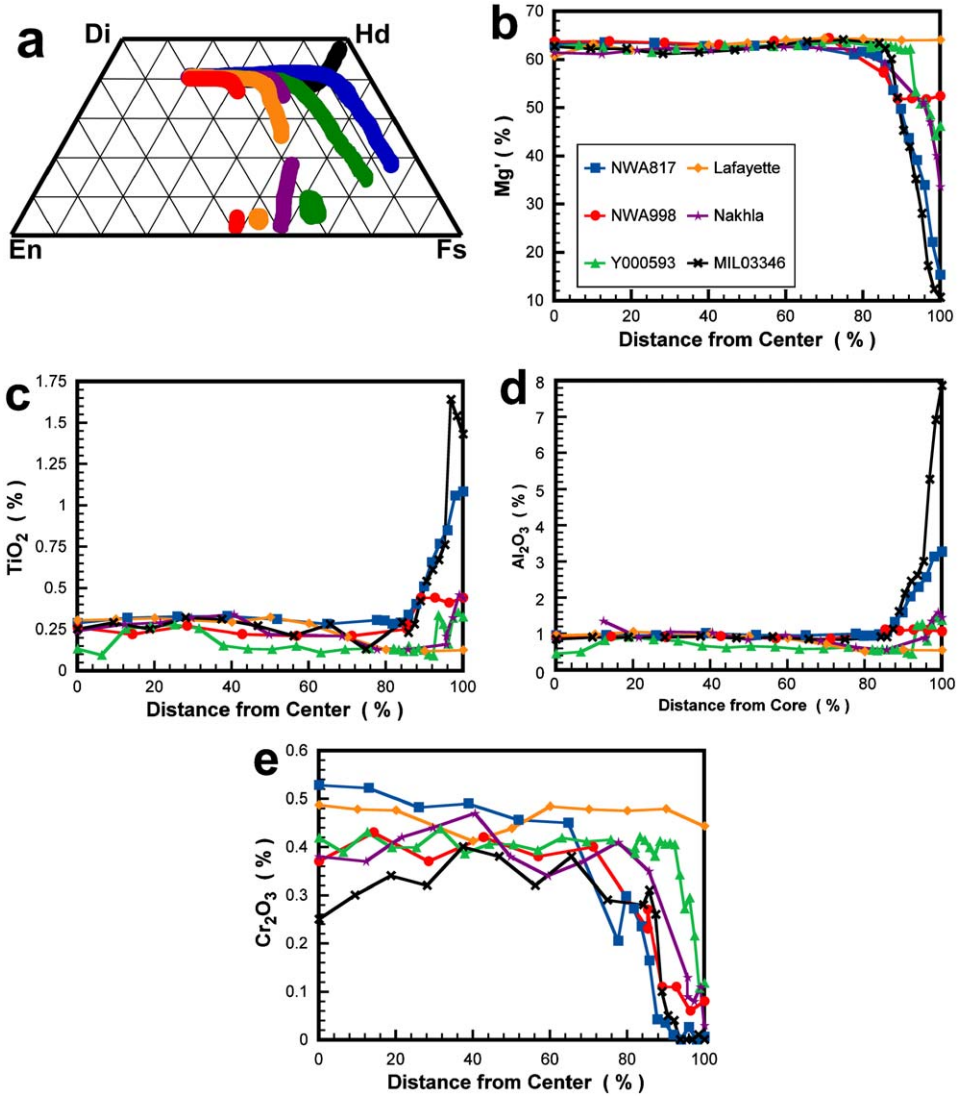

by continuously decreasing Mg′ and abundance of Cr, and by increasing abundances of Ti, Al, and Na (Fig. 3; Treiman, 1990; Harvey and McSween, 1992a; Sautter et al., 2002). MIL03346 is unique in having oscillatory zoning in its pyroxene rims (Anand et al., 2005a; pers. obs.).

In Lafayette and NWA998, rim zones are obscure or absent. Commonly, Mg′ is constant, or changes in a step function to exsolved pyroxenes of relatively constant average composition (Figs. 2d and 3b). Minor elements may vary continuously even when Mg′ is constant (e.g., Cr in NWA998, Fig. 3d), suggesting that a rim zone was once present but that Mg′ has been homogenized.

Uncommonly, the core–rim augite is replaced or erased by a relatively homogeneous ferroan augite (e.g., Figs. 2c, d and 3b). Replacement zones start at rims, adjacent to mesostasis, and extend inward. Boundaries between the core–rim zoning and the replacement augite are sharp – within a few μm, the composition may change from Mg′ = 63% to Mg′∼50% (Fig. 3b).

Along fractures, the core–rim augite is commonly modified to more ferroan compositions (Fig. 2b). In these transgressive zones, compositions vary continuously from very ferroan (e.g., Mg′ ≈ 35%) at the fracture to the normal Mg′ of the surrounding region, with little if any change in abundances of other elements (e.g., Ti, Al, Cr, Na; unpublished data). These gradual changes are unlike those of the sharply bounded replacement zones. Transgressive veinlets like these have been reported in eucrite basalts, and interpreted as products of late- or post-magmatic metasomatism by an Fe–S-rich fluid (e.g., Mittlefehldt and Lindstrom, 1997; Schwartz et al., 2003; Warren, 2002; Herd et al., 2004).

The large augites (except in NWA 817 and MIL03346) are commonly rimmed by low-calcium pyroxene (Harvey and McSween, 1992a; Imae et al., 2003). These rims abut mesostasis areas, and may be either pigeonite or orthopyroxene. Harvey and McSween (1992a) invoke disequilibrium evolution of melt in each mesostasis area, with the level of Ca depletion in each area depending on kinetic delays in nucleating plagioclase.

Fig. 3. Chemistry of large augites. Typical core-to-rim traverses in parts b–d, lengths being: NWA817, 107 μm; NWA998, 185 μm; Y000593, 233 μm; Lafayette, 158 μm; Nakhla, 133 μm; MIL03346, 177 μm. (a) Pyroxene quadrilateral with ranges of pyroxene compositions. After Mikouchi et al. (2003), augmented with data on NWA998 and MIL03346 (McKay and Schwandt, 2005; Mikouchi et al., 2005; new data here). MIL03346 is unique in having a trend toward hedenbergite (Hd) pyroxene. (b) Mg′ (molar Mg/[Mg + Fe]) vs. % distance, core to rim. Three types of rim zoning: none (e.g., Lafayette); continuously decreasing (e.g., NWA817, Nakhla, MIL03346), and stepped (e.g., NWA998, Y000593). Pyroxene grains in a single nakhlite may show one or more of these patterns (Fig. 2c). (c) TiO_2 content. Zoning patterns are the inverse of those for Mg*. In MIL03346, Ti content decreases closest to the rim, possibly indicating co-crystallization of Ti-magnetite. (d) Al_2O_3 content. Zoning patterns are very similar to Ti. The high Al contents of rim pyroxenes in NWA817 and MIL03346 reflect the failure of plagioclase to nucleate in their mesosataes. (e) Cr_2O_3 content. Zoning patterns follow those of Mg*. MIL03346 is unusual in that Cr increases outward from the core, before dropping to zero.

Table 3. Compositions of Nakhlite pyroxenes

	Nakhla Aug Core	Nakhla Aug Core	Nakhla Aug Rim	Nakhla Pig Repl	GV[a] Aug Core	GV[a] Aug Rim	Laf.[a] Aug Core	Laf.[a] Aug Rim	NWA 817 Aug Core	NWA 817 Aug Rim	Y 000 593 Aug Core	Y 000 593 Aug Rim	NWA 998 Aug Core	NWA 998 Aug Rim	NWA 998 Opx Core	NWA 998 Opx Rim	MIL 03346 Aug Core	MIL 03346 Aug Rim
SiO_2	52.2	51.9	49.3	49.6	51.9	49.7	52.4	51.2	51.5	48.95	53.0	48.6	51.6	50.5	50.6	49.8	51.5	42.9
TiO_2	0.11	0.26	0.36	0.37	0.24	0.46	0.15	0.28	0.24	0.64	0.09	0.46	0.17	0.43	0.08	0.04	0.25	1.46
Al_2O_3	0.53	0.94	1.50	0.69	0.79	1.82	0.52	0.62	0.83	1.99	0.45	1.20	0.79	1.19	0.48	0.43	0.86	8.00
Cr_2O_3	0.48	0.47	0.20	0.01	0.39	0.13	0.42	0.17	0.49	0.00	0.41	0.00	0.48	0.05	0.02	0.01	0.25	0.00
FeO	14.2	13.7	19.9	36.2	14.0	19.7	14.3	18.7	14.0	22.24	14.3	28.1	13.5	18.2	30.5	33.1	13.7	24.2
MnO	0.40	0.41	0.55	1.03	0.43	0.55	0.42	0.51	0.40	0.63	0.47	0.76	0.45	0.59	0.86	0.79	0.39	0.52
MgO	13.3	13.5	9.72	7.73	13.3	9.46	13.6	10.9	12.9	6.95	13.5	5.60	13.8	11.5	15.9	14.3	12.9	1.62
CaO	18.5	18.7	17.1	5.15	18.4	17.5	18.5	17.7	19.4	18.43	18.4	15.3	18.8	17.2	1.26	0.95	19.8	19.8
Na_2O	0.19	0.22	0.26	0.12	0.19	0.25	0.29	0.24	0.37	0.42	0.19	0.22	0.23	0.26	0.03	0.01	0.24	0.42
K_2O	0.01	0.00	0.02	–	–	–	0.01	0.00	–	–	0.00	0.00	0.00	0.00	0.01	0.00	0.00	0.02
Sum	100.0	100.1	98.9	100.9	99.8	99.6	100.5	100.3	100.4	100.57	100.3	100.3	99.9	99.9	99.8	99.4	99.8	98.9
Ca %	38.5	39.3	37.1	11.7	38.5	38.0	38.1	37.3	40.2	40.4	38.0	31.6	38.7	36.2	2.7	2.0	40.9	48.3
Mg %	38.5	38.6	29.3	24.4	38.7	28.6	38.9	32.0	37.1	21.2	38.9	16.1	39.5	33.8	46.9	42.7	37.0	5.5
Fe %	23.0	22.1	33.7	64.0	22.8	33.4	23.0	30.7	22.6	38.3	23.1	48.8	21.8	30.0	50.4	55.3	22.0	46.2
Mg′ %	62.5	63.6	33.9	27.6	62.9	46.4	62.9	52.4	66.5	37.9	62.7	26.1	64.5	52.7	48.8	43.6	62.7	10.6

Augite – aug; pigeonite – pig; orthopyroxene – opx; replacement zones – repl.

Core values are representative of 'homogeneous' regions. Nakhla core analyses in same grain, c/o D. Musselwhite.

Rim values are spots in zones of progressive Fe enrichment.

Data new here, except: GV: Friedman-Lentz et al. (1999); NWA817: Sautter et al. (2002).

[a]GV – Governador Valadares; Laf. – Lafayette.

The average abundance of ferric iron in Nakhla's augites is ~2.3% of the iron present (Dyar, 2003). Iron in MIL03346 augite is reported to be ~25% ferric (Dyar et al., 2005). It is not known if the ratio is constant across the grains' zones.

Trace element data on augites are sparse. Nakamura et al. (1982) analyzed Nakhla augite separates, core and rim, by INAA for REE, Rb, Sr, Ba, and K. Wadhwa and Crozaz (1995), Lentz et al. (2001), and Wadhwa and Crozaz (2003) used SIMS to determine abundances of several trace elements (including the rare earths) across pyroxenes of many nakhlites. Abundances of incompatible elements vary inversely with Mg′, while the compatible element Cr varies with Mg′ (Fig. 3). Lentz et al. (2001) analyzed augites in Nakhla and Lafayette for Li, B and Be, and found that their abundances are essentially constant across the augite grains. In NWA817, B and Be act as incompatible elements (Musselwhite et al., 2005). Nakhla augite contains hydrogen at 0.04 wt% equivalent of H_2O (Dyar et al., 2004).

REE contents of the augite cores may differ among the nakhlites – Y000593 with the least and NWA817 the most (Wadhwa and Crozaz, 2003). This suggestion needs verification in light of variable REE and minor element contents in augite cores from individual nakhlites (Table 3; Wadhwa and Crozaz, 2003).

2.2. Olivine

Large olivine grains are less common than large augites – ~10 vol% of each meteorite except MIL03346 with ~3% (Table 2). Large olivines are euhedral in NWA817, Y000539, and MIL03346 – typical pseudo-hexagonal prisms with beveled terminations (Fig. 4a). In the other nakhlites, olivine grains are subhedral to anhedral, and connect to poikilitic olivine that encloses large augite grains (Figs. 4b

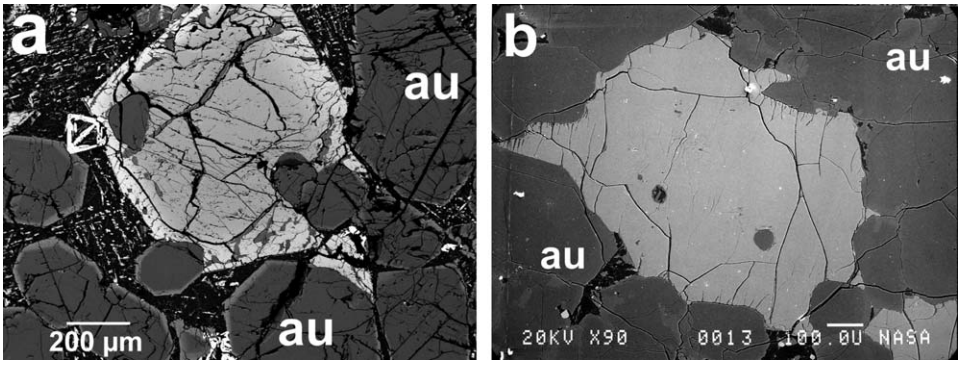

Fig. 4. Large olivine grains. BSE images. Olivine: light gray; augite: au, dark gray; mesostasis: black; oxide minerals; white. (a) NWA817. Euhedral olivine (center), surrounded by augite euhedra (with normal zoning to lighter rims. Olivine rim is more ferroan (lighter tone), note included augite. Irregular gray bands and patches in olivine are iddingsite (Fig. 9). Skeletal magnetite in mesostasis. (b) Nakhla. Subhedral olivine, larger than individual augites, extending among augites. Olivine contains an augite inclusion (right) and a magmatic inclusion (left, see Fig. 8).

and 8a). Olivine euhedra and subhedra are slightly larger than augites, averaging $1.0 \times 0.6\,mm^2$ and up to $\sim 3 \times 2\,mm^2$ (Nakamura et al., 1982; Treiman, 1990). Olivine is commonly cut by jagged veinlets of alteration minerals.

Olivine grains have cores of constant composition, but their patterns and compositions are different from those of the large augites. Olivine in NWA817 and MIL03346 is normally zoned in Mg′ and Ca content – the former decreasing core-to-rim, and the latter increasing (Figs. 4a and 5; Table 4). Olivines in Y000593, Nakhla, and Governador Valadares have slight normal zoning, while those in Lafayette and NWA998 are essentially homogeneous (Fig. 5; Berkley et al., 1980; Treiman, 1986, 1990; Longhi and Pan, 1989; Harvey and McSween, 1992a; Sautter et al., 2002). Compositions of olivine cores are nearly identical within a nakhlite but differ among them; Mg′ ranges from 45% in NWA817 and 44% in MIL03346 to 35% in Lafayette and Y000593 (Fig. 5a; Table 4). In general, the higher the Mg′ of the olivine core, the sharper the Mg′ zoning in the rim (Fig. 5a). Calcium in the olivine's cores varies significantly (Fig. 5b, Table 4), most to least in the order: NWA817 and MIL03346 at 0.6%, Nakhla = Governador Valadares, Y000593, Lafayette, and NWA998 at 0.17%. In the rims, Ca zoning varies widely – essentially flat in Lafayette, increasing in NWA998 and Y000593, and decreasing in Nakhla, NWA817, and MIL03346 (Fig. 5b). In the last two, Ca decreases probably reflect the nucleation and growth of plagioclase in the mesostasis. Large olivines in Y000394 and NWA998 contain TEM-scale exsolution lamellae of monticellite-kirschteinite (Bridges et al., 2004).

The average abundance of ferric iron in Nakhla's olivine is low, 0–1.8% of the iron, basically at the detection limit of the Mössbauer analyses (Dyar, 2003). It is not known if the ratio is constant across the grains' zones.

INAA measurements (Nakamura et al., 1982) of most trace elements are suspect because of low intrinsic abundances and presence of inclusions and alterations (Shih et al., 1982). SIMS analyses presumably avoid inclusions (Wadhwa and Crozaz, 1995, 2003), and show that LREE are highly depleted in the olivines, which is consistent with ${}^{ol}D_{LREE/basalt} \ll {}^{ol}D_{HREE/basalt}$ (Jones, 1995).

2.3. Orthopyroxene

NWA998 is unique among nakhlites in containing grains of low-calcium pyroxene (Fig. 6) comparable in size to the augite grains (Irving et al., 2002; Carlson and Irving, 2004). Chemically, these grains are orthopyroxene, $En_{47}Fs_{49}Wo_4$ (Table 3; Irving et al., 2002), show little Fe/Mg zoning (Fig. 3; Carlson and Irving, 2004), and rarely have rims of pigeonite. Some large orthopyroxene crystals are lath-shaped, and seemingly continuous with adjacent olivine grains (Figs. 6a and b). Other orthopyroxenes contain inclusions of olivine, all of which have the same optical (crystallographic) orientation (Fig. 6c). The orthopyroxene cores are less magnesian (Mg′ = 50%) than the cores of adjacent augites (Mg′ = 64%) but more magnesian than the nearby olivines (Mg′ = 36%).

Rare-earth elements in orthopyroxene have a V-shaped pattern, with the minimum at Eu (Wadhwa and Crozaz, 2003). The HREE pattern is akin to the NWA998 olivine, while the LREE enrichment is ascribed to terrestrial weathering.

Table 4. Compositions of olivine

	Nakhla Core	Nakhla Rim	GV[a] Core	GV[a] Rim	Laf.[a] Core	Laf.[a] Rim	NWA817 Core	NWA817 Rim	Y000593 Core	Y000593 Rim	NWA998 Core	NWA998 Rim	MIL03446 Core	MIL03446 Rim
SiO_2	33.6	32.6	32.9	32.4	32.4	32.1	33.9	30.4	34.2	32.0	33.0	32.6	34.1	31.6
TiO_2	0.05	0.07	–	–	0.00	–	0.03	0.04	–	0.03	0.02	0.05	0.00	0.00
Al_2O_3	0.08	0.04	–	–	0.49	–	0.01	0.00	–	0.06	0.02	0.04	0.02	0.04
Cr_2O_3	0.03	0.02	–	–	0.01	–	0.04	0.00	–	–	0.02	0.00	0.00	0.02
FeO	48.6	53.4	50.0	52.3	51.0	52.6	46.4	62.1	45.5	60.1	50.4	49.8	45.5	55.5
MnO	0.96	1.08	0.99	1.02	0.94	1.01	0.85	1.40	0.92	1.15	0.96	0.96	0.90	1.22
MgO	17.5	13.2	15.0	13.1	14.7	13.9	19.8	5.67	18.2	6.42	15.3	15.6	19.2	8.51
CaO	0.29	0.19	0.39	0.31	0.18	0.18	0.56	0.13	0.50	0.15	0.15	0.13	0.56	0.54
Na_2O	0.05	0.01	–	–	–	–	0.00	0.05	–	–	0.01	0.04	0.00	0.00
K_2O	0.00	0.00	–	–	–	–	0.02	0.03	–	–	0.00	0.00	0.00	0.00
Sum	100.7	100.6	99.3	99.1	99.7	99.7	101.6	101.7	99.8	99.9	99.9	99.2	100.3	97.4
Ca %	0.5	0.3	0.6	0.7	0.3	0.3	0.9	0.2	0.8	0.3	0.2	0.2	0.9	1.0
Mg %	39.1	30.5	34.6	30.7	33.8	31.9	42.8	14.0	41.2	16.0	35.1	35.8	42.5	21.2
Fe %	60.4	69.2	64.7	68.7	65.9	67.8	56.3	85.8	58.0	83.8	64.7	64.0	56.6	77.8
Mg′ %	39.3	30.6	34.8	30.9	33.9	32.0	42.4	14.0	41.5	16.0	35.2	35.9	42.9	21.5

Core and rim values are from large olivines.
GV: Laf rim from Friedman-Lentz et al. (1999).
NWA817: data from Sautter et al. (2002).
Y000593: data from Mikouchi et al. (2003).
Laf.: Core from Treiman (1993).
All other data are new.
[a]GV – Governador Valadares; Laf. – Lafayette.

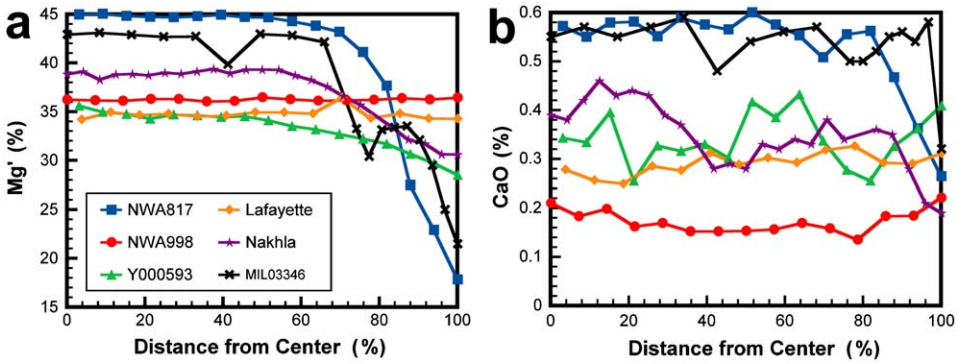

Fig. 5. Chemistry of large olivine grains. Core-to-rim traverses, lengths are: NWA817, 150 μm; NWA998, 152 μm; Y000593, 346 μm; Lafayette, 211 μm; Nakhla, 536 μm; MIL03346, 1031 μm. (a) Mg′ vs. % distance, core to rim. NWA817, Nakhla, Y000593, and MIL03346 are Fe-rich at rims. Cores are homogeneous, with different Mg* in each nakhlite. (b) CaO content. NWA817, Nakhla, and MIL03346 show distinct decreases in Ca content at rims. Cores (except in Lafayette, NWA998) have irregular variations in CaO.

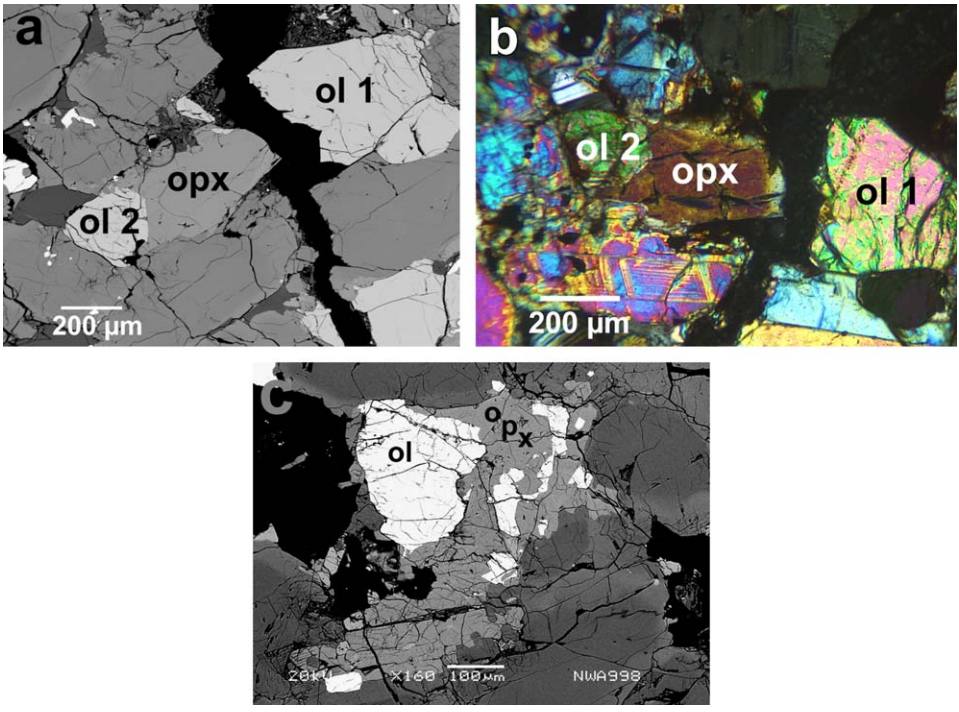

Fig. 6. Large orthopyroxene (opx) grains, NWA998. (a) Opx in Fig. 3 of Carlson and Irving (2004), BSE, 1.16 mm across. Olivine grains 'ol1' and 'ol2' on either side of opx. (b) Same scene as part (a), slightly rotated, optical view, crossed polarizers. 'Ol1' and 'ol2' have identical interference colors and extinction positions, meaning that they are oriented identically. (c) Scattered olivine grains in orthopyroxene, BSE. Augite is dark gray; mesostasis is black. Scale bar 100 μm.

Table 5. Bulk compositions and CIPW norms for the nakhlite meteorites

	Nakhla[a]	Nakhla[b]	Nakhla[c]	Lafayette[d]	Gov. Valad.[e]	NWA817[f]	Y000593[g]	Y000749[g]	MIL 03346[h]
Mass (g):	3.6	8	?	n.a.	?	0.11	2.2	2.0	0.02
SiO_2	48.69	48.24	49.33	46.9	49.52	*50.83*	47.93	48.77	49.2
TiO_2	0.38	0.29	0.35	0.42	0.35	0.61	0.47	0.46	0.07
Al_2O_3	1.74	1.45	1.64	2.74	1.74	3.28	1.91	2.01	3.59
Cr_2O_3	0.33	0.41	0.25	0.19	0.21	0.27	0.24	0.28	0.19
Fe_2O_3	1.29	–	–	–	1.14	–	2.05	2.03	–
FeO	19.63	20.63	21.7	21.6	18.62	19.84	19.82	19.19	19.23
MnO	*0.09*	0.54	0.55	0.5	0.67	0.53	0.59	0.58	0.45
MgO	12.01	12.47	11.82	12.9	10.92	10.31	11.10	11.08	9.33
CaO	15.17	15.08	14.30	13.4	15.82	13.07	14.71	15.08	15
Na_2O	0.41	0.42	0.57	0.40	*0.82*	0.94	0.64	0.68	1.01
K_2O	0.14	0.10	0.17	0.11	*0.43*	0.32	0.18	0.16	0.29
P_2O_5	–	0.12	0.10	0.45	–	–	0.29	0.13	0.22
S	0.06	–	0.02	0.04	–	–	0.07	0.09	–
H_2O	0.24	–	–	0.19	–	–	0.05	0.00	–
Sum	100.45	99.75	100.80	99.6	100.24	*100.00*	99.76	100.50	98.34
CIPW norm[i]									
Or	0.83	0.59	1.00	0.65	*2.54*	1.89	1.06	0.94	1.71
Ab	3.46	3.56	4.78	3.39	*6.55*	7.94	5.41	5.72	8.54
An	2.49	1.78	1.40	5.36	–	3.78	1.81	1.95	4.40
Di	60.36	60.09	56.88	48.35	*65.31*	50.89	57.72	59.64	57.34
Hy	16.82	15.26	20.06	19.46	*7.40*	28.84	15.90	15.89	15.33
Ac	–	–	–	–	*0.25*	–	–	–	–
Ol	12.60	15.48	12.71	18.51	*15.50*	3.36	13.01	11.17	7.97
Il	0.72	0.55	0.66	0.80	*0.66*	1.36	0.89	0.87	0.13
Chr	0.49	0.60	0.36	0.28	*0.31*	0.40	0.35	0.41	0.25
Mt	1.87	1.81	1.88	1.89	*1.48*	1.73	2.97	2.93	1.86
Ap	0.11	0.28	0.23	0.97	–	–	0.62	0.30	0.47
Mg′ (%)	53.5	53.9	51.3	53.7	51.4	53.7	51.2	52.0	47.9

Italicized numbers judged questionable.

Mg′ is molar MgO/(MgO + FeO).

[a]Prior (1912). Wet chemistry. MnO is considerably lower than in other analyses of Nakhla.

[b]McCarthy et al. (1974) X-ray fluorescence.

[c]Dreibus et al. (1982) X-ray fluorescence and instrumental neutron activation. Mass not given, but likely ~100 mg.

[d]Boctor et al. (1976). Electron microprobe of fusion crust.

[e]Gomes and Keil (1980). Wet chemistry. Na_2O and K_2O values high compared to analyses with comparable Al_2O_3. Bogard and Husain (1977) give $K_2O = 0.12\%$, which is similar to other nakhlites. The excess alkalis appear in the CIPW norm as the absence of Anorthite (An) and the presence of Acmite (Ac). The other norm values are distorted.

[f]Sautter et al. (2002). Instrumental neutron activation. SiO_2 by difference, assuming Sum = 100%.

[g]Y000593 and Y000749 are paired. Imae et al. (2003). Wet chemistry.

[h]Anand et al. (2005a, b). ICP-AES.

[i]CIPW norm calculation after Morse (1980). Where Fe^{3+} was not measured, $Fe^{3+}/(Fe^{2+} + Fe^{3+})$ is set to 0.06 as in analysis 1 of Nakhla.

The origin of these large orthopyroxenes is not clear. They cannot have formed at high-temperature equilibrium with the augite, because low-Ca pyroxene would have been pigeonite. The orthopyroxenes may represent a lower-temperature

reaction between olivine and melt, as reported in Lafayette (Harvey and McSween, 1992a).

2.4. Mesostasis

Among the large augite and olivine crystals is mesostasis, a multimineral assemblage of small grains. Mesostasis is commonly brown, as it hosts much of the aqueous alteration material. The abundance of mesostasis varies widely in single samples and among the nakhlites, as seen in petrography (Fig. 1; Table 2) and in chemical analyses (i.e., Al content; Table 5). In areas with little mesostasis, augite and olivine abut each other closely, with no, or very limited, rinds of ferroan pyroxene (Fig. 1b).

In most nakhlites, the mesostasis is marked by radiating sprays of plagioclase laths (Figs. 7a–c and e), with titanomagnetite as subhedra and as small grains among the plagioclase. Spikes of augite and pigeonite/opx project from large augite phenocrysts among the plagioclase laths, and may be optically continuous with other pyroxene grains far into the mesostasis. Among these major minerals are others typical of late crystallization of basaltic magma. Three nakhlites have distinctly different mesostasis textures: NWA817, MIL03346, and NWA998.

Mesostasis in NWA817 contains few laths of plagioclase, and its titanomagnetite crystals are strongly dentritic and cruciform (Fig. 7d). Among these few grains are arrays of needle-shaped, oriented augite and olivine crystals in a very fine-grained brownish matrix, probably devitrified and altered glass (Sautter et al., 2002; Fig. 7d).

Mesostasis in MIL03346 contains no plagioclase, but is marked by elongated skeletal crystals of olivine, titanomagnetite, and pyrrhotite in glass (Figs. 7g–j). The olivine crystals are laths, rods, and feathers – shapes indicative of rapid cooling, like

Fig. 7. Mesostasis. Image pairs, 0.58 mm across, left in plane polarized light (pl), right in crossed polarizers (xp), except as noted. Intereference colors vary. Large crystals are augite, except as noted olivine, ol. (a) Nakhla. Clear plagioclase crystals (with albite-law twins) and euhedral magnetite grains in brownish devitrified, silica-rich glass. (b) Governador Valadares. As in Nakhla, but somewhat finer grained. (c) Lafayette. Clear plagioclase, orange-brown aqueous alterations of glass, and euhedral magnetite grains. (d) NWA 817. Finely devitrified glass with skeletal cruciform titanomagnetite (black), plagioclase (clear in pl), oriented needles of augite (pale in xp). (e) Y000593. As in Nakhla. Iddingsite alteration at left. (f) NWA998. Mesostasis is single plagioclase grains (white in pl, white to gray in xp) among pyroxene, olivine (top left, pink in xp). (g) MIL03346. Typical mesostasis, paired images in plane polarized light, transmitted (left, pl) and reflected (right, rl). Finely devitrified glass with olivine dendrites partially replaced by iddingsite (brown in pl), skeletal titanomagnetite (bright in rl). (h) MIL03346. Paired pl and rl images as in part (g) 0.23 mm across. Oxide boxwork in mesostasis, in rl as bright lines at center and upper right. Titanomagnetite crystal at center left, with an iron sulfide in its core. (i) MIL03346. Spinifex-textured olivine, with small oxide and sulfide grains. Single image, reflected plane light, 0.23 mm across. Olivine slightly brighter than augite (center left and lower right). (j) MIL03346. Skeletal titanomagnetite crystal. Single image, reflected plane light, 0.23 mm across.

'spinifex' olivine in terrestrial komatiites (e.g., Lofgren, 1983). Titanomagnetite forms skeletal grains (Figs. 7g and j), box-works of very thin plates oriented at right angles to each other (Fig. 7(h), and discrete tiny euhedra. Iron sulfide (pyrrhotite?) occurs in the titanomagnetite (Fig. 7(h) and as rare skeletal grains. The remaining mesostasis is silicate glass with uncommon rounded blebs of silica.

NWA 998 does not contain mesostasis as described above, but has the same minerals in compact subhedral or anhedral grains (Fig. 7f). These minerals lie among

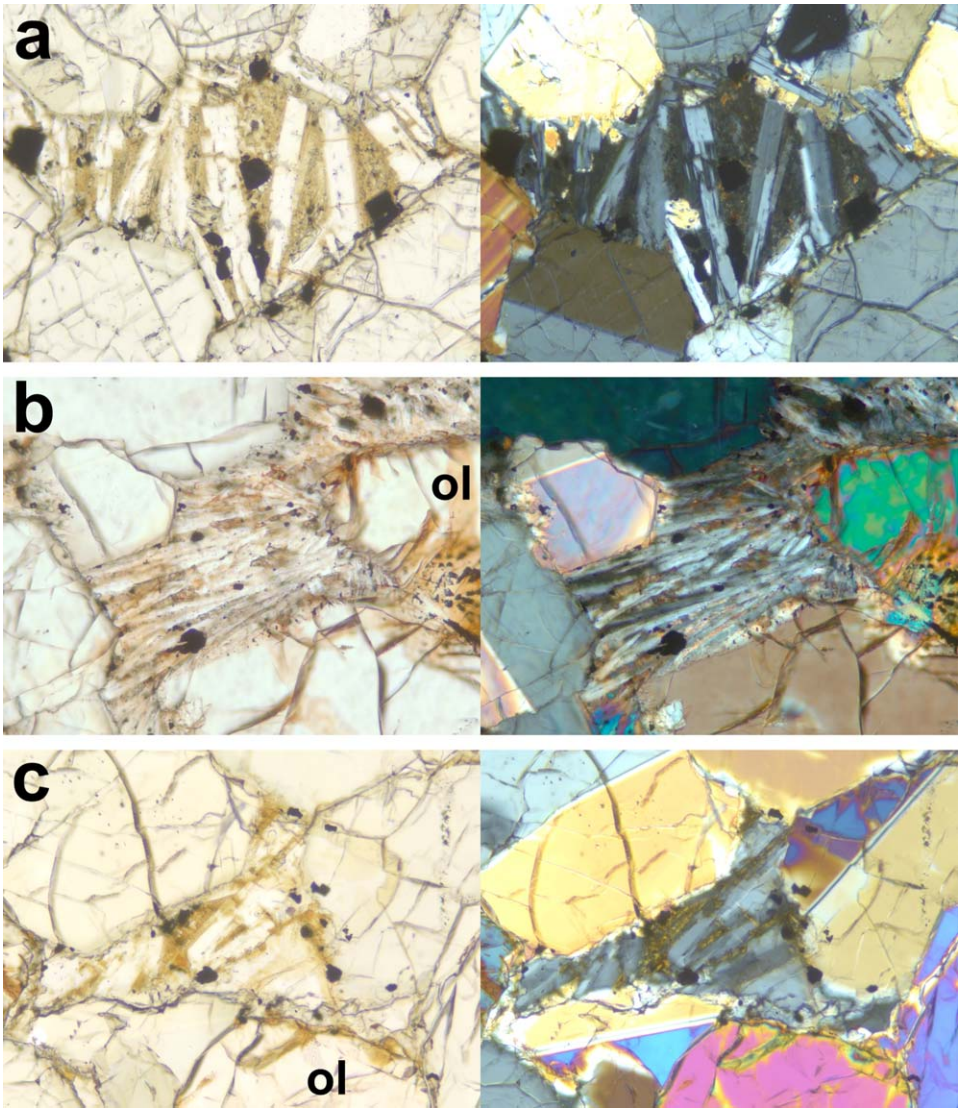

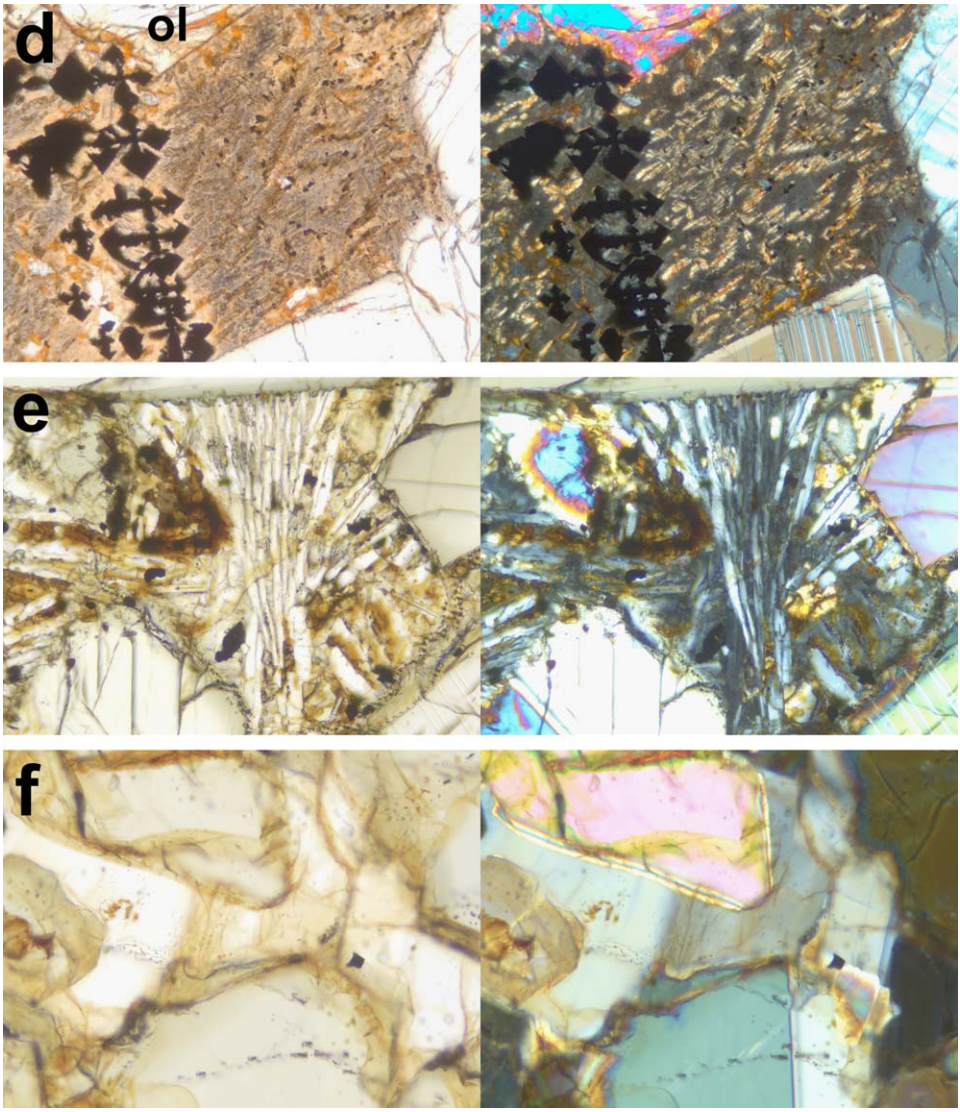

Fig. 7. (*Continued*)

the large pyroxene, olivine, and titanomagnetite grains to form a diabasic texture (e.g., p. 136 of Philpotts, 1989).

2.4.1. Plagioclase

Mesostasis plagioclase is as thin laths or blades (except in NWA998 and MIL03346); in thin section, they appear as long rectangles (Fig. 7). They commonly

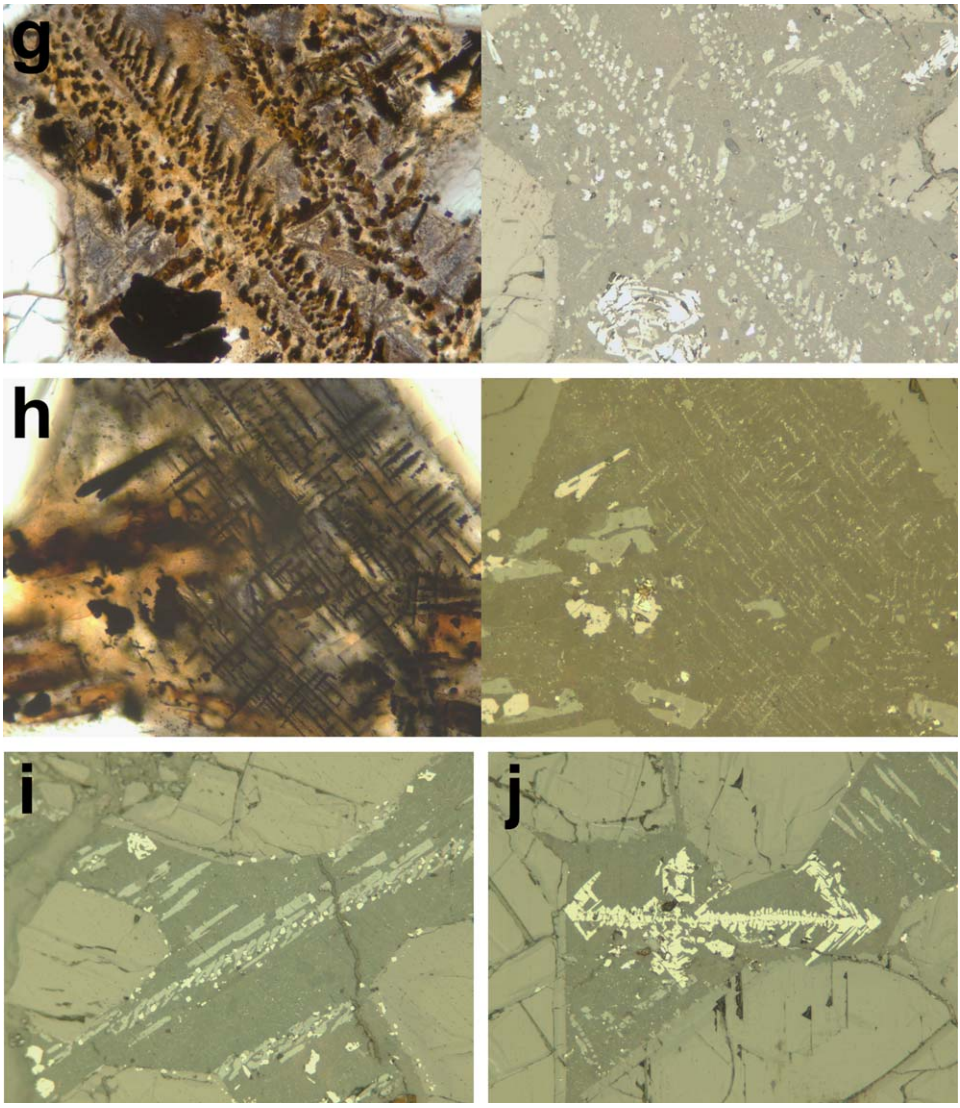

Fig. 7. (*Continued*)

radiate as sprays or sheaves from spots at the edges of mesostasis areas. The widths of the laths vary among meteorites, with NWA817 being thinnest and NWA998 being thickest (Table 6).

The plagioclase is albitic, typically near $Ab_{60}An_{35}Or_{05}$ (Table 7). There are few data on zoning, although analyses range from $Ab_{73}An_{14}Or_{13}$ to $Ab_{59}An_{37}Or_{04}$. Reverse zoning, cores more albitic than rims, is reported for NWA817 plagioclase,

Table 6. Mesostasis plagioclase

Sample	Plagioclase lath width (μm)
MIL 03346	0
NWA817	5
Y000593	20
Nakhla	50
Governador Valadares	50
Lafayette	100
NWA998*	>100

Extended from Mikouchi et al. (2003).
*Plagioclase in NWA998 occurs as blocky grains, to >100 μm width.

which are also exceptional in containing significant Fe and Mg: ~5% Fe_2O_3 and ~0.3% MgO (Sautter et al., 2002). No other nakhlite plagioclase has more than 1% Fe_2O_3 equivalent, nor more than 0.1% MgO (Table 7). The plagioclase is enriched in LREE and has positive Eu anomalies (Wadhwa and Crozaz, 1995, 2003).

2.4.2. Fe–Ti oxides

Titanomagnetite occurs as small euhedra and anhedra between large augite and olivine crystals (Table 8). Plagioclase laths terminate at the small euhedra crystals, suggesting that the titanomagnetite crystallized first. Their grains are skeletal or cellular in NWA817, Y000593 and MIL03346, and compact in the other nakhlites (Figs. 4a and 7g, j: Sautter et al., 2002; Imae et al., 2003; see Figs. 12–7b of Philpotts, 1990). Titanomagnetite also occurs as anhedra among plagioclase and/or olivine laths (Fig. 7).

Ilmenite occurs as plate-shaped lamellae in titanomagnetite, suggestive of oxidative exsolution of original ulvöspinel. Discrete ilmenite grains are reported in Nakhla, Lafayette, and Y000593 (Bunch and Reid, 1975; Boctor et al., 1976; Szymanski et al., 2003), but not in NWA817 (Sautter et al., 2002).

2.4.3. Other phases

Many other minerals are reported in mesostasis. Most abundant are pyroxenes, some of which project from the edges of large augite grains. In Ca-Mg-Fe composition, mesostasis pyroxenes continue the trends of the large augites' rims to higher Fe and lower Ca contents, and with lower Al and Na (Fig. 3a). Mesostasis pyroxenes include augite, pigeonite, and orthopyroxene, and many have 'forbidden zone' compositions (Fig. 3a) or are exsolved to lamellae of augite and pigeonite (e.g., Mikouchi and Miyamoto, 1998; Mikouchi et al., 2003).

Minor phases are typical of late crystallization of basaltic magma and include potassium feldspar (Table 7), apatite, zircon, badellyite, silica, and 'granitic' glass. The silica mineralogy is varied: quartz in Nakhla, tridymite in Y000593, and cristobalite in NWA998 and MIL03346 (Edwards et al., 1999; Sautter et al., 2002;

Table 7. Compositions of Nakhlite Feldspars

	Nakhla pl-1	Nakhla pl-2	Nakhla afs	Laf.[a] pl	Laf.[a] afs	NWA817 afs-1	NWA817 afs-2	Y000593 pl	Y000593 afs	NWA998 pl-1	NWA998 pl-2
SiO_2	60.6	60.1	65.5	60.7	65.8	62.7	63.1	59.6	66.2	58.5	59.6
TiO_2	–	0.02	–	–	–	0.43	0.18	0.06	–	0.03	0.02
Al_2O_3	24.3	23.8	18.1	23.5	18.4	18.8	19.0	24.2	18.5	25.9	25.8
Cr_2O_3	–	–	–	–	–	0.00	0.00	–	–	0.01	0.00
Fe_2O_3	–	–	–	–	–	5.35	4.29				
FeO	0.84	0.92	–	0.83	–	–	–	0.85	0.45	0.92	0.72
MnO	–	0.01	–	–	–	0.09	0.02	0.06	–	0.00	0.00
MgO	0.03	0.06	–	0.10	–	0.25	0.48	0.02	–	0.04	0.00
CaO	6.7	6.44	0.49	7.1	0.51	2.82	1.92	7.18	0.64	7.77	7.12
Na_2O	7.3	7.37	2.69	7.3	2.49	7.84	6.23	7.56	3.92	6.91	7.03
K_2O	1.0	0.91	12.9	0.71	13.4	2.11	4.89	0.58	9.61	0.73	0.88
Sum	100.8	100.7	99.68	100.24	100.60	100.4	99.9	100.1	99.2	100.8	101.2
An	33.6	30.9	2.4	31.8	2.4	14.5	10.2	33.3	3.3	36.7	34.0
Ab	62.4	63.9	23.5	62.6	21.5	72.7	59.6	63.5	37.0	59.2	61.0
Or	4.0	5.2	74.1	5.6	76.1	12.9	30.2	3.2	59.7	4.1	5.0

pl – plagioclase; afs – alkali feldspar.

Data sources: Bunch and Reid (1975), Nakhla pl-1 and afs, Lafayette pl and afs; Nakhla pl-2, Weincke (1978); NWA817, Sautter et al. (2002); Y000593, Mikouchi et al. (2003); NWA998, new data.

[a]Laf. – Lafayette.

Table 8. Compositions of oxide minerals

	Nakhla Ti–Mt	Nakhla Il	Laf.[a] Mt	Laf.[a] Il	NWA817 Ti–Mt	NWA817 Ti–Mt	Y000593 Ti–Mt	Y000593 Il	NWA998 Mt	NWA998 Mt
SiO_2	0.08	0.00	–	–	–	–	0.12	–	0.06	0.05
TiO_2	14.8	51.3	17.3	51.3	12.5	10.6	15.3	49.1	14.3	23.8
Al_2O_3	6.83	0.24	2.21	0.24	2.06	0.69	1.52	0.02	1.23	0.81
Cr_2O_3	0.34	0.12	7.17	0.12	0.02	0.02	0.29	0.22	2.06	2.20
Fe_2O_3 [b]	30.9	0.86	–	–	40.9	46.5	–	–	–	–
FeO	44.2	43.7	63.8	44.5	42.6	40.8	77.0	45.6	74.9	67.1
MnO	0.41	0.62	0.65	0.62	0.37	0.37	0.38	0.66	0.42	0.52
MgO	0.48	0.86	1.41	0.82	0.14	0.05	0.29	0.53	0.71	1.04
CaO	0.19	0.25	0.23	0.25	–	–	0.08	–	0.03	0.40
Na_2O	0.00	–	–	–	–	–	–	–	0.00	0.01
K_2O	0.08	–	–	–	–	–	–	–	0.02	0.01
Sum	98.3	98.0	93.7	97.9	98.8	98.5	95.2	96.2	93.7	95.6

Ti–Mt – titanomagnetite; Mt – magnetite; Il – ilmenite; Homog. – homogeneous.

Data sources: Nakhla: Treiman (1993), new data; Lafayette, Boctor et al. (1976); NWWA817: Sautter et al. (2002); Y000593: Mikouchi et al. (2003); NWA998, new data.

[a]Laf. – Lafayette.

[b]Calculated by stoichiometry.

Imae et al., 2003; Rutherford et al., 2005). The only phosphate is chlorapatite with little F, minimal OH, and abundant REE (Bridges and Grady, 1999, 2000; Wadhwa and Crozaz, 1995, 2003). Magmatic sulfides are pyrrhotite and rare chalcopyrite (Greenwood et al., 2000a, b; Imae et al., 2003). Pyrite and marcasite are uncommon, and are discussed with alteration minerals.

2.5. Inclusions in large crystals

The large augite and olivine grains contain inclusions, many of which are important in nakhlite petrogenesis. Here, they are divided into monomineralic, multimineralic with (or without) glass, and symplectic.

2.5.1. Monomineralic inclusions

The nakhlites' large crystals contain few monomineralic inclusions, except for augite grains enclosed in poikilitic late olivine. Large augites contain only magnetite grains to ~200 μm, which are similar to those in mesostasis, and may be in glassy multiphase inclusions or embayments of mesostasis. One olivine inclusion was noted near the edge of an augite core in NWA998.

In NWA998, the large orthopyroxenes commonly contain inclusions of olivine, which share a common crystallographic orientation (Fig. 6c).

The large olivines contain sparse grains of augite (Fig. 4b). These are ellipsoidal to subhedral, chemically indistinguishable from the large augites, and commonly surrounded by selvages of 'granitic' glass (Harvey and McSween, 1992b).

2.5.2. Multiphase and glassy inclusions

The large olivine and augite grains in all nakhlites contain complex, multiphase inclusions. These are inferred to be magmatic or melt inclusions, remnants of droplets of magma entrapped by growing crystals (e.g., Treiman, 1990, 1993; Harvey and McSween, 1992b).

Many large olivines contain ellipsoidal to irregular multiphase magmatic inclusions (Figs. 8a and b), described in detail by Harvey and McSween (1992b) and Treiman (1993). They range from <10 μm to 350 μm diameter, occur throughout the olivine grains, and may be concentrated in zones surrounding an olivine's center (Fig. 1b of Treiman, 1986). Inclusions in all but NWA817 are marked by radiating laths of Al–Ti-rich augite, 5–20 μm wide (Figs. 8b and 9a; Table 9). Among these augite laths are equant crystals of titanomagnetite in 'granitic' glass, with rare ilmenite, pigeonite, alkali feldspar, chlorapatite, pyrrhotite, and silica (Table 9; Harvey and McSween, 1992b; Treiman, 1993). The silica is cristobalite in NWA817 but tridymite in Y000593 (Sautter et al., 2002; Imae et al., 2003). Spherical or ellipsoidal void spaces are interpreted to represent magmatic vapor (Fig. 8b; Figs. 1a and b of Treiman, 1993). Plagioclase is nearly absent (Treiman, 1993). A reported kaersutite grain (Harvey and McSween, 1992b) is doubtful, as its chemical analysis does not have amphibole stoichiometry. Between the augite laths and the host olivine is a rind, a few μm thick, of Al–Ti–Cr augite and Ti–Al chromite (Table 9). Multiphase inclusions in Lafayette's olivine differ in having pyroxenes that are

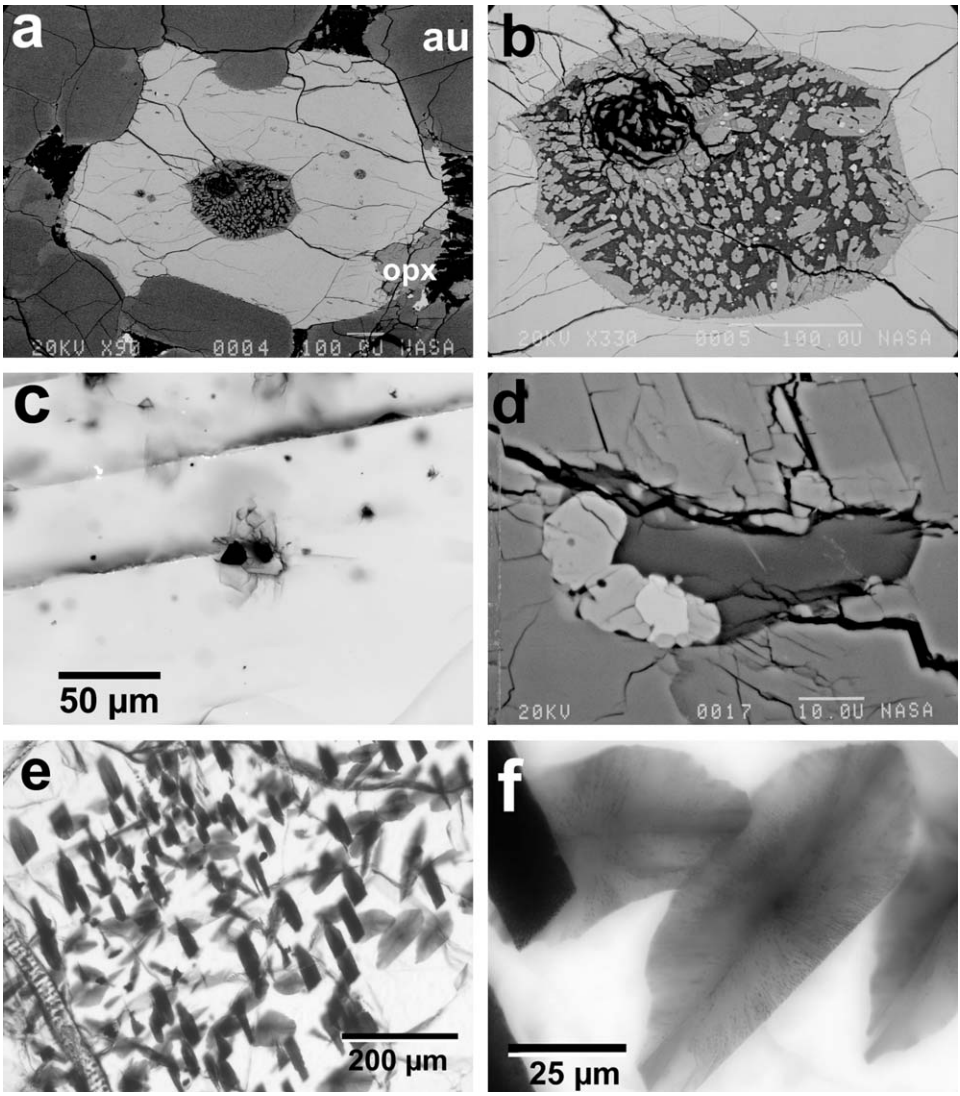

Fig. 8. Inclusions in augite and olivine. (a) Magmatic inclusions (elliptical multimineral mass) in Nakhla olivine (light gray), BSE, scale bar 100 μm. Fig. 1a of Treiman (1993). Augite au is dark gray, orthopyroxene [opx] replacing olivine is medium gray, mesostasis is mostly black. (b) Detail of part (a), BSE, scale bar 100 μm. Inclusion contains augite (medium gray), feldspathic glass/mesostasis (dark gray), Fe–Ti oxides (bright). Darker circular area at upper left is void space, originally a vapor bubble. (c) Magmatic inclusion in augite, Lafayette. Optical view, plane light. Magnetite (triangular shape), pyrrhotite (ellipsoidal, out of focus), feldspathic glass (clear), and low-Ca pyroxene (browner than surrounding augite). (d) Magmatic inclusion in augite, Nakhla. BSE, scale bar 10 μm. Hercynite (Fe–Al spinel, brightest), low-Ca pyroxene (light gray), feldspathic glass (dark), and a phosphate (light needle in glass). (e) Olivine, Y000593, with symplectite inclusions. Plane light. Brown streak, lower left, is epoxy. (f) Symplectite, detail of (e), Y000593. Plane light; reconstructed in-focus image from six frames. Dark streaks of magnetite radiate out from symplectite center.

wider, less elongate, less aluminous, and in carrying orthopyroxene in addition to augite (Fig. 10a).

Olivines in NWA817 contain glassy inclusions of the same size and shape (Fig. 2f of Sautter et al., 2002). These are most reasonably interpreted as uncrystallized inclusions of parent magma, precursors to the multiphase inclusions.

The cores of large augites contain multiphase, glass-bearing inclusions, $<50\,\mu m$ across, with irregular boundaries (Figs. 8c and d). Augite against and in these inclusions is enriched in Al and Ti. The inclusions contain silicate glass, Ti magnetite, ellipsoidal void spaces (vapor bubbles?), pigeonite, hercynite (Fe–Al spinel), pyrrhotite, and chlorapatite (Figs. 8c and d; Varela et al., 2001; Stockstill et al., 2002; pers. obs.). Similar inclusions occur in pyroxenes in shergottites (Treiman, 1985). In MIL03346, they contain only glass and titanomagnetite. The chemical composition of the glass varies among inclusions (Varela et al., 2001).

There is a single report of a fluid inclusion in a nakhlite augite, along a healed fracture (Bodnar, 1998). It contains liquid and vapor CO_2 (or possibly H_2O).

2.5.3. Symplectites

The cores of large olivines in most nakhlites contain dark feathery inclusions – submicron symplectites of augite and magnetite (Figs. 8e and f: Mikouchi et al., 2000; Greshake et al., 2000; Imae et al., 2003). They are not seen in Lafayette, NWA998, and MIL03346. Symplectite inclusions are a few μm thick and up to hundreds of μm long and wide. They lie parallel to crystallographic (1 0 0) of the host, and are elongated along the [0 1 0] and [0 1 3] zones (Mikouchi et al., 2000). They may represent oxidative exsolution of a kirschteinite component ($CaFeSiO_4$) from the host olivine – olivine in some nakhlites contains exsolution lamellae of kirscheinite-monticellite (Bridges et al., 2004).

2.6. Alteration mineral assemblages

A marvelous feature of the nakhlites is that they contain pre-terrestrial mineral assemblages deposited by liquid water (Fig. 9; Bridges et al., 2001), especially veinlets and patches of red-brown 'iddingsite' (Figs. 9a–f; Reid and Bunch, 1975). 'Iddingsite' is a sub-μm mixture of smectite clay, iron oxy-hydroxides, and salt minerals; it is a product of low-temperature aqueous alteration of mafic material, especially olivine and basalt glass (e.g., Smith et al., 1979; Delvigne, 1998). In nakhlites, iddingsite appears as veins through olivine (Figs. 9a–c), stringers along cracks (Figs. 9a and f), and as masses where mesostasis or intercumulus olivine once lay (Figs. 9d and e). Iddingsite veins in olivine typically have serrated or saw-tooth borders formed of segments along the olivines' {0 2 1} planes (Figs. 9b and c). The bulk of most veins is filled with moderately large smectite grains (to $\sim$100 μm long in Lafayette), most with cleavage (crystallographic {0 0 1}) radiating from, and approximately perpendicular to, the vein walls. Also adjacent to vein walls are grains or masses (to $\sim$100 μm) of gypsum and calcic siderite (Fig. 9c; Vicenzi and Fahey, 2001; Bridges and Grady, 2000). Near the centers of the veins are thin veinlets, a few μm wide, of submicron or amorphous material of smectite

composition (Figs. 9b and c; Treiman et al., 1993; Vicenzi and Fahey, 2001; Gillet et al., 2002). These smaller veinlets cut across the structure and cleavages of the coarser smectite grains. This identical pattern is seen in terrestrial olivine replaced by phyllosilicates (e.g., Figs. 130, 131 of Delvigne, 1998).

Iddingsite is most abundant in Lafayette and Y000593. There, it occurs among large augite crystals as masses up to ~500 μm across, in the shapes of poikilitic olivine grains (Figs. 9d and e). The masses are concentrically layered, with alternating bands of rust-colored smectite material and red iron oxide-hydroxide

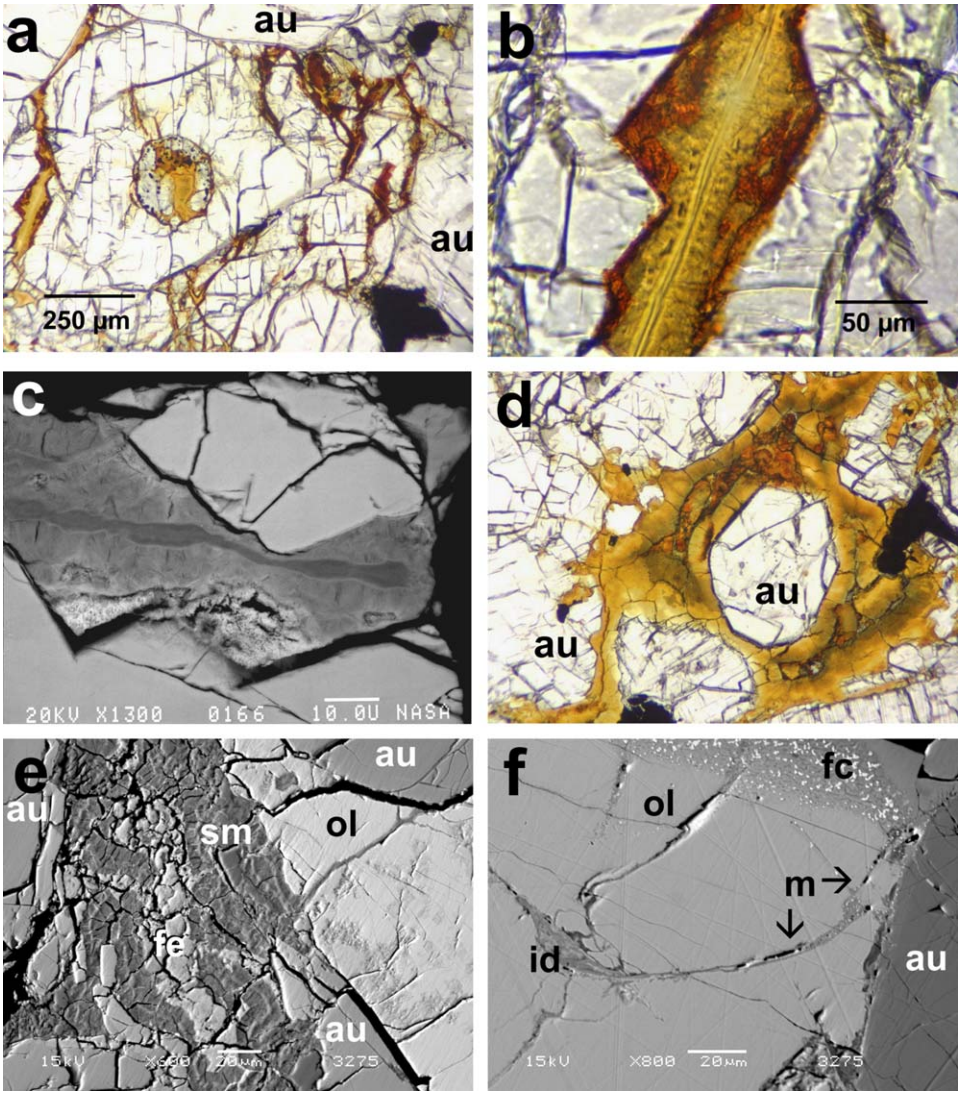

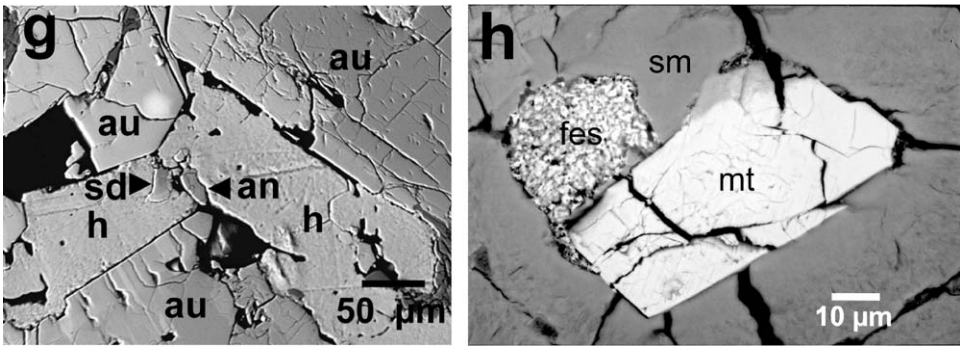

Fig. 9. (*Continued*)

material. Iddingsite veinlets are offset along fractures (Gooding et al., 1991), and are degraded and melted near the fusion crust (Gooding et al., 1991; Treiman et al., 1993; Treiman and Goodrich, 2002).

Iddingsite has a range of compositions, as can be seen on BSE imagery as bands and speckles of varying brightness (Figs. 9c and e). In bulk composition, iddingsite is equivalent (more or less) to mixtures of olivine, iron oxy-hydroxide, mesostasis glass, and water (Gooding et al., 1991; Treiman et al., 1993). Iddingsite in olivine has nearly no Al_2O_3, while that in mesostasis areas contains up to 5% Al_2O_3 (Treiman et al., 1993; Gillet et al., 2002). Lafayette iddingsite has a REE pattern similar to that of the mesostasis, but at lower abundances (Treiman and Lindstrom, 1997; Bridges and

Fig. 9. Aqueous alteration materials. (a) Iddingsite in olivine, Lafayette. Plane light, scale bar 250 μm. Augite is au. Iddingsite fills vein with saw tooth edges (far left, (b)), replaces glass in magmatic inclusions (round shape, center), fills irregular cracks and grain boundaries (right). (b) Detail of saw-tooth edge, from (a). Plane light, scale bar 50 μm. Reddish rind is calcic siderite and gypsum (c), partially oxidized. Yellow-brown core material is smectite. Veinlet of ultrafine-grained smectite at center of vein. (c) Saw-tooth iddingsite vein cutting olivine (ol), Lafayette. BSE. Salts (sa) are gypsum and siderite, partially oxidized. Smectite flakes (sm) radiate from the vein walls and centers; veinlet core is fine-grained darker (Fe-poorer) smectite or amorphous silicate. (d) Iddingsite fills space among augites (au, light greenish gray), Lafayette. Plane light, scale bar 250 μm. Yellow-brown is poorly crystalline smectite. Larger smectite grains radiate in towards centers of iddingsite masses. Red at the center of iddingsite is nearly amorphous Fe oxy-hydroxide. (e) Space-filling iddingsite among augite (au) and olivine (ol), Y000593. BSE, scale bar 20 μm. Smectite (sm) layers parallel the augite and olivine, and are cored by iron oxide/hydroxide (fe). (f) Iddingsite veinlet, melted near fusion crust, Y000749. BSE, scale bar 20 μm. Olivine (ol), fusion crust (fc, with tiny magnetite crystals), augite (au). Veinlet of iddingsite, id, is melted to homogeneous glass, bubbles, and Fe-oxide grains (m) near fusion crust. (g) Salt assemblage in Nakhla (Bridges et al., 1998). Halite (h), anhydrite (an) and siderite (sd) among augite (au) in mesostasis. (h) Sulfide alteration, Lafayette. Spongy intergrowth of iron sulfide and oxide (fes), adjacent to smectite (sm) in iddingsite and titanomagnetite (mt).

Table 9. Mineral compositions from magmatic inclusions

Host mineral:	Nakhla	Nakhla	Nakhla	Nakhla	Nakhla	Nakhla	Nakhla	GV[a]	GV[a]	GV[a]	Nakhla	Laf.[a]
	Olivine	Olivine	Olivine	Olivine	Olivine	Olivine	Olivine	Olivine	Olivine	Olivine	Augite	Augite
Location:	Rind	Rind	Core	Core	Core	Core	Core	–	–	–	–	–
	Cr–Mt	Aug	Mt	Ilm[b]	Aug	Aug	Afs	Aug[b]	Mt[b]	Sp[b]	Pig[c]	Mt[d]
SiO_2	0.01	45.8	0.08	–	48.5	44.3	*63.4*	49.4	0.04	*4.96*	49.7	*0.15*
TiO_2	10.5	1.32	14.8	*45.0*	0.91	1.1	*0.05*	0.71	16.5	*0.69*	–	*7.98*
Al_2O_3	4.00	4.60	6.83	*0.86*	2.81	5.27	*18.1*	2.50	6.31	*47.1*	1.9	*5.50*
Cr_2O_3	21.9	0.15	0.34	–	0.02	0.01	*0.00*	0.17	3.36	*5.26*	–	*2.97*
FeO	58.2	18.8	71.9	*43.4*	18.3	19.8	*2.05*	16.3	68.0	*36.3*	30.7	*74.1*
MnO	0.51	0.43	0.41	*0.59*	0.50	0.44	*0.05*	0.40	0.51	*0.33*	0.9	*0.39*
MgO	1.10	7.36	0.48	*1.43*	8.27	6.63	*0.10*	11.2	0.94	*4.92*	12.9	*0.88*
CaO	0.09	21.2	0.19	*2.24*	19.5	20.2	*0.18*	18.6	0.11	*0.09*	3.0	*0.39*
Na_2O	0.00	0.25	0.00	–	0.25	0.25	*0.71*	0.31	0.02	*0.03*	0.3	*0.00*
K_2O	0.00	0.02	0.08	–	0.11	0.12	*14.4*	–	–	–	–	*0.00*
Sum	96.3	99.9	95.1	*93.5*	99.5	100.2[e]	*94.33*	99.6	95.8	*99.6*	99.4	*92.4*

Italicized analyses have low sums or are clearly mixtures, and are included only as indications of the phases present.

Cr–Mt – chromian magnetite; Mt – magnetite; Aug – augite; Ilm – ilmenite; Afs – alkali feldspar; Sp – aluminous spinel; Pig – pigeonite.

[a]GV – Governador Valadares. Laf. – Lafayette.

[b]From Harvey and McSween (1992b).

[c]From Varela et al. (2001).

[d]New data.

[e]Includes 2.05% P_2O_5.

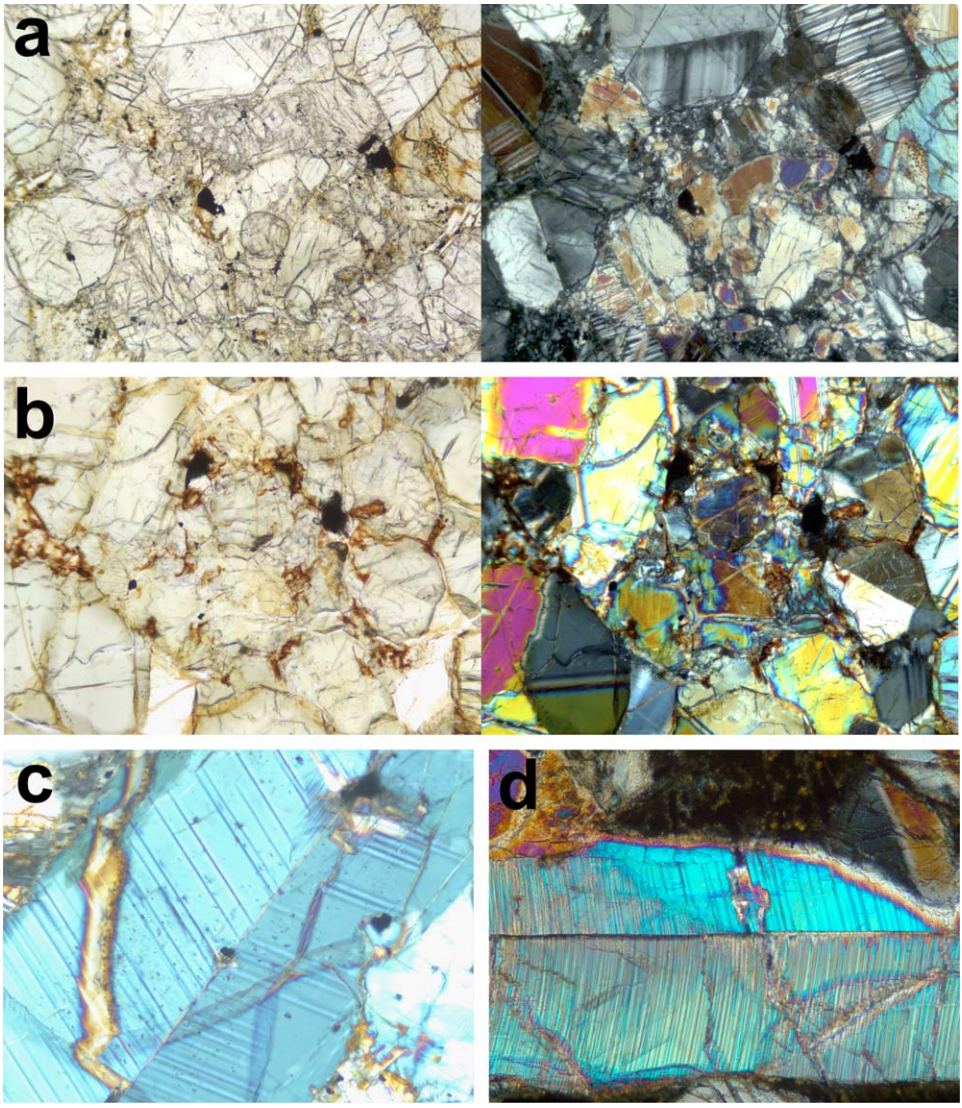

Fig. 10. Deformation features. (a) Granulated zone, Nakhla. Image pair of same scene, 1.16 mm across: left, plane polarized light (pl); right, crossed polarizers (xp). (b) Granulated zone, NWA998. Image pair of same scene, 1.16 mm across: left, pl; right, xp. (c) Deformation twins, Y000593, single image, xp, 0.58 mm across. Typical chevron-pattern twins. (d) Deformation twins, MIL03346, single image, xp. Typical chevron-pattern twins.

Grady, 2000). Iddingsite in NWA817 has LREE like those of the mesostasis diluted 10-fold, and HREE like those of the olivine, but enriched 10-fold (Gillet et al., 2002).

Iddingsite in Lafayette is known best, being both abundant and coarse grained. It contains platy smectite crystals to ~100 μm long (Treiman et al., 1993) with strong

basal {0 0 1} cleavage – d-spacing perpendicular to the cleavage are ~1.4 nm (Treiman et al., 2004). This basal diffraction is broad, indicating significant disorder in stacking and intercalation. Raman spectra show peaks characteristic of two tri-octahedral layer silicates (including smectites; Kuebler et al., 2004). The iddingsite also occurs as very fine-grained material (Treiman et al., 1993; Vicenzi and Heaney, 2000), which appears in TEM as irregular, short (to 100 nm) packets of smectite clay (layer spacing at ~1.1 nm) in amorphous material (Gooding et al., 1991; Treiman et al., 1993). Lafayette iddingsite also contains iron oxide-hydroxide material, seen in thin section as red isotropic masses coating smectite layers. This material is nearly amorphous, and some diffracts as 'two-ring ferrihydrite' (Treiman, unpublished data).

Iddingsite in other nakhlites is less well characterized. That in NWA817 has Raman spectra of smectite, and X-ray diffractions at 1.1–1.2 nm (Gillet et al., 2002). Iddingsite in Y000593 contains goethite, montmorillonite, a smectite clay, amorphous clay-composition material, and jarosite (Imae et al., 2003; Noguchi et al., 2003; Treiman et al., 2004). MIL03346 contains similar veinlets of red-orange vein material, probably this same iddingsite material (Stopar et al., 2005; pers. obs.).

The salt mineral assemblage includes siderite, anhydrite, and halite together in the mesostasis of Nakhla (Bridges and Grady, 1999, 2000; Fig. 9g). These salts occur as unzoned, anhedral grains among feldspar and 'granitic' glass in the mesostasis, possibly associated with phosphates. The siderite is Mn-rich and Ca-poor, unlike the Ca-siderite of the iddingsite veinlets. MIL03346 contains gypsum in a similar setting (Stopar et al., 2005). The salts were deposited from saline water (Bridges and Grady, 2000; Bridges et al., 2001), either by filling void spaces or replacement of other minerals.

In Nakhla, Lafayette, and Y000593, a sulfide alteration assemblage is present as pyrite or marcasite (Fig. 9h; Bunch and Reid, 1975; Boctor et al., 1975; Shearer and Adcock, 1998; Greenwood et al., 2000a, b; Mikouchi et al., 2003). Pyrite is stable only below 743 °C (Craig and Scott, 1974); marcasite on Earth forms in hydrothermal and diagenetic environments (Nesse, 2000). Pyrite in Nakhla and Lafayette has sulfur isotope ratios not far from the solar-system initial, $\delta^{34}S = -3.4 - +1.5‰$, but with some non-mass-fractionation effects (Greenwood et al., 2000a, b; Farquhar et al., 2000). It is not clear if the sulfide assemblage is related to the other alteration assemblages.

2.7. Shock effects

Shock effects in the nakhlites are minor (Fig. 10), especially compared to the abundant strong shock effects seen in other SNC (Martian) meteorites (Stöffler, 2000). Plagioclase is fully crystalline with normal birefringence, some augite and olivine grains show undulatory extinction (Greshake et al., 2004), and some augite grains have lamellar shock twins (Fig. 10c; Berkley et al., 1980). Structural signs of shock deformation include microfaults and rare brecciated zones. Microfaults offset grain boundaries and veinlets of iddingsite (e.g., Gooding et al., 1991), and the brecciated zones are associated with chevron twinning in augite (Fig. 10).

2.8. Terrestrial effects

All nakhlites have interacted with the terrestrial environment. Terrestrial effects are commonly minor and poorly documented, but are critically important for understanding ultra-trace elements, organic matter, and possible biogenic materials.

Nakhla is the least affected of the nakhlites. Pre-terrestrial halite is still preserved in samples collected shortly after its fall (Bridges and Grady, 1999, 2000). Observed terrestrial effects include addition of lead (Nakamura et al., 1982), interaction with water and oxygen (i.e., rusting, dissolution, hydration), inoculation with microbes, and deposition of microbial organic secretions (Toporski et al., 1999, 2001; Toporski and Steele, 2004). Much of the organic carbon in Nakhla is terrestrial, based on ^{14}C abundances and on the specific compounds present (Jull et al., 2000; Glavin et al., 1999).

Other Nakhla samples were collected several years after their fall, and should contain terrestrial effects like in the NWA nakhlites (e.g., Barrat et al., 1998; Crozaz et al., 2003; Lee and Bland, 2004). These include deposition of carbonate minerals along veinlets and grain boundaries, weathering to form ferric oxy-hydroxides and clays (Barrat et al., 1998; Lee and Bland, 2004), REE additions and losses (Crozaz et al., 2003), disruption of some radioisotope systems (e.g., Borg et al., 2003), and water exchange with hydrous phases like clays.

The Yamato nakhlites have been altered like other Antarctic meteorites (e.g., Gooding, 1986; Lee and Bland, 2004). Veinlets of clay-like material and silica cut across their fusion crusts, and penetrate their interiors (Treiman and Goodrich, 2002). It is likely that pre-terrestrial carbonates and other salt minerals have interacted with Antarctic waters (see Kopp and Humayan, 2003). Biotic contamination is a strong possibility (Steele et al., 2001).

3. Bulk chemical composition

3.1. Major elements

The chemical compositions of the nakhlites are very similar (Table 5), consistent with the similarities in their mineral proportions and compositions (Tables 2–4 and 7). Compared to typical basalts, they are rich in CaO (from augite) and poor in Al_2O_3 and alkalis (from mesostasis).

Each nakhlite is moderately homogeneous among samples of grams to tenths of grams (Table 5). For instance, the three analyses of Nakhla represent three different techniques and more than an order of magnitude differences in mass. The most obvious differences among nakhlite compositions (beside questionable and missing values) are in Al_2O_3 and alkalis; abundances of these elements decrease in the order MIL03346 > NWA817 ≈ NWA998 > Lafayette > Y000593 > Nakhla ≈ Governador Valadares (Table 5). These elements are concentrated in mesostasis, and proportions of mesostasis generally follow this order (Table 2). These differences suggest that

Lafayette is distinct from Nakhla, but that Governador Valadares and Nakhla may not be distinct.

The nakhlites' bulk compositions share several characteristic element ratios with the shergottites and Chassigny, notably Fe/Mn, Na/Al, K/La, P/Ti, etc. (Wänke and Dreibus, 1988; Treiman et al., 1986, 2000; Longhi et al., 1992). The similarities in these ratios suggest that these meteorite groups share a common parent planet (i.e., Mars).

3.2. Trace elements

Trace element abundances in most nakhlites have been tabulated by Lodders (1998) and Meyer (2003). The nakhlites are strongly enriched in REE (Fig. 11a) – most with La at ~10 × CI chondritic, but NWA817 has La~25 × CI. All are also enriched in LREE; CI-normalized La/Lu values are 5 × CI in NWA817, 4.2 × CI in Nakhla and Y000593, and 3.5 × CI in Lafayette. All have slight negative Eu anomalies and no Ce anomalies, such might result from terrestrial weathering or loss of magmatic volatiles (Lentz et al., 2001; Crozaz et al., 2003).

Uranium and Th are critical for isotopic dating, as heat sources in the Martian mantle (Kiefer, 2003), and as highly incompatible trace elements (Fig. 11a). Their abundances are unusual in being depleted relative to La (i.e., U/La and Th/La are lower than CI), and that U is depleted relative to Th (i.e., U/Th is lower than CI). Abundances of U and Th are significantly lower than those of La, the most incompatible of the REEs (Fig. 11a). As U, Th, and La are all highly incompatible in igneous processes (e.g., Jones, 1995), simple igneous events would affect them similarly. The depletion in U and Th could reflect an earlier event which depleted the nakhlites' source mantle in highly incompatible elements, comparble to the genesis of mantle sources of terrestrial N-MORB (e.g., Hess, 1980; Sun and McDonough, 1989). Isotopic evidence also implies that the nakhlites' source mantle had been strongly depleted.

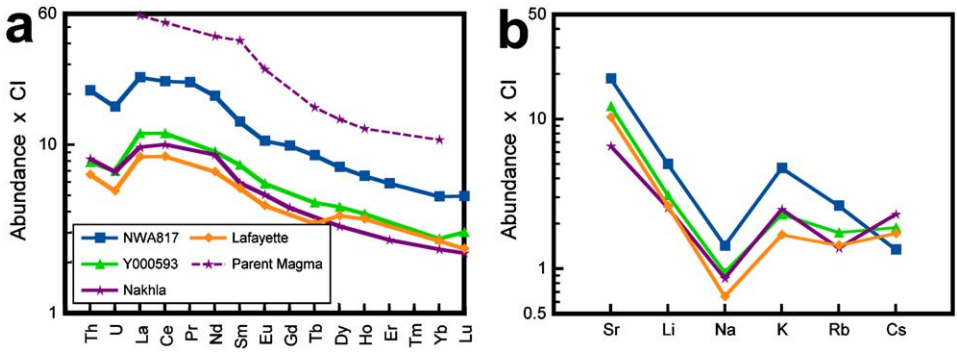

Fig. 11. Trace element abundances. (a) REE, U, and Th, and calculated parental magma composition. Data in Table 10. (b) Sr and alkali elements. Patterns are essentially parallel (except for Cs), with same relative abundances as the REE (a).

Table 10. Abundances of selected trace elements in Nakhlites

	Nakhla	G.V.[a]	Lafayette	NWA817	Y000593	MIL 03346
K	1162	996	950	3850	1300	2410
Rb	3.8	3.9	3.3	6.1	4	
Sr	59	55.8	80	145	95	106
Cs	0.39		0.32	0.25	0.35	
La	2.1		2.0	5.9	2.76	
Ce	5.9		5.3	14.7	7.23	
Nd	3.2	3.4	3.2	9.0	4.22	
Sm	0.77	0.76	0.79	1.97	1.09	
Eu	0.235		0.24	0.576	0.321	
Gd	0.86			1.96	1.1	
Tb	0.12		0.12	0.305	0.16	
Dy	0.77		0.93	1.81	0.99	
Yb	0.39		0.445	0.817	0.457	
Lu	0.055		0.059	0.121	0.074	
Hf	0.27		0.27	0.78	0.39	
Th	0.20		0.19	0.60	0.23	
U	0.052		0.043	0.136	0.056	
K/Rb	305	255	288	630	325	
Rb/Sr	0.064	0.069	0.041	0.042	0.042	
La/Lu	38		34	49	37	
Th/U	3.8		4.4	4.4	4.1	

Values in parts per million (ppm, or μg/g).
Nakhla: Lodders (1998), similar to Dreibus et al. (2003).
Governador Valadares: Bogard and Husain (1977), Shih et al. (1999).
Lafayette: Dreibus et al. (2003), similar to Lodders (1998).
NWA817: Sautter et al. (2002).
Y000593: Dreibus et al. (2003), average of Y000593 and Y000749; Gd from Oura et al. (2003).
MIL 03346: Anand et al. (2005a, b).
See original sources for uncertainties.
Gale data on Nakhla give Rb/Sr = 0.060, 0.069.
Shih et al. on Lafayette gives Rb/Sr = 0.037!!.
[a]G.V. – Governador Valadares.

Second, the nakhlites' Th/U abundance ratio is 4.0–4.4 ppm/ppm (Fig. 11a, Table 10), significantly higher than the CI value of 3.5 (Anders and Grevesse, 1989). This non-chondritic Th/U is indigenous, as it is seen in falls (Nakhla), hot desert finds (NWA817), and Antarctic finds (Y000593). In the Earth's mantle, melt extraction or other depletion events tend to leave Th more depleted than U, opposite to the nakhlites' ratio.

The alkali and alkaline earth elements (Fig. 11b) show some important trends. In the Martian meteorites, Na abundance correlates well with moderately incompatible elements like Ti, while abundances of the other alkalis correlate well with highly incompatible elements like La (Treiman et al., 1986; Treiman, 2003a). CI-normalized

abundances of Na are consistently below those of the other alkali elements, following the nakhlites strong enrichments in highly incompatible elements compared to moderately incompatible elements. Among these latter alkali elements, CI-normalized abundances decrease with increasing volatility (Longhi et al., 1992). All nakhlites have similar abundances of Li, consistent with a lack of water-induced mobilization and redistribution (Lentz et al., 2001). Interestingly, strontium has a CI-normalized abundance similar to that of highly incompatible elements (like La).

3.3. Organic matter

The nakhlites contain small quantities of organic carbon, ~90 to ~800 ppm (Wright et al., 1989; Jull et al., 2000). Much of the C is terrestrial; even in a pristine Nakhla fragment, live ^{14}C in the organics is approximately half the recent level (Jull et al., 1995, 2000). Much of Nakhla's organics are polymerized aromatic compounds (Flynn et al., 1999; Sephton et al., 2002), and its organics (~30 ppm in a pristine Nakhla fragment) are mostly pre-terrestrial (Jull et al., 2000). Nakhla contains a small load of terrestrial amino acids (Glavin et al., 1999).

4. Stable isotopes

4.1. Oxygen

The O isotope compositions of the igneous minerals of the nakhlites (bulk, pyroxene, olivine) are like in other SNC meteorites (Clayton and Mayeda, 1996; Franchi et al., 1999). The Martian meteorites have somewhat 'lighter' oxygen than terrestrial basaltic rocks ($\delta^{18}O = 4.3$–$5.2‰$ vs. 5–6‰ in nearly all Earth basalts; Clayton and Mayeda, 1996; Franchi et al., 1999; Eiler, 2001). Anhydrous silicates in the nakhlites have $\Delta^{17}O = +0.32‰$ (Clayton and Mayeda, 1996; Franchi et al., 1999) like other SNC meteorites, and distinct from the Earth ($\Delta^{17}O \equiv 0.00‰$), the moon, and other meteorite groups.

The O isotope composition of iddingsite is distinct. Lafayette iddingsite has $\Delta^{17}O = +1.45 \pm 0.12‰$ and $\delta^{18}O = +14.4 \pm 2‰$ (Romanek et al., 1998). Confusingly, water from the iddingsite has high $\Delta^{17}O$ ($+0.6‰$ for Lafayette; $+0.9‰$ for Nakhla), but $\delta^{18}O$ similar to the anhydrous silicates ($+5‰$ for Lafayette; $+4$–$6‰$ for Nakhla; Karlsson et al., 1992; Baker et al., 1998). The different $\Delta^{17}O$ values for the anhydrous and hydrous silicates were unexpected, as it had been thought that all the materials of a differentiated planet shared a common oxygen reservoir.

Oxygen in siderite in Nakhla's salt assemblage (by SIMS) is heavy, $\delta^{18}O \approx +34‰$ (Saxton et al., 2000a, b). Thermal decomposition of bulk samples gives similar values, $\delta^{18}O = \sim +30‰$ (Leshin et al., 1996; Farquhar and Thiemens, 2000). The bulk carbonate has $\Delta^{17}O = +1.0‰$, within uncertainty of that in the iddingsite water. Oxygen in Lafayette carbonate is less extreme, $\Delta^{17}O = +0.7‰$ (Farquhar and Thiemens, 2000), within uncertainty of the $\Delta^{17}O$ of Lafayette iddingsite.

Water-soluble sulfate in Nakhla, which could be in the iddingsite or salt assemblages, is distinct, at $\delta^{18}O = -3.7‰$ and $\Delta^{17}O = +1.3‰$ (Farquhar and Thiemens, 2000). Anhydrite from the salt assemblage has $\delta^{18}O = +7.4‰$ (Saxton et al., 1999).

4.2. Hydrogen

The nakhlites contain significant hydrogen, mostly associated with iddingsite (Leshin et al., 1996). Nakhla has ~130 ppm H (0.12 wt% H_2O); Governador Valadares has ~120 ppm H (0.11 wt% H_2O); and Lafayette has 420 ppm H (0.38 wt% H_2O). The H isotopic compositions of minerals and release fractions range from $\delta D = -280‰$ to $+900‰$. The lightest values are from NWA817, and their origins are not clear (Gillet et al., 2002; Boctor et al., 2003). The lightest H in other nakhlites, to $\delta D = -74‰$, is from low-temperature thermal extractions (<300 °C) and may represent terrestrial contamination (Leshin et al., 1996), possibly from exchange of interlayer water in smectite in the iddingsite. Heavier H (higher δD) is found in mineral separates and in high-temperature thermal releases. High-temperature thermal releases of Lafayette give δD to +900‰ (Leshin et al., 1996), with similar results for Nakhla and Governador Valadares. Siderite in Nakhla's salts has a high δD, possibly up to ~+1300‰ (Saxton et al., 2000b). These high δD values are reminiscent of the extreme values, to +4300‰, in minerals of other Martian meteorites (Watson et al., 1994) and of $\delta D \approx +4000‰$ in the Martian atmosphere (Bjoraker et al., 1989). However, minerals in the nakhlites have highly variable δD, and adjacent phases are generally not in equilibrium with respect to H isotopes (Saxton et al., 2000a, b; Boctor et al., 2003).

4.3. Carbon

Carbonate minerals are the sources of inorganic C in the nakhlites, except possibly from the highest temperature release fractions. Carbon in Nakhla's carbonate is heavy, at $\delta^{13}C = +15–50‰$ (Carr et al., 1985; Wright et al., 1989, 1992; Leshin et al., 1996; Jull et al., 1995, 2000). Lafayette and Governador Valadares, on the other hand, show little indication of ^{13}C enrichment (Wright et al., 1992; Leshin et al., 1996) despite having relatively large abundances of carbonate minerals.

Carbon released above 700 °C is commonly interpreted as magmatic, and it is light at $\delta^{13}C = \sim -30‰$ (Carr et al., 1985; Wright et al., 1992; Leshin et al., 1996; Jull et al., 2000). However, it is released with heavy O, $\delta^{18}O = \sim +30‰$ (Leshin et al., 1996), like nakhlite carbonate and unlike igneous silicates ($\delta^{18}O = \sim +5‰$). Possibly, some of this C is from small inclusions of carbonate protected in igneous minerals.

Much of the C in the nakhlites is organic, i.e., reduced species with carbon-carbon bonds. Nakhla's extra-terrestrial organics (no live ^{14}C) have $\delta^{13}C = -10‰$ to $-35‰$ (Wright et al., 1998; Jull et al., 2000), as do extracted organics of high molecular weight (Sephton et al., 2002).

4.4. Sulfur

Isotopic ratios of S in the nakhlites vary widely (Greenwood et al., 2000a, b). Pyrrhotite in Nakhla has $\delta^{34}S_{CDT}$ from –4.5‰ to +4.5‰, in Governador Valadares from –2.4‰ to +3.8‰, and in Lafayette from –6.1‰ to –0.1‰. The sole analysis of a sulfide grain that was protected from alteration gave $\delta^{34}S_{CDT} = -0.1‰$ – a bulk solar-system value. Pyrite in Lafayette appears to replace pyrrhotite, and spans essentially the same range of $\delta^{34}S_{CDT}$ (–4.8‰ to +0.1‰). Spot analyses of moderate sensitivity show no mass-independent fractionations (i.e., $\Delta^{33}S = 0 \pm 0.5‰$; Greenwood et al., 2000b). Bulk analyses at greater mass sensitivity do show mass-independent effects fractionations Nakhla pyrrhotite ($\Delta^{33}S = -0.18 \pm 0.01‰$, $\Delta^{36}S = +2.2 \pm 0.8‰$) but not in Lafayette (Farquhar and Thiemens, 2000).

4.5. Nitrogen and noble gases

Nitrogen and noble gases are inert, strongly partitioned into a gas phase, and complex in the nakhlites (Mathew and Marti, 2002). Nearly all available analyses are on Nakhla (Ott, 1988; Gilmour et al., 1999, 2001; Mathew and Marti, 2002), with a few of Lafayette, Governador Valadares, and Y000593 (Drake et al., 1995; Swindle et al., 2000; Okazaki et al., 2003). Abundances of light noble gases (He, Ne, Ar) in the nakhlites are dominated by radiogenic products and exogenous contributions. Indigenous N, Kr, and Xe, which are the focus here, are mixtures of several components (Table 11): current Martian atmosphere, Chas-S, Chas-E, and fractionated Martian atmosphere (Mathew and Marti, 2002).

The nakhlites contain trapped Martian atmosphere, as exemplified by gas in the shock glass of EETA79001 (Bogard and Johnson, 1983; Bogard and Garrison, 1998). Martian atmosphere is marked by excess ^{129}Xe, near-solar Kr, and very heavy N (Table 11) In Nakhla, this component is concentrated at grain boundaries, particularly in the mesostasis (Gilmour et al., 2001).

The Chas-S component, abundant in the Chassigny meteorite, has Xe isotope abundances like solar but strongly non-solar element abundance ratios (Table 11; Ott, 1988; Mathew and Marti, 2001). Chas-S represents a reservoir where Xe was not fractionated from iodine or plutonium while their short-lived radioisotopes were live (^{129}I yielding ^{129}Xe; ^{244}Pu yielding heavy Xe isotopes). Gilmour et al. (2001) suggest that this component is magmatic, and represents the mantle source of the nakhlites.

Chas-E, also defined from Chassigny, is like Chas-S but with greater abundances of heavy Xe isotopes and with heavier N (Table 11; Mathew and Marti, 2002). Its Xe isotopic signature is like Chas-S with Xe from fission of ^{244}Pu, but its element abundance ratios are different. This could arise by chemical fractionations from a Chas-S-like source after ^{129}I went extinct but while ^{244}Pu was still live. The Chas-E component in Nakhla is isotopically identical to Chas-E in Chassigny, but again has different element abundance ratios.

Finally, fractionated Martian atmosphere has a Xe isotopic composition like that of the current Martian atmosphere (i.e., high ^{129}Xe and $^{136}Xe/^{132}Xe$), but much

Table 11. Inert gas components in Nakhla and the solar system

	Chas-S Chassigny	Chas-E Chassigny	Chas-E Nakhla	Fract. Mars atmosphere	Mars atmosphere	Solar wind
$\delta^{15}N$	−30‰	+13‰	+13‰	∼+40‰	+620‰	< −240‰
$^{14}N/^{36}Ar_t$	4×10^7	8×10^5	3×10^7	1×10^6	8×10^3	24
$^{14}N/^{84}Kr$	2×10^8	2×10^7	4×10^8	2×10^7	$\sim 2 \times 10^5$	$\sim 1 \times 10^5$
$^{86}Kr/^{84}Kr$	0.3	–		–	∼0.3	0.303
$^{84}Kr/^{132}Xe$	1	2	4	4	20	12.5
$^{129}Xe/^{132}Xe$	1.05	1.05	1.05	2.4	2.6	1.05
$^{136}Xe/^{132}Xe$	0.295	0.32	0.32	0.347	0.345	0.297

Ratios are atomic. See text for descriptions of gas components. Compositions of components calculated from data in: Hashizume et al. (2000), Owen (1992), Mathew and Marti (2001, 2002), Treiman et al. (2000), Weiler and Baur (1994, 1995), Wimmer-Schweingruber (2002). Mars atmosphere and solar wind included for reference.

lower Kr/Xe and much higher N/Xe (Ott, 1988; Drake et al., 1995). This component was thought to be current Martian atmosphere fractionated through gas/water partitioning and associated with the iddingsite (aqueous alteration) material in the nakhlites. However, Gilmour et al. (1999, 2001) showed that this component is concentrated in pyroxene and along grain boundaries, and a scribe it to adsorbed atmosphere gas, fractionated during adsorption, and then implanted by shock.

4.6. Iron

Only a few analyses of isotope ratios for iron have been performed on Nakhla. Poitrasson et al. (2004) found that Nakhla (and other SNC meteorites) have $\delta^{56}Fe$ and $\delta^{57}Fe$ lower than Earth basalts by ∼ 0.1‰. On the other hand, Anand et al. (2005b) find iron isotope ratios in Nakhla (and other SNCs) are indistingishable from those of Earth basalts.

5. Geological history

What geological history could produce rocks with the characteristics of the nakhlites? Nearly all the data cited above can be explained within a seven-part framework:

(1) The nakhlites are igneous rocks, formed from basaltic magmas. The magmas had low Al_2O_3 contents, and were enriched in incompatible elements (e.g., U, Th, LREE). This composition requires that the nakhlites formed on a differentiated planetary body.

(2) The nakhlites are cumulate rocks, formed by accumulation of pyroxene and olivine in excess of their parent magmas' normal proportions. Thus, the bulk compositions of the nakhlites are not those of their parent magmas.
(3) After pyroxene and olivine had accumulated, the nakhlites experienced igneous and post-igneous processes to varying degrees, correlated with inferred cooling rates. MIL03346 cooled the fastest, with successively slower cooling (and thus greater modification) of NWA817, Y000593, Nakhla, Governador Valadares, Lafayette, and NWA998. Pyroxene and olivine continued to grow onto the cumulus crystal cores, yielding normally zoned rims. Magma may have percolated through the nakhlites, providing the elements needed for growth of the zoned rims. The crystals and magma continued to interact, both by chemical diffusion and replacement reactions. Eventually, the intercumulus magma crystallized, and its textures were strongly affected by the cooling rate. Some chemical reactions continued after the nakhlites solidified, mostly affecting iron oxide and sulfide minerals.
(4) After the nakhlites solidified they were infiltrated by liquid water. This water formed the alteration mineral assemblages by deposition of salt minerals, dissolution of olivine and silica-rich glass, and precipitation of iddingsite (smectite clays and hydrous iron oxides).
(5) All these events happened on Mars.
(6) The nakhlites were ejected from Mars by an impact event, and orbited the sun until their falls to Earth.
(7) On Earth, the nakhlites were affected by abiotic chemical interactions with their environments, by biological activities, and by human actions.

5.1. Basaltic igneous rocks

The nakhlites are igneous rocks, solidified from basaltic magma (Treiman, 2003b), although the composition of that magma is not certain. An igneous origin is dictated by their mineralogy, mineral chemistry, textures, and sequences of mineral formation. Their mineral chemistry and mineral zoning patterns are similar to those in terrestrial, lunar, and eucrite (asteroidal) basalts. The overall textures of the nakhlites are also similar to terrestrial basalts, as are their mesostasis textures. Similarly, minerals in the nakhlites contain multiphase, glass-bearing inclusions identical to those identified as magmatic inclusions in terrestrial basaltic rocks. Finally, rocks nearly identical to the nakhlites have been found on Earth, in geologic settings that are clearly volcanic and basaltic.

Early interpretations of the nakhlites relied on their mineralogic and textural similarities with terrestrial basaltic rocks. Their mineralogy is dominated by pyroxenes, olivine, plagioclase, and Fe–Ti oxides – as expected from basalt. Their overall texture, large crystals in fine-grained matrix, is typical of phenocrystic or porphyritic basalt. NWA817 and MIL03346 are exceptional in that their mesostases are mostly glassy (Sautter et al., 2002; Ant. Met. Bull., 2004) – a remnant of the basalt that fractionated among the large crystals. Mesostasis textures of the other

nakhlites are consistent with slower cooling of similar fractionated basaltic magma, with NWA998 having the texture of a typical diabase. Another texture consistent with an igneous origin is of low-Ca pyroxene replacing olivine, via the liquidus reaction Mg_2SiO_4(olivine) + SiO_2(magma) = 2 $MgSiO_3$(low-Ca pyroxene), see Morse (1980). Textural evidence of this reaction is clear in Lafayette and NWA998 (Fig. 6; Harvey and McSween, 1992a). The sequence of mineral appearance is consistent with crystallizing picritic basalt (Table 12).

The mineral chemistry of the nakhlites is consistent with mineral–basalt fractionations, affected variously by post-igneous equilibration. Augite is chemically zoned (except in Lafayette and NWA998) in a manner consistent with augite/basalt partition coefficients (Jones, 1995). Augite cores are magnesian, rich in compatible elements like Cr, and relatively poor in incompatible elements like Na, Ti, Al, REE, etc. Variations in abundances of minor elements (Al, Ti, REE) could arise from rapid, non-equilibrium crystal growth, and from the presence of small magmatic inclusions (Fig. 8). In NWA817 and MIL03346 (which experienced little late modification), the composition of the core olivines and augites are consistent with magmatic Fe–Mg equilibrium, based on natural equilibrated minerals and the experiments of Longhi and Pan (1989). Across their rim zones, augites become progressively depleted in compatible elements and progressively enriched incompatible elements (Fig. 3, Table 3). The relative elemental enrichments and depletions are consistent with mineral/basalt partition coefficients; e.g., $^{La}D_{augite/basalt} < {}^{Yb}D_{augite/basalt}$, and La becomes more enriched than Yb (e.g., Oe et al., 2002). Olivine in NWA817 and Y000593 is similarly zoned: magnesian cores, and rim zones progressively enriched in incompatible elements like Fe and Ca (Fig. 5).

As in terrestrial basaltic rocks, olivines and augites in the nakhlites contain multiphase, glass-bearing magmatic inclusions (Fig. 8) – remnants of magma trapped in growing mineral grains (Harvey and McSween, 1992b; Treiman, 1993). Similar multiphase inclusions are known in many terrestrial and lunar basalts (Roeder and Weiblen, 1977; Roeder, 1979).

These lines of evidence converge in a few terrestrial rocks that are eerily similar to the nakhlites. The best known of these are in the Archaean-age Theo's Flow complex, Munro Township, Ontario (Arndt, 1977; Friedman-Lentz et al., 1999).

Table 12. Crystallization sequences of nakhlites

Aug
Aug + Ol
Aug + Ol + TiMt
Aug + Ol + TiMt + Pl
Ol + TiMt + Pl + Pig/OPX
Ol + TiMt + Pl + Pig/OPX + Il
(Ol +) TiMt + Pl + Pig/OPX + Il + Sil + Ap

Aug – augite; Ol – olivine; Ti–Mg – titanomagnetite; Pl – plagioclase; Pig/OPX – pigeonite and/or orthopyroxene; Il – ilmenite; Sil – silica; Ap – chlor-apatite.

Theo's Flow is a differentiated basaltic body; its lower third was augite-olivine cumulate rock (original olivine is now serpentine) strikingly similar to the nakhlites (Friedman-Lentz et al., 1999). Its cumulus augite grains have homogeneous cores with small multiphase inclusions of glass, pyroxene, and opaques (Treiman, 2003b); the rims of the augite grains are normally zoned to very ferroan compositions. The large olivine grains, replaced by serpentine and calcite, contained ellipsoidal multiphase magmatic inclusions. Among the augites and original olivine grains was a fine-grained mesostasis (now altered to phyllosilicates) marked originally by elongated laths of plagioclase. There is no doubt that Theo's Flow is an igneous body, and thus that its nakhlite look-alike rocks are also igneous. Terrestrial analogs to the nakhlites occur sparsely in other Archaean greenstone belts, including those on the Kola Peninsula, Russia (Hanski, 1992), and in Minnesota, USA (Berkley and Himmelberg, 1978).

5.2. Cumulate igneous rocks

The nakhlites are considered cumulates because they are derived from basaltic magma, but are too rich in crystals and too depleted in incompatible (magmaphile) elements to represent magma themselves (Bunch and Reid, 1975). The nakhlites contain ~75% augite (Table 2), which is much more than any known basalt. The nakhlite contain ~1.5–3.5% Al_2O_3, while their inferred parent magmas contain 6–9% Al_2O_3 (Tables 5 and 13). Similarly, the nakhlites themselves contain 9–25 × CI abundances of La, while their inferred parent magma contains La at 40–60 × CI (Fig. 11, Table 10; Wadhwa and Crozaz, 1995).

Texturally, nakhlites are also similar to terrestrial basaltic cumulates, especially rapidly cooled cumulates like those in lava lakes or thick flows (e.g., Wager and Brown, 1967; Arndt, 1977; Wright and Okamura, 1977; Wright and Peck, 1978). These tend to contain euhedral to subhedral crystals in a fine-grained or glassy matrix. Commonly, these crystals show a preferred orientation, with their long axes somewhat aligned from magma flow, as are the nakhlite augites (Berkley et al., 1980). Finally, the nakhlites are texturally and compositionally similar to undoubted cumulate rock on Earth – pyroxenite of the Theo's Flow complex (Arndt, 1977; Friedman-Lentz et al., 1999). Theo's Flow is a differentiated basaltic body, with a basal dunite (now serpentinite), pyroxenite, gabbro, and a quench-textured brecciated flow top. The composition of the flow top matches that of the whole flow, implying that the flow differentiated in place and that the pyroxenite is a cumulate (Arndt, 1977).

Because the nakhlites are cumulates, the compositions of their parent magma(s) must be inferred indirectly. Estimates of the composition of Nakhla's parent magma have been based on: mass balance among bulk and mineral compositions (Treiman, 1986); augite/basalt partition coefficients (Longhi and Pan, 1989; Treiman, 1993); magmatic inclusions in olivines, constrained by phase equilibria (Harvey and McSween, 1992b; Treiman, 1993); magmatic inclusions in augites (Stockstill et al., 2001); and experiments to duplicate the compositions of augite cores (Kaneda et al.,

Table 13. Proposed nakhlite parent magmas

	NK01	HC	N′	NK93	NK3
SiO_2	49.8	49.75	50.5	50.2	45.8
TiO_2	0.8	0.80	1.4	1.0	3.1
Al_2O_3	7.5	5.73	6.8	8.6	7.2
Cr_2O_3	0.1	0.05	0.1	0.1	–
FeO	22.3	22.96	21.9	19.1	26.2
MnO	0.5	0.58	0.4	0.4	–
MgO	4.6	4.56	4.3	4.0	5.7
CaO	10.4	12.22	13.0	11.9	10.4
Na_2O	1.1	1.00	1.2	1.2	0.8
K_2O	2.4	1.04	0.3	2.6	1.4
P_2O_5	0.6	0.17	–	0.7	–
CIPW norm					
Q	0	0	1.8	0	0
Or	14.2	6.2	1.8	15.4	8.3
Ab	9.3	8.6	10.2	10.2	6.8
An	8.4	8.2	12.3	10.4	11.9
Di	33.8	44.9	45.0	38.0	34.0
Hy	21.4	28.6	26.1	15.5	14.3
Ol	9.9	1.6	0	6.9	20.0
Il	1.5	1.5	2.7	1.9	5.9
Chr	0.2	0.1	0.2	0.2	–
Ap	1.39	0.4	–	1.6	–
Mg′ %	27	26	27	28	28

NK01 – Treiman and Goodrich (2001).
HC – Kaneda et al. (1998).
N′: NK93 – Treiman (1993).
NK3 – Harvey and McSween (1992a, b).

1998). These inferred parent magmas span a fairly small range of compositions (Table 13), although none is consistent with all constraints.

A critical issue in interpreting the nakhlites is how many magmas were involved in their origins – both whether an individual nakhlite represents a single magma, and whether all the nakhlites formed from the same parent magma.

There are no compelling data to suggest that the nakhlites represent multiple magmatic sources, despite perceived complexities in the nakhlites which could imply multiple magmas. Berkley et al. (1980) suggested that the intercumulus liquid in the nakhlites was not closely related to the cumulus augites, but Wadhwa and Crozaz (1995) showed that the augites and intercumulus liquid were cogenetic (Wadhwa and Crozaz, 1995). Treiman (1990) suggested that the large olivine and augite crystals of Nakhla, having cores out of Mg′ equilibrium, must have formed in different magmas. Longhi and Pan (1989) showed that the olivine cores exchanged Fe and Mg

with the evolving magma, and originally were in Mg′ equilibrium. Varela et al. (2001) suggested that the glassy inclusions in Nakhla augites represented multiple magmas or other complex formation mechanisms; Treiman (2003b) showed that similar glassy inclusions are found in simple, monogenetic basalts.

Available data are mostly consistent with the nakhlites being co-magmatic or co-genetic – either from the same igneous event or from very similar magmas emplaced nearly simultaneously. Wadhwa and Crozaz (1995) suggested that some nakhlites were more evolved than others because their core augite compositions had different abundances of minor elements Ti, Y, REE, etc. However, compositional ranges of core augites in a single nakhlite are similar to those reported between different nakhlites, consistent again with formation from a single magma. Similarly, stable and radiogenic isotope data are mostly consistent with the nakhlites forming from a single magma. The nakhlites share the same crystallization age, 1.3 Ga, within analytical uncertainties (Table 14). Initial isotopic ratios (at 1.3 Ga) are a sensitive test for co-genetic magmas, and available data are probably consistent with a single magmatic source (Table 15). It is possible that Nakhla and Governador Valadares

Table 14. Igneous crystallization ages for nakhlites – in Ga (10^9 years before present)

	^{39}Ar–^{40}Ar	^{87}Rb–^{87}Sr	^{143}Sm–^{147}Nd	U–Th–Pb	^{176}Lu–^{176}Hf	^{187}Re–^{187}Os
Nakhla	1.3[a] 1.328±0.008	1.23±0.01 1.30±0.02 1.36±0.02	1.26±0.07	1.28±0.05 1.24±0.11 1.233±0.008	–	1.4±0.1[b]
Governador Valadares	1.32±0.04	1.32±0.01	1.37±0.02	–	–	–
Lafayette	1.34±0.03 1.322±0.010	1.25±0.08	1.32±0.05	1.15±0.34	–	1.4±0.1[b]
NWA817	1.35[a]			–	–	–
Y000593	1.24±0.22	1.30±0.02 1.27±0.24	1.31±0.03	–	–	–
NWA998	1.33±0.01	–	1.29±0.05	–	1.54±0.3	–

Based on the review of Nyquist et al. (2001). Unless otherwise noted, data from sources cited there.
Nakhla: Ar–Ar: Swindle and Olson (2004); Precise U–Th–Pb: Chen and Wasserburg (1986); Re–Os: Brandon et al. (2000); Walker et al. (2002).
Lafayette: Swindle and Olson (2004); U–Th–Pb: on apatite Terada et al. (2002); Re–Os: Brandon et al. (2000); Walker et al. (2002).
NWA 817: K–Ar age from Marty and Marti (2001), Mathew et al. (2003).
Y000593: K–Ar: Okazaki et al. (2003); Rb–Sr and Sm–Nd: Misawa et al. (2003a, b) and Shih et al. (2002).
NWA 998: Ar–Ar: Garrison and Bogard (2005); Sam–Nd and Lu–Hf: Carlson and Irving (2004).
[a]K–Ar age.
[b]Whole rock isochron based on nakhla, lafayette and chassigny.

Table 15. Intital isotope ratios at ~1.3 Ga (10^9 years before present)

	$^{87}Sr/^{86}Sr_i$	$\varepsilon^{143}Nd_i$
Nakhla	0.70232 ± 0.6	
	0.70254 ± 0.3	
		+16.8 ± 1.4
		+16.4
Governador Valadares	0.70236 ± 0.1	+16.7 ± 0.4
Lafayette	0.70260 ± 4.0	+16.3 ± 0.4
Y000593	0.70251 ± 3.8	
	0.70253 ± 0.3	+15.7 ± 0.2
NWA998	0.7024	+15.3 ± 0.9[a]
		+11.9[b]

Nakhla: Data, in order, from Papanastassiou and Wasserburg (1974), Gale et al. (1975), Nakamura et al. (1982), Jagoutz and Jotter (2000).
Governador Valadares: Shih et al. (1999).
Lafayette: Shih et al. (1998).
Y000593: Data, in order, from Namamura et al. (2002) and Misawa et al. (2003b).
NWA 998: Carlson and Irving (2004).
[a]Isochron among pyroxenes, plagioclase, and magnetite.
[b]Isochron between olivine and a leach fraction.

have different Sr isotopic initials, and possible that Y000593 has a different Nd isotopic initial than Governador Valadares and Lafayette (Table 15). Nd–Sm data for these last three were all taken by the same laboratory, and the Yamato Nd initial is outside the 2σ uncertainty limits of the others.

The parent magmas of the nakhlites were basaltic, rich in calcium, and poor in alumina compared to common terrestrial magmas. Estimates of parent magma compositions (Table 13) are quite similar considering that they were derived by several different methods: element partitioning, experimental petrology, and analyses of magmatic inclusions. Most of the compositions are olivine-normative, which seems reasonable for magma that formed so much olivine and so little silica.

The Mg′ values for all the magma compositions (Table 13) come from the compositions of the augite cores and Fe/Mg partitioning coefficients for augite and basalt magma. Augite pyroxene cores of Mg′ = 63% (Fig. 3b, Table 3) would be in equilibrium with basalt magma of Mg′ = 27% (Treiman, 1986, 1993; Longhi and Pan, 1989; Harvey and McSween, 1992b). This Mg′ value would have been in equilibrium with olivine of Mg′ ≈ 45% (see core olivine composition for NWA817 and MIL03346; Table 4, Fig. 5a), which is significantly lower than estimates of the Martian mantle composition (e.g., Longhi et al., 1992; Ghosal et al., 1998). Thus, the nakhlites' parent magma was not a primitive mantle product.

The major differences among these estimates of nakhlite parent magma compositions (Table 13) are in Na and K. The nakhlites themselves and their intercumulus mesostases have $Na_2O > K_2O$ (Table 5, Berkley et al., 1980; Treiman,

1986), which should imply parent magmas with $Na_2O > K_2O$. However, magmatic inclusions in olivine and parent magma compositions estimated from them have $Na_2O < K_2O$ (NN01, NK93, NK3; Table 13). The source of this disagreement is not clear.

The volatile contents of nakhlite parent magmas are not known. The vapor bubbles in magmatic inclusions suggest a significant proportion of volatiles (Figs. 8a and b; Varela et al., 2001; Treiman, 2003a, b), and there is one report of a liquid-gas inclusion in Nakhla (Bodnar, 1998). Lentz et al. (2001) found no evidence that magmatic water was lost, based on their analyses of Li, B, and Be in augites. The H contents of the parent magmas were low. The nakhlites contain no magmatic minerals with essential hydrogen – even their apatite is chlorine-rich with little hydrogen. Magmatic inclusions in olivine contain no amphibole or biotite, unlike those in Chassigny (Floran et al., 1978; Watson et al., 1994). Magmatic inclusions in pyroxene contain no amphibole, unlike those in the shergottites (Treiman, 1985).

The REE composition of Nakhla's parent magma (Fig. 11) was estimated from SIMS analyses of augite cores and augite/basalt partition coefficients (Wadhwa and Crozaz, 1995). The calculated magma composition relies on use of appropriate partition coefficients, but is certainly enriched in LREE, with $La \approx 40–60 \times CI$ and $Yb \approx 10 \times CI$, paralleling Nakhla itself (Fig. 11).

The oxygen fugacity of the parent magma is poorly known. Coexisting Fe–Ti oxides give $f(O_2)$ near the fayalite–magnetite–quartz buffer (FMQ), but at submagmatic temperatures near 800 °C (Szymanski et al., 2003). Earlier estimates gave $f(O_2)$ orders of magnitude lower (Reid and Bunch, 1975; Delano and Arculus, 1980).

The O isotopic composition of the nakhlite parent magma had $\Delta^{17}O = +0.32‰$ (like the bulk), and $\delta^{18}O \approx +5.1‰$ as calculated from the olivine composition and the olivine–basalt fractionation factor (Clayton and Mayeda, 1996; Franchi et al., 1999; Eiler, 2001). Magmatic S probably had $\delta^{34}S_{CDT} \approx 0‰$ (Greenwood et al., 2000a). The H isotope composition is poorly known, and probably between $\delta D = 0‰$ and $-1500‰$ (e.g., Jakosky and Jones, 1997; Boctor et al., 2003). Magmatic C may have $\delta^{13}C \approx -30‰$. Noble gases and nitrogen would be like Chas-E and/or Chas-S (Table 11).

The proportion of intercumulus melt in a nakhlite can be estimated by mass balance from the REE compositions of the bulk meteorite and its inferred parent magma as derived from the REE content its core augite (Wadhwa and Crozaz, 1995). For Nakhla, this calculation suggests 15–25% intercumulus magma (Fig. 11), consistent with the measured proportion of mesostasis (Table 2) and the certainty that some rim augite and olivine grew from the intercumulus magma. The same calculation for other nakhlites is problematic because the REE contents of their core augites may be different from Nakhla's (Wadhwa and Crozaz, 2003). Assuming that the nakhlites had a parent magma like that of Nakhla, then Lafayette and Y000593 contained 15–30% intercumulus magma, and NWA817 contained ~45–65% intercumulus magma (see Fig. 1). These values are fairly consistent with the proportions of mesostases in the nakhlites (Table 2) and with the major element compositions of the nakhlites (Tables 5 and 13).

5.3. Post-accumulation effects

Although the nakhlites have nearly identical mineralogies and compositions, they are different in the zoning of their minerals, mesostasis textures, and extent of mineral replacement/reaction textures. These contrasts arose in late- and post-magmatic processes. After the nakhlite cumulates formed, their magmas deposited overgrowths onto the large augites and olivines, and thereby evolved to more ferroan compositions. The overgrowths were normally zoned: increasingly ferroan, enriched in incompatible elements (e.g., Ti, REE), and depleted in compatible elements (e.g., Cr). Simultaneously, and continuing after crystallization was complete, chemical diffusion among minerals and melt subdued these compositional gradients, and chemical reactions erased the original minerals. Olivine and augite grains continued to grow from the (now) intercumulus magma. The olivines show this continued growth most clearly in their poikilitic textures (Figs. 4b and 8a), and in normally zoned rims preserved in NWA817, Y000593, and MIL03346 (Figs. 4a and 5). In the other nakhlites, cation diffusion in olivine and interdiffusion with magma have softened or erased the zoning.

The intercumulus magma deposited normally zoned overgrowths onto cumulus augites: increasingly ferroan, enriched in incompatible elements (e.g., Ti, REE), and depleted in compatible elements (e.g., Cr). Chemical zoning is most extreme in NWA817 and MIL03346, where large augites have cores of $Mg' = 64\%$ and rims to $Mg' \sim 10\%$ (Fig. 3). Large augites in the other nakhlites show smaller ranges of Mg', and the minimum Mg' of the augite appears to coincide with transition to lower-Ca pyroxene (Fig. 3a). This change may signal the crystallization of magnetite and plagioclase, as these lower-Ca, lower-Mg pyroxenes also have low Al and Ti. Crystallization of magnetite would limit Fe-enrichment in the intercumulus melt, and therefore in the pyroxenes. Crystallization of plagioclase would deplete the intercumulus melt of Ca, and allow formation of low-Ca pyroxene. But why would magnetite and plagioclase crystallize at different augite Mg' in the different nakhlites? A reasonable answer is cooling rate – under fast cooling, nucleation of these minerals may be delayed long after the point expected in equilibrium crystallization. In this view, the average cooling rates of the nakhlites can be ordered, from fastest to slowest, as: MIL03346 > NWA817 > Y000593 > Nakhla ≈ Governador Valadares > Lafayette > NWA998.

Texturally, the grain size distributions of nakhlite augites show deficiencies in the smallest grains, compared to that expected from continuous nucleation and growth (Friedman-Lentz et al., 1999). The order of deficits of smallest grains is MIL03346 > Y000593 > Governador Valadares > Nakhla > NWA998 > Lafayette (Lentz and McSween, 2003; Stopar et al., 2005). This order is consistent with that of cooling rates above, and so reasonably represent diminished nucleation rates associated with rapid cooling.

A critical question for understanding the nakhlites is whether they represent closed chemical systems, or whether they were affected by significant movement of magma after accumulation of their large olivines and augites, i.e., magma metasomatism (e.g., Irvine, 1980; Boudreau and McCallum, 1992). Berkley et al. (1980) suggested

that magma metasomatism was responsible for the low Mg′ of the olivines, but that is now ascribed to diffusive re-equilibration (Longhi and Pan, 1989). The importance of magma metasomatism remains unclear, especially in light of evidence for magma metasomatism in Theo's Flow (Friedman-Lentz et al., 1999). Treiman (1993) argued that Nakhla had been affected by magma metasomatism, because the magma composition he inferred from magmatic inclusions was far from those predicted by mass balance if Nakhla had been a closed system. His proposed magma composition (and in fact all others, Table 13), has too little normative orthopyroxene to be consistent with simple mass balance, however the calculation may be flawed because it ignored ferric iron. On the other hand, Wadhwa and Crozaz (1995) inferred that infiltration metasomatism was not significant for Nakhla. They found that the REE abundances of Nakhla bulk were adequately modeled by cumulus augite and olivine plus ~25% magma. This calculation depends critically on the REE partition coefficients, which in turn depend greatly on magma Al_2O_3. This value is generally consistent with mass-balance constraints, i.e., on Al_2O_3 abundances. Taking average Al_2O_3 in parental magma, bulk Nakhla, and augite cores as ~7%, ~1.6%, and ~0.7% respectively (Tables 3, 5 and 13), and assuming that 5% of Nakhla is cumulus olivine (not crucial), then Nakhla contained ~15% parental magma. This 15–25% intercumulus magma are consistent with modal abundances of mesostasis or glass in the most rapidly cooled nakhlites, NWA817 and MIL03346 (Table 2).

On the other hand, petrography suggests rather more intercumulus magma. In Nakhla, original intercumulus magma would be represented now by mesostasis, overgrowth augite, and overgrowth olivine. Nakhla contains ~8.5% mesostasis (Table 2). Of its 81% augite, ~35% is overgrowth (Fig. 2) implying that ~28% of Nakhla is augite grown from intercumulus magma. Nakhla is 10% olivine, but the proportion of overgrowth is unknown because the olivine is effectively unzoned; taking 35% of that as overgrowth is reasonable considering the poikilitic texture of the olivine (Figs. 4b and 8a). Summing these values, Nakhla would have contained ~40% intercumulus magma. REE and Al_2O_3 abundances suggest much less intercumulus magma, and this mismatch in could readily arise from magma metasomatism.

Olivine in all nakhlites must have been zoned originally, as is the magmatic augite, but the zoning was subdued by chemical diffusion within grains and with their environment (Fe–Mg interdiffusion in olivine is orders of magnitude faster than in augite). The differences in olivine zoning profiles and in core compositions can be explained by differences in cooling rate. The difference between the Mg′ values of the olivines' cores and rims represents the chemical gradient remaining in the olivine after complete cooling – longer time-at-temperature would yield a smaller difference. Ordered by olivine chemical gradient, the nakhlites are: NWA817 > MIL03346 > Y000593 > Nakhla > Governador Valadares > Lafayette > NWA998 (Fig. 5a). One can also compare the olivines' core composition, which represent larger-scale equilibria; that sequence, from most magnesian (least equilibrated) to most ferroan, is: NWA817 > MIL03346 > Y000593 > Nakhla ≈ Governador Valadares > NWA998 > Lafayette (Fig. 5a). These sequences are nearly the same,

and nearly identical to the sequence of cooling rates inferred from pyroxene zoning and from mesostasis texture.

Crystallization of basalt magma can induce chemical reactions among crystallized minerals and the remaining magma, and the nakhlites show evidence for two such reactions. Orthopyroxene rims and replaces olivine in Lafayette, Nakhla, and NWA998, (Figs. 6b and c; Fig. 7 of Harvey and McSween, 1992a), which suggest the peritectic reaction 'olivine + melt ⇒ orthopyroxene' (Morse, 1980). Textures from this reaction have not been reported in the other nakhlites; perhaps they cooled too fast for the peritectic reaction textures to be recognizable.

An unusual texture, especially prominent in Nakhla, is of ferroan augite replacing magnesian augite – patches and bands of homogenous ferroan augite around and within large augite grains (Fig. 2c). Similar textures occur in other nakhlites (rarely in NWA817 and not in MIL03346). The replacement augite is rich in Al and Ti like the normal augite rims, so it likely represents reaction with the intercumulus magma. The chemical process for this replacement is not clear.

The intercumulus magma crystallized to form mesostasis. Only in MIL03346 and NWA817 is abundant glass preserved. Mesostases, except in NWA998 and MIL03346, contain lath-shaped plagioclase crystals, which imply rapid cooling (e.g., p. 79 of Philpotts, 1989). Experimental studies of basalt crystallization show that faster cooling produces thinner plagioclase laths (Grove, 1978; Table 6 of Lofgren, 1983). Thus, one may correlate widths of plagioclase laths (Table 6) with cooling rate, yielding, from fastest to slowest: NWA817 > Y000593 > Nakhla ≈ Governador Valadares > Lafayette. MIL03346 cooled faster than these, as its mesostasis contains spinifex olivine. NWA998 cooled the slowest of all, as its plagioclase crystals are blocky and not lath-shaped. This order of cooling rates is the same as inferred from mineral chemical zoning.

Chemical reactions continued after complete crystallization. Chemical diffusion must have continued, although its effects in silicates may be negligible because of slow diffusion rates. Iron-titanium oxide minerals equilibrated to subsolidus temperatures – Fe–Ti oxide thermo-barometry for Nakhla and Y000593 give temperatures of ~800 °C (far subsolidus), and oxygen fugacities near FMQ (Szymanski et al., 2003). Iron and sulfur were also mobile in the post-magmatic history, probably with external influences. Pyrite formed below 743 °C, in part by replacement of pyrrhotite (Greenwood et al., 2000a). Nearly all pyrite and pyrrhotite show significant exchange of S isotopes with external reservoirs (Greenwood et al., 2000a, b; Farquhar and Thiemens, 2000). The iron-enriched veinlets crossing pyroxene imply that iron was mobile in the subsolidus, possibly in an Fe–S fluid (Schwartz et al., 2003).

5.4. Aqueous alteration

Alteration assemblages in the nakhlites represent rock-water interactions, mostly on Mars. Nakhla's short exposure to the terrestrial environment suggests that its aqueous alterations are pre-terrestrial (Reid and Bunch, 1975; Bridges and Grady, 1999, 2000). In most nakhlites, the iddingsite assemblage is clearly pre-terrestrial,

being dehydrated and melted at fusion crusts (Fig. 9f. Nakhla: Gooding et al., 1991; Lafayette, Treiman et al., 1993; Y000593, Treiman and Goodrich, 2002). Similarly, iddingsite veinlets in Nakhla are offset by microfaults, which bespeak stronger deformation than could have occurred on Earth (Gooding et al., 1991). Stable and radioisotope data also imply pre-terrestrial origins. Iddingsite O has non-terrestrial isotope ratios ($\Delta^{17}O \sim +1‰$; Romanek et al., 1998). Hydrogen from Lafayette iddingsite is extreme by terrestrial standards, δD to $\sim +1500‰$ (Saxton et al., 2000b). The iddingsite formed at ~620 Ma, long before their falls to Earth. In the salt assemblage, siderite has $\delta^{18}O = +33.8‰$ (Saxton et al., 2000a), unusually high for terrestrial materials. Carbon isotope ratios for carbonate in the nakhlites are heavy, $\delta^{13}C = +10 - +55‰$ (Wright et al., 1992; Romanek et al., 1998; Jull et al., 1995); at the upper end, these values are extreme for the Earth.

The salt assemblage has been ascribed to evaporite solutions (Bridges and Grady, 2000; Bridges et al., 2001), similar a playa-like environment like that inferred by some for alteration of ALH84001 (McSween and Harvey, 1998; Warren, 1998).

The iddingsite formed below 500 °C (Gooding et al., 1991; Gillet et al., 2002), and most likely between 100 and 50 °C (Treiman et al., 1993). Unlike most terrestrial 'iddingsite,' it did not form by epitaxial or topotaxial replacement of olivine (e.g., Smith et al., 1987) because the lattice planes of its smectite are not parallel to those of the olivine (Fig. 9c). Rather, it was deposited into open cavities in the rock where igneous minerals had been dissolved out (Figs. 9d and e) – a koiloaltermorph texture (Delvigne, 1998). These dissolution cavities were filled by precipitation of salt minerals, hydrous silicates, and hydrous iron oxides (Gooding et al., 1991) – holo-altermorph or cumuluo-alteromorph textures (Delvigne, 1998).

The compositions of the iddingsite retain some characteristics of its local site; iddingsite in olivine has nearly no Al, and iddingsite in mesostasis areas is relatively rich in Al (Treiman et al., 1993; Gillet et al., 2002). However, much of the chemistry is controlled externally, including the Fe/Mg ratio, the REE abundances, the REE pattern, and the O isotope ratios. In Lafayette and Nakhla, iddingsite is more magnesian than its host olivine or mesostasis, while that in NWA817 is more ferroan that its hosts (Gooding et al., 1991; Treiman et al., 1993; Gillet et al., 2002). Iddingsite in Lafayette has nearly no detectable REE (Treiman and Lindstrom, 1997), while that in NWA817 has variable LREE enrichment with variable positive Eu anomalies (Gillet et al., 2002).

Treiman et al. (1993) suggested that the iddingsite formed by dissolution, short-range chemical transport and precipitation, so that its composition was effectively olivine + mesostasis + water. This model does not explain Fe/Mg and REE in the iddingsite (Treiman and Lindstrom, 1997; Gillet et al., 2002); other components must be dissolved into the water, but the variability of the iddingsite REE composition in NWA817 still suggests that chemical transport was fairly limited. Treiman and Lindstrom (1997) suggested that iddingsite was deposited originally as gel, which then transformed to crystalline smectite; however, this mechanism would not yield the banded smectite/Fe-oxy-hydroxide masses in Lafayette and Y000593 (Figs. 9d and e).

The isotopic character of the iddingsite-forming water is not clear. Hydrogen in iddingsite in Lafayette, Nakhla, and Governador Valadares is quite heavy, with $\delta D > +800‰$ (Leshin et al., 1996), whereas in NWA817 it is extraordinarily light, $\delta D = -170‰$ (Gillet et al., 2002). So, did nearly identical iddingsite in different nakhlites involve completely different waters, or could H in the iddingsite have exchanged extensively? Oxygen is equally confusing. Iddingsite in Lafayette has $\Delta^{17}O$ much greater than that for the anhydrous silicates, which suggests an exogenous (extra-Martian?) source for its water (Karlsson et al., 1992; Romanek et al., 1998). However, the $\delta^{18}O$ of this O uncertain – is it +5‰ (Karlsson et al., 1992) or +15‰ (Romanek et al., 1998)?

5.5. Origin on Mars

Many lines of evidence suggest that the nakhlites (N) and several other meteorite groups [the shergottites (S) and chassignite (C), collectively called SNCs] with similar geochemistry formed on the planet Mars (Treiman et al., 2000). The most crucial evidence is that several of these meteorites contain a gas component that is identical (within analytical uncertainty) to the Martian atmosphere analyzed on Mars by the Viking landers (Bogard and Johnson, 1983; Weins et al., 1986; Bogard and Garrison, 1998). Implicit in this comparison are the observations that the nakhlites came from a planet with an atmosphere, and that its atmosphere experienced strong mass-dependent fractionations (Treiman et al., 2000). In bulk chemical composition, the nakhlites and these other meteorite groups share several important geochemical parameters with rock and soil analyses from Mars: Fe/Mn, Cr vs. Mg/(Mg + Fe), Na/Al, and oxidation state. The nakhlites' formation ages are near 1.3 Ga, consistent with formation on a large active planet. Similarly, the spread of ages among the nakhlites and other Martian meteorites, 4.5 Ga for ALH84001 to 0.17 Ga for Zagami, are consistent with formation on a planet with preserved ancient surfaces and active volcanism. The aqueous alteration of the nakhlites implies that their parent planet had active groundwater at ~620 m.y. Together, all these lines of evidence point to Mars as the only reasonable source of the nakhlites.

5.6. From Mars to Earth

If the nakhlites formed on Mars, they must have been removed from Mars and traveled to Earth. Only asteroid impacts can generate enough energy to propel a rock to escape speed for Mars, ~5 km/s. Questions about the physics and mechanics or ejecting rocks from Mars have been resolved – the rocks were ejected as impact spalls from near the ground surface (Head et al., 2002). In the nakhlites, petrologic effects of this impact are minor: brecciation (Fig. 10), undulatory extinction in minerals, twinning in pyroxene (Fig. 10), and micro-faulting (Gooding et al., 1991). The extent of undulatory extinction and the lack of maskelynite imply bulk shock pressures $< \sim 15$ GPa (Stöffler et al., 1991; Greshake et al., 2004). The brecciation suggests rapid deformation (Spry, 1969; Spray, 1998;

van der Bogert et al., 2004). The chemical consequences of ejection have been minor, probably limited to entrapment of atmospheric gases on grain boundaries (Gilmour et al., 1999, 2001).

After the nakhlites' precursors were ejected from Mars, orbital perturbations and collisions with other meteoroids in space modified their orbits to cross the Earth's on timescales consistent with their cosmic-ray exposure ages (Gladman, 1997). These transits through space probably had few effects beyond production of CRE nuclides.

5.7. Terrestrial effects

The effects of human collection, museum curation, and sample treatment are poorly described and understood. For instance, the find of indigenous halite (NaCl) in Nakhla (Bridges and Grady, 1999) was only possible because thin sections were prepared without water. Similarly, one neutron activation analysis of a fragment of Lafayette iddingsite contained ~350 ppm Hg (Treiman and Lindstrom, 1997) – this huge excess probably represents human-induced contamination.

5.8. A dissenting interpretation

Recently, Varela et al. (2001, 2003) suggested that this whole 'standard interpretation' of Nakhla (and by extension all nakhlites) is incorrect. They argued that Nakhla is an agglomeration of non-igneous mineral grains from several sources, likely to be primitive chondritic materials unrelated to Mars. The foundation of this idea is that Nakhla's augite grains contain glassy inclusions (Figs. 8c and d), in which the glasses show a significant range of compositions. To Varela et al., this lack of a single glass composition implies that the augites could not have formed from a single parent magma, and thus could not be igneous. Further, they invoke isotopic heterogeneities (N, H, and C) as inconsistent with an igneous history, and infer that Nakhla (and other nakhlites) are agglomerations of unrelated mineral grains, formed in the solid state, and probably related to carbonaceous chondrites, and likely not from Mars.

Treiman (2003b) rebutted this hypothesis and ascribed variability in compositions of magmatic inclusions in augite to processes in their formation: boundary layers, entrapment of solids, liquid immiscibility, necking of entrapped inclusions, and the undocumented processes that produce bizarre inclusions in the minerals of undoubted igneous rocks (e.g., Roeder and Weiblen, 1977; Roeder, 1979; Bacon, 1989). Some of the isotopic heterogeneities invoked by Varela et al. (2001, 2003) are seen in Martian basalt meteorites (shergottites), and appear characteristic of Mars; others arise from comparing igneous minerals (augite, olivine) with later aqueous alterations and deposits (siderite, anhydrite).

Thus, I find no merit in the hypothesis of Varela et al. (2001); it explains hardly anything, and is inconsistent with nearly all observations and analyses.

6. Chronology

The radioisotope chronology of the nakhlites is simple (e.g., Nyquist et al., 2001), especially compared to the disturbed complexities of the shergottites. Seven events can be recognized: core formation near 4.55 Ga; two mantle differentiations near ~4.5 Ga; magma generation and igneous crystallization at 1.3 Ga; aqueous alteration at ~0.6 Ga; ejection from Mars at 11 Ma; and fall to Earth in recent times. For reference, the oldest materials of the solar system formed at 4.571 Ga, and chondritic asteroids formed at ~4.567 Ga (e.g., Shukolyukov and Lugmair, 2002).

6.1. Core formation and mantle differentiation

All SNC meteorites retain radioisotopic signatures of Mars' early planetary events: core formation and mantle differentiations (e.g., Halliday et al., 2001). The signatures of these events are so similar to those of the Moon, which reflect fractionations in a magma ocean, that Mars probably also had a magma ocean (Harper et al., 1995; Lee and Halliday, 1997; Brandon et al., 2000; Jones, 2003). One can infer that Mars' metallic core separated from its silicate mantle early in the magma ocean phase at ~4.557 Ga (Kleine et al., 2004). The magma ocean would then have cooled and crystallized, permitting silicate fractionations at least through 4.513 Ga, when the mantle sources of the shergottites formed (Borg et al., 2003).

The formation of Mars' core is dated principally with Hf-W isotope system; ^{182}Hf decayed to ^{182}W with $T_{1/2} = 9$ my (Lee and Halliday, 1997; Halliday and Lee, 1999; Halliday et al., 2001). Separation of W-bearing metal from a silicate mantle while ^{182}Hf was alive would lead to an excess of ^{182}W in the silicate compared to chondritic. The nakhlites have such an excess, $\varepsilon^{182}\mathrm{W} = \sim +3.3$ compared to chondrites at $\varepsilon^{182}\mathrm{W} = -1.9$ (Kleine et al., 2002, 2004; Borg et al., 2003; Foley et al., 2004). This ^{182}W excess suggests core formation (W loss) at ~4.557 Ga (Kleine et al., 2004), consistent with other chronometers like Re–Os (Brandon et al., 2000).

The formation of the nakhlites' parent mantle is constrained by Sm–Nd and isotope chronometers. The extinct isotope ^{146}Sm decayed to ^{142}Nd with $T_{1/2} = 103$ my, and nakhlites have ^{142}Nd in excess of that in chondrites, $\varepsilon^{142}\mathrm{Nd} = +0.75 \pm 0.05$ (Harper et al., 1995). This excess means that nakhlites' parent material was depleted in Nd while ^{146}Sm was still live – within a few hundred million years of solar-system origin (Harper et al., 1995; Jones, 2003). The Sm and Nd isotopic compositions of the shergottites are consistent with formation of their mantle source(s) in a single event at 4.513 Ga (Borg et al., 2003). However, Sm and Nd isotopes in the nakhlites require more complexity. First, the difference between ε^{182}W in the shergottites vs. the nakhlites is too great for core-mantle differentiation alone (Halliday et al., 2001; Borg et al., 2003). And second, Sm–Nd isotopic ratios of the nakhlites (both ^{146}Sm–^{142}Nd and ^{147}Sm–^{143}Nd) could arise in a single fractionation only if it were before the origin of the solar system (Harper et al., 1995; Borg et al., 2003). This is impossible, so the nakhlites' source must have experienced multiple silicate fractionations, possibly including events near 4.0 Ga (Shih et al., 1999) and/or

nearly simultaneous with core formation 4.557 Ga (Kleine et al., 2004; from Hf-W systematics).

Xenon isotopes, which track two short-lived radioisotope systems, are also consistent with early mantle differentiation. Decay of ^{129}I ($T_{1/2} = 16$ my) produced ^{129}Xe; the nakhlites' non-atmosphere components (Chas-S and Chas-E) contain no excess ^{129}Xe. This implies that I and Xe were not fractionated from each other in the nakhlites' source region within the effective lifetime of ^{129}I, say 160 my. However, the Chas-E gas component in Nakhla and NWA817 contains excess Xe from fission of short-lived ^{244}Pu, $T_{1/2} = 82$ my (Marty and Marti, 2002). Several scenarios are possible: the nakhlites' source lost some of its Xe after ^{129}I had expired but while ^{244}Pu was live; or that Xe from ^{244}Pu was added to the nakhlites' source.

This early mantle differentiation event is also suggested by the nakhlites' relative depletions of U and Th relative to La (Fig. 11a; McLennan, 2003), and provides a mechanism or event to allow fractionation of Th from U (Fig. 11a).

6.2. Magma formation and crystallization

Because the nakhlites are igneous rocks, their crystallization from magma should be prominently recorded in all suitable geochronometers. In fact, all were reset at ~1.3 Ga (Table 14), which is accepted as the time of igneous crystallization (Nyquist et al., 2001). Disturbances in the Rb–Sr system are ascribed to aqueous alteration (Nyquist et al., 2001; Misawa et al., 2003b) or terrestrial weathering. Some samples and mineral fractions (especially the 'brownies' of Papanastassiou and Wasserburg, 1974) are interpreted to contain iddingsite, which formed later and thus give discordant ages. An unusual result for NWA998 is that its olivine leaches have a different Nd isotopic initial than its other minerals and leaches (Table 15; Carlson and Irving, 2004).

Uranium–thorium–lead systematics of Nakhla give mixing/evolution lines that intersect the chondritic concordia curve at ~1.3 and ~4.3 Ga (Nakamura et al., 1982; Chen and Wasserburg, 1986; Jagoutz et al., 2002). The younger age is igneous crystallization. The lead component representing the older age is very similar to terrestrial lead, and likely represents a contaminant (Nakamura et al., 1982; J. Jones, pers. comm.), either terrestrial or Martian.

Several groups have argued that this chronology wrong – that the 1.3 Ga event represents metasomatism or metamorphism, not igneous crystallization. Papanastassiou and Wasserburg (1974) interpreted their Rb–Sr isochron for Nakhla as incomplete homogenization during metamorphism, because several mineral fractions fell off the overall isochron. In retrospect, these fractions contained aqueous alteration material that formed long after the anhydrous minerals. More recently, it was suggested that the 1.3 Ga event was hydrothermal alteration or metasomatism that reset essentially all the nakhlites' radioisotope chronometers (Blichert-Toft et al., 1999; Jagoutz and Jotter, 2000; Varela et al., 2001). If so, this alteration or metasomatism event must have been highly selective – equilibrating many radioisotopic systems (Rb–Sr, Sm–Nd, Lu–Hf, U–Th–Pb) while affecting neither Mg–Fe–Ca in nakhlite olivines and pyroxenes nor Na–K–Ca in Nakhla feldspars.

This selectivity seems entirely artificial, especially considering that Fe–Mg diffusion in pyroxenes is significantly faster than diffusion of most elements in the radiochronometers (e.g., Sm, Nd, Lu, Hf). Thus, the petrology of the nakhlites is inconsistent with alteration or metasomatism at 1.3 Ga.

6.3. Aqueous alteration

The tightest age of iddingsite formation, 614 ± 30 Ma, is from Rb–Sr isotopic data on olivine leach residues in Y000593 (Misawa et al., 2003b). The leaches themselves give the same age, although with less precision and with a different Sr initial isotopic ratio. A two-point 'isochron' between Lafayette olivine and leachate from iddingsite-rich samples gives an age of 680 ± 66 Ma (Shih et al., 1998), and the oldest Ar–Ar age for fragments of Lafayette iddingsite is 670 ± 90 Ma (Swindle et al., 2000). Recognizing the large uncertainties on these data, it seems likely that the nakhlites were altered by water at ~620 Ma. The iddingsite assemblage shows evidence of multiple episodes of deposition (Treiman et al., 1993; Vicenzi and Fahey, 2001), but their ages cannot be resolved with available data. The ages of the salt and sulfide assemblages are not known.

6.4. Cosmic ray exposure and residence on Earth

Several radioisotope chronometers record a meteorite's exposure to cosmic rays, mostly in interplanetary space but also at the surface of an airless planet. Cosmic ray exposure data are consistent with a single exposure to cosmic rays lasting ~10.75 m.y. (Nyquist et al., 2001; Marty and Marti, 2002; Okazaki et al., 2003) – the tightest constraint is from ^{81}Kr in Nakhla (Terrebilini et al., 2000). This age is interpreted as the age of ejection from Mars – the time when the nakhlites were removed from Mars into solar orbits (Nyquist et al., 2001).

Nakhla was observed to fall in 1911 (Prior, 1912), and Governador Valadares was reported collected soon after its fall in 1958. Lafayette was recognized as a meteorite in 1931, and is reported to have fallen in the 1920s (Nininger, 1935). However, Lafayette's ^{14}C and ^{10}Be contents imply residence on Earth for $\sim 2900 \pm 1000$ years (Jull et al., 1997), and ^{14}C in NWA998 gives a terrestrial residence of 6000 ± 1000 years (Nishiizumi et al., 2004). No terrestrial ages are available yet for Y000593, NWA817, and MIL03346.

7. Magma source and generation

The nakhlite parent magma was generated at 1.3 Ga from the Martian mantle, and something of the mantle source and of magma generation can be divined from the chemical and isotopic characteristics of the nakhlites. In particular, radiogenic isotopic systems can be modeled to delimit the chemical properties of the source mantle and its chemical history.

Although the nakhlites are enriched in highly incompatible elements relative to moderately incompatible elements (Fig. 11) their source mantle was highly depleted. This surprising inference comes from the initial isotopic ratios, at 1.3 Ga, of suitable radiogenic isotope systems (Table 15). For instance, the nakhlites and their parent magmas have Sm/Nd ratios well below CI chondritic (Fig. 11), at $Sm/Nd \approx 0.6 \times CI$. However, to produce the nakhlites' super-chondritic $^{143}Nd/^{144}Nd_i$ ratios (at 1.3 Ga), their sources must have been strongly depleted in Nd, with a time-averaged $^{147}Sm/^{144}Nd \approx 1.2 \times CI$ (Nakamura et al., 1982; Shih et al., 1998, 1999, 2002; Misawa et al., 2003b)! Evidence for this depletion is preserved in the Rb–Sr and Lu–Hf systems and in trace element abundances (i.e., non-chondritic U/La, Th/La, and Th/U). This fractionation occurred while ^{146}Sm was still alive, i.e., within a few hundred million years of planet formation (Harper et al., 1995; Borg et al., 2003). Evidence of this is also preserved in the W-Hf isotopic system, in that $\varepsilon^{182}W$ (i.e., early depletion in W) in Martian meteorites is correlated with $\varepsilon^{142}Nd$ (i.e., early enrichment in Sm; Borg et al., 2003). This means that the fractionation occurred while ^{182}W was still live, i.e., within ten or so million years of planet formation (Lee and Halliday, 1997; Halliday and Lee, 1999; Halliday et al., 2001; Foley et al., 2004; Kleine et al., 2004).

Like the nakhlites, their source mantle must have been rich in augite and olivine, and must have had little low-Ca pyroxene or aluminum-rich phases as melting residua. If the source had been otherwise, it would not yield augite-olivine cumulates like the nakhlites. This bulk composition and depletion in incompatible elements, unlike that of an average (chondrite-like) planetary mantle, has been rationalized as an augite-rich cumulate from an early Martian magma ocean (e.g., Borg et al., 1997, 2003; Blichert-Toft et al., 1999; Brandon et al., 2000; Borg and Draper, 2003; Jones, 2003; Elkins-Tanton et al., 2003).

The nakhlites are enriched in LREE and other highly incompatible elements, but formed from a source mantle strongly depleted in them. Cases of similar enrichment are known on Earth (e.g., Neal and Davidson, 1989), but the mechanism(s) for enrichment are not clear. Models for generation of nakhlite magmas have relied on low fractions of partial melt (<0.1–10%) from a garnet-bearing source mantle, followed or not by extensive fractional crystallization (Nakamura et al., 1982; Shih et al., 1999; Borg et al., 2003). Garnet is crucial to these models, as it supports the largest known fractionation between Sm and Nd and thus permits the extreme fractionation of Sm vs. Nd seen between the nakhlites' sources and parent magmas. Garnet also can accommodate U in preference to Th, unlike pyroxenes or olivine (Jones, 1995), and so could be invoked to explain the nakhlites' superchondritic Th/U ratios (Fig. 11a; Table 10). However, the stability of garnet in the Martian mantle appears relatively limited (Bertka and Fei, 1997; Draper et al., 2003), and other mechanisms for LREE enrichment could be explored, e.g., mantle metasomatism (e.g., Menzies and Hawkesworth, 1987; Treiman, 2003a), mantle zone refining (e.g., Harris, 1957; Neal and Davidson, 1989), and periodic recharge of fractionating magma chambers (e.g., O'Hara and Mathews, 1981; Bohrson and Spera, 2003).

8. Geologic setting

The geologic setting of the nakhlites, the outcrop- and regional-scale geology in which they formed, has been part of their recent study. Reid and Bunch (1975) compared their textures to those of Earth gabbros, implying formation at some depth in their parent planet. Berkley et al. (1980) recognized that their fine-grained mesostases required rapid cooling, and suggested a two-stage cooling history (slow, then rapid). Following the paradigm for the ureilite achondrite meteorites, Berkley et al. (1980) suggested that the rapid cooling was initiated by '…impact-induced removal of insulating overburden…' from a large body of basaltic magma.

The generally referenced geologic settings for the nakhlites are flows or shallow intrusions ultrabasic magma (Treiman, 1986), in great part by comparison with the similar rocks of Theo's Flow, a 125-m thick pyroxene-rich lava flow in the Archaean rocks of the Munro Township, Ontario (Friedman-Lentz et al., 1999). Based on Theo's Flow, Friedman-Lenz suggested that nakhlites develop from in situ crystallization of a nearly crystal-free magma in a convecting lava pool or lake. Augite crystals would nucleate on the walls and lid of the pool, and be swept back into the magma by its vigorous convection. After the augite crystals accumulated to a porous mass at the flow bottom, the intercumulus magma remained in chemical communication with the overlying magma as it convected and evolved. Thus, evolved magma could infiltrate among the more primitive cumulus augite grains. Nearby field exposures and cooling rate calculations suggested that flows (of Theo's Flow composition) thicker than ~15 m could produce nakhlite-like rocks. Further quantification of cooling rates based on chemical zoning in olivine confirm these estimates (Mikouchi and Miyamoto, 2002; Mikouchi et al., 2003), though with some inconsistencies.

A broader question is where on Mars the nakhlites could have formed. Their crystallization ages of ~1.3 Ga (Table 14) places them in the Middle Amazonian period of Martian history (Hartmann and Neukum, 2001). Most Martian surfaces of this age are in the Tharsis and Elysium volcanic provinces – regions of many huge shield volcanos and extensive flow fields (Scott et al., 1986; Hartmann and Berman, 2000) – which are likely sources of nakhlites (and other Martian meteorites except ALH84001). However, Martian surfaces may be younger than generally inferred (Treiman, 1995; Nyquist et al., 1998), which would permit other sources for the nakhlites (e.g., Syrtis Major, Harvey and Hamilton, 2005).

It is interesting that the Martian meteorite basalts (and parent magmas) have low Al_2O_3 contents and low Al/Ca ratios compared to 'normal' terrestrial basalts (Tables 5, 13; Lodders, 1998; Meyer, 2003), while the presumably older Martian basalts of the Mars Pathfinder and Gusev Crater sites have more 'normal' Al_2O_3 contents (11–12.5% Al_2O_3: Brückner et al., 2003; Foley et al., 2003; McSween et al., 2004) and near-chondritic Al/Ca ratios (McSween et al., 2004). It is possible that these geochemical differences reflect different mantle tectonic environments, e.g., that the Tharsis and Elysium basalts originated in large long-lived plumes (e.g., Kiefer, 2003), and that the older Pathfinder and Gusev lavas had a different origin.

9. Summary

The seven nakhlite meteorites, igneous clinopyroxenites, formed on Mars from eruptions or shallow intrusions of basaltic or ultrabasic magma. Their source mantle was affected by core formation and several differentiation events within a few hundred million years of Mars' formation – possibly associated with formation and crystallization of a magma ocean. The nakhlites' source mantle was strongly depleted in incompatible elements (like La, K, U, Th), and remained so until just before formation of nakhlite magmas at ~1.3 Ga. This mantle source was then greatly enriched in incompatible elements and partially melted to form nakhlite parent magmas. It is not clear whether all the nakhlites formed from a single batch of magma, or whether several closely related batches were involved. The magmas had low abundances of Al_2O_3 relative to common basalts, and high Fe/Mg compared to Earth basalts – characteristics shared by the Martian meteorite basalts (but not by all basalts on Mars).

On eruption at ~1.3 Ga, the nakhlite parent magmas began crystallization in an environment that permitted formation of the chemically homogeneous cores the augite and olivine – perhaps a large subsurface magma chamber. Then, the magma and crystals moved to environments where the crystals could accumulate and the interstitial magma could cool at varying rates. Accumulation of augite and olivine crystals set the mineral proportions and bulk compositions of the nakhlites. The various cooling rates produced a wide range of textures, ranging from glassy mesostasis (MIL03346, NWA817) to completely crystalline diabasic (NWA998). The nakhlites' cooling rates affected mineral compositions and mesostasis textures in many ways; nearly all are consistent with order of cooling rates, fastest to slowest, as: MIL03346, NWA817, Y000593, Nakhla ≈ Governador Valadares, Lafayette, and NWA998.

After the crystallization and cooling, at ~0.62 Ga, the nakhlites were infiltrated by liquid water, which dissolved olivine and mesostasis glass, deposited iddingsite (smectite and iron oxy-hydroxides), deposited salt minerals, and replaced magmatic sulfides. No other events are recorded until ejection from Mars at ~11 Ma, and falls to Earth in recent times. Ejection from Mars, by asteroidal impact, produced brecciated zones and implanted atmosphere gases, but had few other effects. On Earth, the nakhlites have been affected to varying degrees by their environment. Effects include deposition of salts, oxidation and weathering, and attack by microbiota.

Many features of the nakhlites can be rationalized within this simple geologic story. The alert reader will see many opportunities for continued work that will improve our understanding of petrogenesis and aqueous processes on Mars.

Acknowledgments

Over the years, I have learned much about the nakhlites and Mars from discussions with J. Berkley, R.C.F. Lentz, R. Harvey, J.H. Jones, C. Goodrich, J.

Gooding, and D. Bogard. I am grateful for their help. Thin sections were graciously loaned by Harvard University (J. Wood), The Smithsonian Institution (G. MacPherson), the Naturhistorisches Museum Wien (F. Brandstaetter), the American Museum of Natural History (D. Ebel, J. Bosenberg), Johnson Space Center (K. Righter), and the National Institute of Polar Research Japan (H. Kojima). K. Mathew kindly checked my calculations of noble gas components. Fig. 9g appears with gracious permission from J. Bridges. I am grateful to K. Keil for inviting this review paper. Financial support is from NASA Cosmochemistry grant NAG5-13279, and NASA Mars Fundamental Research grant NAG5-12771. Lunar and Planetary Institute Contribution #1229.

References

Anand, M., Williams, C.T., Russell, S.S., Jones, G., James, S., Grady, M.M., 2005a. Petrology and geochemistry of nakhlite MIL 03346: a new Martian meteorite from Antarctica. Lunar Planet. Sci. XXXVI Lunar and Planetary Institute (CD-ROM), #1639.

Anand, M., Russell, S.S., Mullane, E., Grady, M.M., 2005b. Fe isotopic comopsition of Martian meteorites. Lunar Planet. Sci. XXXVI Lunar and Planetary Institute (CD-ROM), #1859.

Anders, E., Grevesse, N., 1989. Abundances of the elements: meteoritic and solar. Geochim. Cosmichim. Acta 53, 197–214.

Antarctic Meteorite Newsletter, 2004. Special edition announcing the availability of a new Martian meteorite. Ant. Meteorite Newslett. 27 (2) 2pp.

Arndt, N.T., 1977. Thick, layered peridotite-gabbro lava flows in Munro township, Ontario. Can. J. Earth Sci. 14, 2620–2637.

Ashworth, J.R., Hutchison, R., 1975. Water in non-carbonaceous stony meteorites. Nature 256, 714–715.

Bacon, C.R., 1989. Crystallization of accessory phases in magmas by local saturation adjacent to phenocrysts. Geochim. Cosmochim. Acta. 53, 1055–1066.

Baker, L., Franchi, I.A., Wright, I.P., Pillinger, C.T., 1998. Oxygen isotopes in water from martian meteorites (abstract). Meteorit. Planet. Sci. 33, A11.

Barrat, J.A., Gillet, Ph., Lécuyer, C., Sheppard, S.M.F., Lesourd, M., 1998. Formation of carbonates in the Tatahouine meteorite. Science 280, 412–414.

Berkley, J.L., Himmelberg, G.R., 1978. Cumulus mineralogy and petrology of the Deer Lake complex, Itasca County, Minnesota. Minn. Geol. Surv. Rep. Invest. 20-A 18pp.

Berkley, J.L., Keil, K., Prinz, M., 1980. Comparative petrology and origin of Governador Valadares and other nakhlites. Proc. Lunar Planet. Sci. Conf. 11, 1089–1102.

Bertka, C.M., Fei, Y., 1997. Mineralogy of the martian interior up to core–mantle boundary pressures. J. Geophys. Res. 102, 5251–5264.

Bjoraker, G.L., Mumma, M.J., Larson, H.P., 1989. Isotopic ratios of hydrogen and oxygen in the martian atmosphere (abstract). Bull. Am. Astron. Soc. 21, 991.

Blichert-Toft, J., Gleason, J.D., Telouk, K., Albaréde, F., 1999. The Lu–Hf geochemistry of the shergottites, and the evolution of the Martian mantle-crust system. Earth Planet. Sci. Lett. 173, 25–39.

Boctor, N.Z., Meyer, H.O.A., Kellerud, G., 1976. Lafayette meteorite: petrology and opaque mineralogy. Earth Planet. Sci. Lett. 32, 69–76.

Boctor, N.Z., Alexander, C.M.O'D., Wang, J., Hauri, E., 2003. The sources of water in Martian meteorites: clues from hydrogen isotopes. Geochim. Cosmochim. Acta 67, 3971–3989.

Bodnar, R.J., 1998. Fluid inclusions in Allan Hills 8400 and other martian meteorites: evidence for volatiles on Mars (abstract). In: Workshop on the Issue Martian Meteorites: Where Do We Stand, And Where Are We Going? Lunar and Planetary Institute, pp. 3–5 Contribution # 956.

Bogard, D.D., Garrison, D.H., 1998. Relative abundances of argon, krypton, and xenon in the Martian atmosphere as measured in Martian meteorites. Geochim. Cosmochim. Acta 62, 1829–1835.

Bogard, D.D., Husain, L., 1977. A new 1.3 Aeon-young achondrite. Geophys. Res. Lett. 4, 69–71.

Bogard, D.D., Johnson, P., 1983. Martian gases in an Antarctic meteorite. Science 221, 651–654.

Bohrson, W.A., Spera, F.J., 2003. Energy-constrained open-system magmatic processes IV: geochemical, thermal and mass consequences of energy-constrained recharge, assimilation and fractional crystallization (EC-RAFC). Geochem. Geophys. Geosyst. 4 (2), 8002.
Borg, L.E., Draper, D.S., 2003. A petrogenetic model for the origin and compositional variation of the Martian basaltic meteorites. Meteorit. Planet. Sci. 38, 1713–1731.
Borg, L.E., Nyquist, L.E., Wiesmann, H., Shih, C.-Y., 1997. Constraints on Martian differentiation processes from Rb–Sr and Sm–Nd isotopic analyses of basaltic shergottite QUE94201. Geochim. Cosmochim. Acta 61, 4915–4931.
Borg, L.E., Nyquist, L.E., Wiesmann, H., Shih, C.-Y., Reese, Y., 2003. The age of Dar al Gani 476 and the differentiation history of the martian meteorites inferred from their radiogenic isotopic systematics. Geochim. Cosmochim. Acta 67, 3519–3536.
Boudreau, A.E., McCallum, I.S., 1992. Infiltration metasomatism in layered intrusions—an example from the Stillwater Complex, Montana. J. Volc. Geotherm. Res. 52, 171–183.
Brandon, A.D., Walker, R.J., Morgan, J.W., Goles, G.G., 2000. Re–Os isotopic evidence for early differentiation of the Martian mantle. Geochim. Cosmochim. Acta 64, 4083–4095.
Bridges, J.C., Grady, M.M., 1999. A halite–siderite–anhydrite–chlorapatite assemblage in Nakhla: mineralogical evidence for evaporites on Mars. Meteorit. Planet. Sci. 34, 407–416.
Bridges, J.C., Grady, M.M., 2000. Evaporite mineral assemblages in the nakhlite (martian) meteorites. Earth Planet. Sci. Lett. 176, 267–279.
Bridges, J.C., Catling, D.C., Saxton, J.M., Swindle, T.D., Lyon, I.C., Grady, M.M., 2001. Alteration assemblages in Martian meteorites: implications for near-surface processes. In: Kallenbach, R., Geiss, J., Hartmann, W.K. (Eds.), Chronology and Evolution of Mars. Kluwer Academic Publishers, Dordrecht, pp. 365–392.
Bridges, J.C., Warren, P.H., Lee, M.R., 2004. Olivine decomposition features in Y000593 and NWA998 (abstract). Meteoritics 39 #5140.
Brückner, J., Driebus, G., Rieder, R., Wänke, H., 2003. Refined data of Alpha Proton X-ray Spectrometer analyses of soils and rocks at the Mars Pathfinder site: implications for surface chemistry. J. Geophys. Res. 108 (12), 8094.
Bunch, T.E., Reid, A.M., 1975. The nakhlites, part 1: petrography and mineral chemistry. Meteoritics 10, 303–315.
Burragato, F., Cavaretta, G., Funiciello, R., 1975. The new Brazilian achondrite of Governador Valadares (Minas Gerais) (abstract). Meteoritics 10, 374–375.
Carlson, R.W., Irving, A.J., 2004. Pb–Hf–Sr–Nd isotopic systematics and age of nakhlite NWA 998 (abstr.). Lunar Planet. Sci. XXXV, 0 Lunar and Planetary Institute CD-ROM, #1442.
Carr, R.H., Grady, M.M., Wright, I.P., Pillinger, C.T., 1985. Martian atmospheric carbon dioxide and weathering products in SNC meteorites. Nature 314, 248–250.
Chen, J.H., Wasserburg, G.J., 1986. S≠N = ?C (abstract). Lunar Planet. Sci. XVII, 113–114.
Clayton, R.N., Mayeda, T., 1996. Oxygen isotope studies of achondrites. Geochim. Cosmochim. Acta 60, 1999–2017.
Craig, J.R., Scott, S.D., 1974. Sulfide phase equilibria. In: Ribbe, P.H. (Ed.), Sulfide Mineralogy. Mineralogical Society of America Short Course Notes 1, Mineralogical Society of America, Washington, DC Chapter 5, 110pp.
Crozaz, G., Floss, C., Wadhwa, M., 2003. Chemical alteration and REE mobilization in meteorites from hot and cold deserts. Geochim. Cosmochim. Acta 67, 4727–4741.
Delano, J.W., Arculus, R.J., 1980. Nakhla: oxidation state and other constraints (abstract). Lunar Planet. Sci. XI, 219–221.
Delvigne, J., 1998. Atlas of Micromorphology of Mineral Alteration and Weathering. Canadian Mineralogist Special Publication #3, Mineralogical Association of Canada, Ottawa 495pp.
Drake, M.J., Swindle, T.D., Owen, T., Musselwhite, D.S., 1995. Fractionated martian atmosphere in the nakhlites? Meteoritics 29, 854–859.
Draper, D.S., Xirouchakis, D., Agee, C.B., 2003. Trace element partitioning between garnet and chondritic melt from 5 to 9 Gpa: implications for the onset of the majorite transition in the martian mantle. Phys. Earth Planet. Interiors 139, 149–169.
Dreibus, G., Palme, H., Rammensee, W., Spettel, B., Weckwerth, G., Wänke, H., 1982. Composition of the Shergotty parent body: further evidence of a two-component model for planet formation (abstract). Lunar Planet. Sci. XIII, 186–187.
Dreibus, G., Huisl, W., Spettel, B., Haubold, R., 2003. Comparison of the chemistry of Y-000593 and Y-000749 with other nakhlites (abstract). Lunar Planet. Sci. XXXIV Lunar and Planetary Institute CD-ROM, #1586.

Dyar, M.D., 2003. Ferric iron in SNC meteorites as determined by Mossbauer spectroscopy: implications for martian landers and martian oxygen fugacity. Meteorit. Planet. Sci. 38 (12), 1733–1751.
Dyar, M.D., Mackwell, S.J., Seaman, S.J., Marchand, G.J., 2004. Evidence for a wet, reduced Martian interior (abstract). Lunar Planet. Sci. XXXV Lunar and Planetary Institute CD-ROM, #1348.
Dyar, M.D., Pieters, C.M., Hiroi, T., Lane, M.D., Marchand, G.J., 2005. Integrated spectroscopic studies of MIL03346. Lunar Planet. Sci. XXXVI Lunar and Planetary Institute CD-ROM, #1261.
Edwards, H.G.M., Farwell, D.W., Grady, M.M., Wynn-Williams, D.D., Wright, I.P., 1999. Comparative Raman spectroscopy of a Martian meteorite and Antarctic lithic analogues. Planet. Space Sci. 47, 353–362.
Eiler, J.M., 2001. Oxygen isotope variations of basaltic lavas and upper mantle rocks. In: Valley, J.W., Cole, D.R. (Eds.), Stable Isotope Geochemistry, Reviews in Mineralogy and Geochemistry, vol. 43. Mineralogical Society of America, Washington, DC, pp. 319–364.
Elkins-Tanton, L.T., Parmentier, E.M., Hess, P.C., 2003. Magma ocean fractional crystallization and cumulate overturn in terrestrial planets: implications for Mars. Meteorit. Planet. Sci. 38, 1753–1772.
Farquhar, J., Thiemens, M.H., 2000. Oxygen cycle of the Martian atmosphere-regolith system: $\Delta^{17}O$ of secondary phases in Nakhla and Lafayette. J. Geophys Res. 105, 11991–11997.
Farquhar, J., Savarino, J., Jackson, T.L., Thiemens, M.H., 2000. Evidence of atmospheric sulphur in the martian regolith from sulphur isotopes in meteorites. Nature 404, 50–52.
Floran, R.J., Prinz, M., Hlava, P.F., Keil, K., Nehru, C.E., Hinthorne, J.R., 1978. The Chassigny meteorite: a cumulate dunite with hydrous amphibole-bearing melt inclusions. Geochim. Cosmochim. Acta 42, 1213–1229.
Flynn, G.J., Keller, L.P., Jacobsen, C., Wirick, S., 1999. Organic carbon in Mars meteorites: a comparison of ALH84001 and Nakhla (abstract). Lunar Planet. Sci. XXX Lunar and Planetary Institute, CD-ROM, #1087.
Foley, C.N., Economou, T., Clayton, R.N., 2003. Final chemical results from the Mars Pathfinder alpha proton X-ray spectrometer. J. Geophys. Res. 108 (12), 8096.
Foley, C.N., Wadhwa, M., Borg, L., Janney, P.E., 2004. The differentiation history of mantle reservoirs on Mars from W and Nd isotopic compositions of SNC meteorites (abstract). Lunar Planet. Sci. XXXV Lunar and Planetary Institute (CD-ROM), #1879.
Franchi, I.A., Wright, I.P., Sexton, A.S., Grady, M.M., 1999. The oxygen isotopic composition of the Earth and Mars. Meteorit. Planet. Sci. 34, 657–661.
Friedman-Lentz, R.C., Taylor, G.J., Treiman, A.H., 1999. Formation of a martian pyroxenite: a comparative study of the nakhlite meteorites and Theo's Flow. Meteorit. Planet. Sci. 34, 919–932.
Gale, N.H., Arden, J.W., Hutchison, R., 1975. The chronology of the Nakhla achondrite meteorite. Earth Planet. Sci. Lett. 26, 195–206.
Garrison, D.H., Bogard, D.D., 2005. Ar–Ar ages of nakhlites Y000593, NWA998, and Nakhla and CRE age of NWA998. Lunar Planet. Sci. XXXVI Lunar and Planetary Institute (CD-ROM), #1137.
Ghosal, S., Sack, R.O., Ghiorso, M.S., Lipschutz, M.E., 1998. Evidence for a reduced, Fe-depleted martian mantle source region of shergottites. Contrib. Miner. Petrol. 130, 346–357.
Gillet, Ph., Barrat, J.A., Deloule, E., Wadhaw, M., Jambon, A., Sautter, V., Devouard, B., Neuville, D., Benzerara, K., Lesourd, M., 2002. Aqueous alteration in the Northwest Africa 817 (NWA 817) Martian meteorite. Earth Planet. Sci. Lett. 203, 431–444.
Gilmour, J.D., Whitby, J.A., Turner, G., 1999. Martian atmospheric xenon contents of Nakhla mineral separates: implications for the origin of elemental mass fractionation. Earth Planet. Sci. Lett. 166, 139–147.
Gilmour, J.D., Whitby, J.A., Turner, G., 2001. Disentangling xenon components in Nahkla: Martian atmosphere, spallation, and Martian interior. Geochim. Cosmochim. Acta 65, 343–354.
Gladman, B., 1997. Destination: Earth. Martian meteorite delivery. Icarus 130, 228–246.
Glavin, D.P., Bada, J.L., Brinton, K.L.F., McDonald, G.D., 1999. Amino acids in the Martian meteorite Nakhla. Proc. Natl. Acad. Sci. USA 96, 8835–8838.
Gomes, C.B., Keil, K., 1980. Brazilian Stone Meteorites. University of New Mexico Press 159pp.
Gooding, J.L., 1986. Clay-mineraloid weathering products in Antarctic meteorites. Geochim. Cosmochim. Acta 50, 2215–2223.
Gooding, J.L., Wentworth, S.J., Zolensky, M.E., 1991. Aqueous alteration of the Nakhla meteorite. Meteoritics 26, 135–143.
Grady, M.M., 2000. Catalogue of Meteorites, fifth ed. Cambridge University Press, Cambridge 690pp.
Greenwood, J.P., Mojzsis, S.J., Coath, C.D., 2000a. Sulfur isotopic compositions of individual sulfides in Martian meteorites ALH84001 and Nakhla: implications for crust–regolith exchange on Mars. Earth Planet. Sci. Lett. 184, 23–35.

Greenwood, J.P., Riciputi, L.R., McSween Jr., H.Y., Taylor, L.A., 2000b. Modified sulfur isotopic compositions of sulfides in the nakhlites and Chassigny. Geochim. Cosmochim. Acta 64, 1121–1131.

Greshake, A., Stephan, T., Rost, D., 2000. Combined TEM and TOF-SIMS study of symplectic exsolutions in olivine from the martian meteorites Nakhla and Governador Valadares (abstract). Lunar Planet. Sci. XXXI Lunar and Planetary Institute (CD-ROM), #1150.

Greshake, A., Fritz, J., Stöffler, D., 2004. Petrology and shock metamorphism of the olivine-phyric shergottite Yamato 980459: evidence for a two-stage cooling and a single-stage ejection history. Geochim. Cosmochim. Acta 68, 2359–2377.

Grossman, J.N., Zipfel, J., 2001. The Meteoritical Bulletin No. 85, 2001 September. Meteorit. Planet. Sci. 36, A293–A322.

Grove, T.L., 1978. Cooling histories of Luna 24 very low Ti (VLT) ferrobasalts: an experimental study. Proceedings of the Ninth Lunar and Planetary Science Conference, 565–584.

Halliday, A.N., Lee, D.-C., 1999. Tungsten isotopes and the early development of the earth and the moon. Geochim. Cosmochim. Acta 63, 4157–4179.

Halliday, A.N., Wänke, H., Birck, J.-L., Clayton, R.N., 2001. The accretion, composition, and early differentiation of Mars. In: Kallenbach, R., Geiss, J., Hartmann, W.K. (Eds.), Chronology and Evolution of Mars. Kluwer Academic Publishers, Dordrecht, pp. 197–230.

Hanski, E., 1992. Petrology of Pechenga ferropicrites and cogenetic Ni-bearing gabbro-wehrlite intrusions, Kola Peninsula, Russia. Geol. Surv. Finland Bull. 367 193pp.

Harper Jr., C.L., Nyquist, L.E., Bansal, B., Wiesmann, H., Shih, C.-Y., 1995. Rapid accretion and early differentiation of Mars indicated by $^{142}Nd/^{144}Nd$ in SNC meteorites. Science 267, 213–217.

Harris, P.G., 1957. Zone refining and the origin of potassic basalts. Geochim. Cosmochim. Acta 12, 195–208.

Hartmann, W.K., Berman, D.C., 2000. Elysium Planitia lava flows: crater count chronology and geological implications. J. Geophys. Res. 105 (E6), 15011–15025.

Hartmann, W.K., Neukum, G., 2001. Cratering chronology and the evolution of Mars. In: Kallenbach, R., Geiss, J., Hartmann, W.K. (Eds.), Chronology and Evolution of Mars. Kluwer Academic Publishers, Dordrecht, pp. 165–194.

Harvey, R.P., Hamilton, V.E., 2005. Syrtis Major as the source region of the nakhlite/Chassigny group of Martina meteorites: implications for the geological history of Mars. Lunar Planet. Sci. XXXVI Lunar and Planetary Institute (CD-ROM), #1019.

Harvey, R.P., McSween Jr., H.Y., 1992a. The petrogenesis of the nakhlites: evidence from cumulate mineral zoning. Geochim. Cosmochim. Acta 56, 1655–1663.

Harvey, R.P., McSween Jr., H.Y., 1992b. The parent magma of the nakhlite meteorites: clues from melt inclusions. Earth Planet. Sci. Lett. 111, 467–482.

Hashizume, K., Chaussidon, M., Marty, B., Robert, F., 2000. Solar wind record on the Moon: deciphering presolar from planetary nitrogen. Science 290, 1142–1145.

Head, J.N., Melosh, H.J., Ivanov, B., 2002. Martian meteorite launch: high-speed ejecta from small craters. Science 298, 1752–1756.

Herd, C.D.K., Treiman, A.H., McKay, G.A., Shearer, C.K., 2004. The behavior of Li and B during planetary basalt crystallization. Am. Miner. 89, 832–840.

Hess, P.C., 1980. Origin of Igneous Rocks. Harvard University Press, Cambridge, MA 336pp.

Imae, N., Ikeda, Y., Shinoda, K., Kojima, K., Iwata, N., 2003. Yamato nakhlites: petrography and mineralogy. Antarctic Meteorite Research (NIPR) 16, 13–33.

Irvine, T.N., 1980. Magmatic infiltration metasomatism, double-diffusive fractional crystallization, and adcumulus growth in the Muskox Intrusion and other layered intrusions. In: Hargraves, R.B. (Ed.), Physics of Magmatic Processes. Princeton University Press, Princeton, NJ, pp. 325–384.

Irving, A.J., Kuehner, S.M., Rumble III, D., Carlson, R.W., Hupé, A.C., Hupé, G.M., 2002. Petrology and isotopic composition of orthopyroxene-bearing nakhlite NWA 998 (abstract). Meteorit. Planet. Sci. 37, A70 (#5225).

Jagoutz, E.J., Jotter, R.J., 2000. New Sm-Nd isotope data on Nakhla minerals (abstract). Lunar Planet. Sci. XXXI Lunar and Planetary Institute (CD-ROM), #1609.

Jagoutz, E., Dreibus, G., Jotter, R., Kubny, A., Zartman, R., 2002. New U–Pb data on clean Nakhla minerals (abstract). Meteorit. Planet. Sci. 37, A71 #5197.

Jakosky, B.M., Jones, J.H., 1997. The history of Martian volatiles. Rev. Geophys. 35, 1–16.

Jones, J.H., 1995. Experimental trace element partitioning. In: Ahrens, T.J. (Ed.), Rock Physics and Phase Relations: A Handbook of Physical Constants. American Geophysical Union, Washington, DC, pp. 73–104.

Jones, J.H., 2003. Constraints on the structure of the martian interior determined from the chemical and isotopic systematics of SNC meteorites. Meteorit. Planet. Sci. 38, 1807–1814.
Jull, A.J.T., Eastoe, C.J., Xue, S., Herzog, G.F., 1995. Isotopic composition of carbonate in the SNC meteorites ALH84001 and Nakhla. Meteoritics 30, 311–318.
Jull, A.J.T., Cloudt, S., Courtney, C., Eastoe, C.J., 1997. Carbon-14 and stable-isotopic composition of organic material and carbonates from some SNC meteorites (abstract). Meteorit. Planet. Sci. 32, A66.
Jull, A.J.T., Beck, J.W., Burr, G.S., 2000. Isotopic evidence for extraterrestrial organic matter in the Martian meteorite Nakhla. Geochim. Cosmochim. Acta 64, 3763–3772.
Kaneda, K., McKay, G., Le, L., 1998. Synthetic Nakhla pyroxenes: a close match at last (abstract). Lunar Planet. Sci. XXIX Lunar and Planetary Institute CD-ROM, #1620.
Karlsson, H.R., Clayton, R.N., Gibson Jr., E.K., Mayeda, T.K., 1992. Water in SNC meteorites: evidence for a Martian hydrosphere. Science 255, 1409–1411.
Kiefer, W., 2003. Melt in the Martian mantle: Shergottite formation and implications for present-day mantle convection on Mars. Meteorit. Planet. Sci. 38, 1815–1832.
Kleine, T., Mu, C., Mezger, K., Palme, H., 2002. Rapid accretion and early core formation on asteroids and the terrestrial planets from Hf–W chronometry. Nature 418, 952–955.
Kleine, T., Mezger, K., Münker, C., Palme, H., Bischoff, A., 2004. ^{182}Hf–^{182}W isotope systematics of chondrites, eucrites, and martian meteorites: chronology of core formation and early mantle differentiation in Vesta and Mars. Geochim. Cosmochim. Acta 68, 2935–2946.
Kopp, R.E., Humayan, M., 2003. Kinetic model of carbonate dissolution in Martian meteorite ALH84001. Geochim. Cosmochim. Acta. 67, 3247–3256.
Kuebler, K., Jolliff, B.L., Wang, A., Haskin, L.A., 2004. A survey of olivine alteration products using Raman spectroscopy. Lunar Planet. Sci. XXXV, Abstract #1704. Lunar and Planetary Institute, Houston (CD-ROM).
Laul, J.C., Keays, R.R., Ganapathy, R., Anders, E., Morgan, J.W., 1972. Chemical fractionations in meteorites-V. Volatile and siderophile elements in achondrites and ocean ridge basalts. Geochim. Cosmochim. Acta 36, 329–345.
Lee, D.-C., Halliday, A.N., 1997. Core formation on Mars and differentiated asteroids. Nature 388, 854–857.
Lee, M.R., Bland, P.A., 2004. Mechanisms of weathering of meteorites recovered from hot and cold deserts and the formation of phyllosilicates. Geochim. Cosmochim. Acta 68, 893–916.
Lentz, R.C.F., McSween Jr., H.Y., 2003. Crystal size distribution analysis of new nakhlites and Los Angeles: how do they compare with SNCs of old? (abstract). Lunar Planet. Sci. XXXIV Lunar and Planetary Institute CD-ROM, #1914.
Lentz, R.C.F., McSween Jr., H.Y., Ryan, J., Riciputi, L.R., 2001. Water in martian magmas: clues from light lithophile elements in shergottite and nakhlite pyroxenes. Geochim. Cosmochim. Acta 56, 4551–5465.
Leshin, L.A., Epstein, S., Stolper, E.M., 1996. Hydrogen isotope geochemistry of SNC meteorites. Geochim. Cosmochim. Acta 60, 2635–2650.
Lodders, K., 1998. A survey of shergottite, nakhlite, and Chassigny meteorites whole rock compositions. Meteorit. Planet. Sci. 33, A183–A190.
Lofgren, G.E., 1983. Effect of heterogeneous nucleation of basaltic textures: a dynamic crystallization study. J. Petrol. 24, 229–255.
Longhi, J., Pan, V., 1989. The parent magmas of the SNC meteorites. Proceedings of the 19th Lunar and Planetary Science Conference 0, 451–464.
Longhi, J., Knittle, E., Holloway, J.R., Wänke, H., 1992. The bulk composition, mineralogy, and internal structure of Mars. In: Kiefer, H.H., Jakosky, B.M., Snyder, C.W., Matthews, M.S. (Eds.), Mars. University of Arizona Press, pp. 184–208.
Marty, B., Marti, K., 2002. Signatures of early differentiation of Mars. Earth Planet. Sci. Lett. 196, 251–263.
Marty, B., Marti, K.Th., Monod Consortium, 2001. Noble gases in new SNC meteorites NWA817 and NWA 480 (abstract). Meteorit. Planet. Sci. 36, A122–A123.
Mathew, K.J., Marti, K., 2001. Early evolution of Martian volatiles: nitrogen and noble gas components in ALH84001 and Chassigny. J. Geophys. Res. 106, 1401–1422.
Mathew, K.J., Marti, K., 2002. Martian atmospheric and interior volatiles in the meteorite Nakhla. Earth Planet. Sci. Lett. 199, 7–20.

Mathew, K.J., Marty, B., Marti, K., Zimmermann, L., 2003. Volatiles (nitrogen, noble gases) in recently discovered SNC meteorites, extinct radioactivities and evolution. Earth Planet. Sci. Lett. 214, 27–42.

McCarthy, T.S., Erlank, A.J., Willis, J.P., Ahrens, L.H., 1974. New chemical analyses of six achondrites and one chondrite. Meteoritics 9, 215–222.

McKay, G., Schwandt, C., 2005. Mineralogy and petrology of new Antarctic nakhlite MIL 03346. Lunar Planet. Sci. XXXVI Lunar and Planetary Institute CD-ROM, #2351.

McLennan, S.M., 2003. Evidence for a distinctive rare earth element-enriched mantle reservoir on Mars. Lunar Planet. Sci. XXXIV, Abstract #1710. Lunar and Planetary Institute, Houston (CD-ROM).

McSween Jr., H.Y., Harvey, R.P., 1998. An evaporation model for formation of carbonates in the ALH84001 martian meteorite. Int. Geol. Rev. 40, 774–783.

McSween Jr., H.Y., Arvidson, R.E., Bell III, J.F., Blaney, D., Cabrol, N.A., Christensen, P.R., Clark, B.C., Crisp, J.A., Crumpler, L.S., DesMarais, D.J., Farmer, J.D., Gellert, R., Ghosh, A., Gorevan, S., Graf, A., Grant, J., Haskin, L.A., Herkenhoff, K.E., Johnson, J.R., Joliff, B.L., Klingelhoefer, G., Knudson, A.T., McLennan, S., Milam, K.A., Moersch, J.E., Morris, R.V., Rieder, R., Ruff, S.W., deSouza Jr., P.A., Squyres, S.W., Wänke, H., Wang, A., Wyatt, M.B., Yen, A., Zipfel, J., 2004. Basaltic rocks analyzed by the Spirit rover in Gusev Crater. Science 305, 842–845.

Menzies, M.A., Hawkesworth, C.J., 1987. Mantle Metasomatism. Academic Press, London 472pp.

Meyer, C., 2003. Mars meteorite compendium—2003 Report JSC #27672. Johnson Space Center, Houston TX.

Mikouchi, T., Miyamoto, M., 1998. Pyroxene and olivine microsctructures in nahlites martian meteorites: implications for their thermal history (abstract). Lunar Planet. Sci. XXIX Lunar and Planetary Institute CD-ROM, #1574.

Mikouchi, T., Miyamoto, M., 2002. Comparative cooling rates of nakhlites as inferred from iron-magnesium and calcium zoning of olivines (abstract). Lunar Planet. Sci. XXXII Lunar and Planetary Institute CD-ROM, #1343.

Mikouchi, T., Yamada, I., Miyamoto, M., 2000. Symplectic exsolution in olivine from the Nakhla martian meteorite. Meteorit. Planet. Sci. 35, 937–942.

Mikouchi, T., Koizumi, E., Monkawa, A., Ueda, Y., Miyamoto, M., 2003. Mineralogy and petrology of Yamato 000593: comparison with other Martian nakhlite meteorites. Antarctic Meteorite Research (NIPR) 16, 34–57.

Mikouchi, T., Monkawa, A., Koizumi, E., Chokai, J., Miyamoto, M., 2005. MIL03346 nakhlite and NWA2737 (“Diderot”) chassignite: two new martian cumulate rocks from hot and cold deserts. Lunar Planet. Sci. XXXVI Lunar and Planetary Institute (CD-ROM) #1944.

Misawa, K., Kojima, K., Imae, N., Nakamura, N., 2003a. The Yamato nakhlite consortium. Antarctic Meteorite Research (NIPR). Antarctic Meteorite Research (NIPR) 16, 1–12.

Misawa, K., Shih, C.-Y., Wiesmann, H., Nyquist, L.E., 2003b. Crystallization and alteration ages of the Antarctic nakhlite Yamato 000593 (abstract). Lunar Planet. Sci. XXXIV Lunar and Planetary Institute CD-ROM, #1556.

Mittlefehldt, D.W., Lindstrom, M.M., 1997. Magnesian basalt clasts from the EET 92014 and Kapoeta howardites and a discussion of alleged primary magnesian HED basalts. Geochim. Cosmochim. Acta 61, 453–462.

Morse, S.A., 1980. Basalts and Phase Diagrams. Springer, New York 493pp.

Musselwhite, D., Treiman, A.H., Shearer, C., 2005. Light lithophyle element trends in nahklite NWA 817 pyroxenes. Lunar Planet. Sci. XXXVI Lunar and Planetary Institute, CD-ROM, #1230.

Nakamura, N., Unruh, D.M., Tatsumoto, M., Hutchison, R., 1982. Origin and evolution of the Nakh la meteorite inferred from the Sm–Nd and U–Pb systematics and REE, Ba, Sr, Rb, and K abundances. Geochim. Cosmochim. Acta 46, 1555–1573.

Nakamura, N., Yamakawa, A., Yamashita, K., Kobayashi, T., Imae, N., Misawa, K., Kojima, H., 2002. REE abundances and Rb–Sr age of a new Antarctic nakhlite Yamato 000593 (abstract). Antarctic Meteorites (NIPR, Japan) XXVII, 112–114.

Neal, C.R., Davidson, J.P., 1989. An unmetasomatized source for the Malatian alnöite (Solomon Islands): petrogenesis involving zone refining, megacryst formation, and assimilation of oceanic lithosphere. Geochim. Cosmochim. Acta 53, 1975–1990.

Nesse, W.D., 2000. Introduction to Mineralogy. Oxford University Press, New York 442pp.

Nininger, H.H., 1935. The Lafayette Meteorite. Popular Astronomy XLIII, 404–408.

Nishiizumi, K., Hillegonds, D.J., McHargue, L.R., Jull, A.J.T., 2004. Exposure and terrestrial histories of new lunar and Martian meteorites (abstract). Lunar Planet. Sci. XXXV Lunar and Planetary Institute CD-ROM, #1130.

Noguchi, T., Imae, N., Misawa, K., Nakamura, T., 2003. Mineralogy of "iddingsite" and symplectite in Y000593 and 000749: implication for their post-crystallization and aqueous alteration. NIPR Symposium 2003.
Nyquist, L.E., Borg, L.E., Shih, C.-Y., 1998. The shergottite age paradox and the relative probabilities for Martian meteorites of differing ages. J. Geophys. Res. 103, 31,445–31,455.
Nyquist, L.E., Bogard, D.D., Shih, C.-Y., Greshake, A., Stöffler, D., Eugster, O., 2001. Ages and geologic histories of martian meteorites. In: Kallenbach, R., Geiss, J., Hartmann, W.K. (Eds.), Chronology and Evolution of Mars. Kluwer Academic Publishers, Dordrecht, pp. 105–164.
Oe, K., McKay, G., Le, L., Miyamoto, M., Mikouchi, T., 2002. REE and Sr partition coefficients for Nakhla pyroxenes: their relationships to other element abundances. Lunar Planet. Sci. XXXIII Lunar and Planetary Institute CD-ROM, #2065.
O'Hara, M.J., Mathews, R.E., 1981. Geochemical evolution in an advancing, periodically replenished, periodically tapped, continuously fractionated magma chamber. Bull. Geol. Soc. (London) 138, 237–277.
Okazaki, R., Nagai, K., Imae, N., Kojima, H., 2003. Noble gas signatures of Antarctic nakhlites, Yamato (Y) 000593, Y000749, and Y000802. Antarctic Meteorite Research (NIPR) 16, 58–79.
Ott, U., 1988. Noble gases in SNC meteorites Shergotty, Nakhla, and Chassigny. Geochim. Cosmochim. Acta 52, 1937–1948.
Oura, Y., Shiai, N., Ebihara, M., 2003. Chemical composition of Yamato (Y) 000593 and Y000749: neutron induced prompt gamma-ray analysis study. Antarctic Meteorite Research (NIPR) 16, 80–93.
Owen, T., 1992. In: Kieffer, H.H., Jakosky, B.M., Snyder, C.W., Matthews, M.W. (Eds.), The Composition and Early History of the Atmosphere of Mars. Mars University of Arizona Press, Tucson, AZ, pp. 818–834.
Papanastassiou, D.A., Wasserburg, G.J., 1974. Evidence for late formation and young metamorphism in the achondrite Nakhla. Geophys. Res. Lett. 1, 23–26.
Philpotts, A.R., 1989. Petrography of Igneous and Metamorphic Rocks. Prentice-Hall, New Jersey 178pp.
Philpotts, A.R., 1990. Principles of Igneous and Metamorphic Petrology. Prentice-Hall, New Jersey 498pp.
Poitrasson, F., Halliday, A.N., Lee, D.-C., Levasseur, S., Teutsch, N., 2004. Iron isotope differences between Earth, Moon, Mars and Vesta as possible records of contrasted accretion mechanisms. Earth Planet. Sci. Lett. 223, 253–266.
Prior, G.T., 1912. The meteoritic stones of El Nakhla El Baharia (Egypt). Min. Mag. XVI, 274–281.
Reid, A.M., Bunch, T.E., 1975. The nakhlites—II: where, when, and how. Meteoritics 10, 317–324.
Roeder, E., 1979. Origin and significance of magmatic inclusions. Bull. Miner. 102, 487–510.
Roeder, E., Weiblen, P.W., 1977. Anomalous low-K silicate melt inclusions in ilmenite from Apollo 17 basalts. Proc. Lunar. Planet. Sci. Conf. 6, 147–164.
Romanek, C.S., Perry, E.C., Treiman, A.H., Socki, R.A., Jones, J.H., Gibson Jr., E.K., 1998. Oxygen isotopic record of mineral alteration in the SNC meteorite Lafayette. Meteorit. Planet. Sci. 33, 775–784.
Russell, S.S., Zipfel, J., Folco, L., Jones, R., Grady, M.M., McCoy, T., Grossman, J.N., 2003. The Meteoritical Bulletin, No. 87. Meteorit. Planet. Sci. 38, A189–A248.
Rutherford, M.J., Calvin, C., Nicholis, M., McCanta, M., 2005. Petrology and melt compositions in nakhlite MIL-03346: significance of data from natural sample and from experimentally fused groundmass and M.I's. Lunar Planet. Sci. XXXVI Lunar and Planetary Institute CD-ROM, #2233.
Sautter, V., Barrat, J.A., Jambon, A., Lorand, J.P., Gillet, Ph., Javoy, M., Joron, J.L., Lesourd, M., 2002. A new Martian meteorite from Morocco: the nakhlite North West Africa 817. Earth Planet. Sci. Lett. 195, 223–238.
Saxton, J.M., Lyon, I.C., Turner, G., 1999. Oxygen-isotopic composition of Nakhla anhydrite (abstract). Meteorit. Planet. Sci. 34, A101–A102.
Saxton, J.M., Lyon, I.C., Chatzitheodoridis, E., Turner, G., 2000a. Oxygen isotopic composition of carbonate in the Nahkla meteorite: implications for the hydrosphere and atmosphere of Mars. Geochim. Cosmochim. Acta 64, 1299–1309.
Saxton, J.M., Lyon, I.C., Turner, G., 2000b. Ion probe studies of deuterium/hydrogen in the nakhlite meteorites (abstract). Meteorit. Planet. Sci. 35, A142–A143.
Schmitt, R.A., Smith, R.H., 1963. Implications of similarity in rare earth fractionation of nakhlitic meteorites and terrestrial basalts. Nature 199, 550–551.
Schwartz, J.M., McCallum, I.S., Camara, F., Domeneghetti, C., Zema, M., 2003. Pasamonte eucrite: subsolidus thermal history (abstract). Lunar Planet. Sci. XXXIII Lunar and Planetary Institute CD-ROM, #1846.

Scott, D.H., Tanaka, K., Greely, R., Guest, J.E., 1986. Geologic maps of the western equatorial, eastern equatorial, and polar regions of Mars. USG.S Maps I-1802A, B, C. US Geological Survey.
Sephton, M.A., Wright, I.P., Gilmour, I., de Leeuw, J.W., Grady, M.M., Pillinger, C.T., 2002. High molecular weight organic matter in martian meteorites. Planet. Space Sci. 50, 711–716.
Shearer, C.K., Adcock, C., 1998. A comparison between sulfide assemblages in Martian meteorites ALH84001 and Governador Valadares (abstract). In: Workshop on the Issue Martian Meteorites: Where Do We Stand, And Where Are We Going? Lunar and Planetary Institute Contribution #956, pp. 45–47.
Shih, C.-Y., Nyquist, L.E., Bogard, D.D., McKay, G.A., Wooden, J.L., Bansal, B.M., Wiesmann, H., 1982. Chronology and petrogenesis of young achondrites, Shergotty, Zagami, and ALHA77005: late magmatism on a geologically active planet. Geochim. Cosmochim. Acta 46, 2323–2344.
Shih, C.-Y., Nyquist, L.E., Reese, Y., Wiesmann, H., 1998. The chronology of the nakhlite Lafayette: Rb–Sr and Sm–Nd isotopic ages (abstract). Lunar Planet. Sci. XXIX Lunar and Planetary Institute CD-ROM, #1145.
Shih, C.-Y., Nyquist, L.E., Wisemann, H., 1999. Samarium–neodymium and rubidium–strontium systematics of the nakhlite Governador Valadares. Meteorit. Planet. Sci. 34, 647–656.
Shih, C.-Y., Wiesmann, H., Nyquist, L.E., Misawa, K., 2002. Crystallization age of Antarctic nakhlite Y000593: further evidence of nakhlite launch pairing. NIPR Symposium on Antarctic Meteorites XXVII, 151–153.
Shukolyukov, A., Lugmair, G.W., 2002. Chronology of asteroid accretion and differentiation. In: Bottke, Jr., W.F., Cellini, A., Paolicchi, P., Binzel, R.P. (Eds.), Asteriods III. Univeristy of Arizona Press, Tucson, AZ, USA, pp. 687–695.
Smith, K.L., Milnes, A.R., Eggleton, R.A., 1979. Weathering of basalt: formation of iddingsite. Clays and Clay Minerals 35, 418–428.
Smith, K.L., Milnes, A.R., Eggleton, R.A., 1987. Weathering of basalt: formation of iddingsite. Clays Clay Miner. 35, 418–428.
Spray, J.G., 1998. Localized shock- and friction-induced melting in response to hypervelocity impact. In: Grady, M.M., Hutchinson, R., McCall, G.J.H., Rotherby, D.A. (Eds.), Meteorites: FLUX with Time and Impact Effects, vol. 140. Geological Society of London, Special Publication, pp. 171–180.
Spry, A., 1969. Metamorphic Textures. Pergamon Press, New York 350pp.
Steele, A., Toporski, J.K.W., McKay, D.S., 2001. The terrestrial contamination of meteorites: an update (abstract). Meteorit. Planet. Sci. 36 (Suppl.), A197 (#5420).
Stockstill, K.R., Bodnarn, R.J., McSween, Jr., H.Y., Benedix, G.K., 2001. Melt inclusions in Nakhla and ALHA77005: Indicators of parental magmas on Mars. Meteorit. Planet. Sci. 36, A198–199(abstr. #5321).
Stockstill, K.R., Bodnar, R.J., McSween Jr., H.Y., Lentz, R.C.F., 2002. Melt inclusions in SNC meteorites as indicators of parental melts on Mars. Lunar Planet. Sci. XXXIII Lunar and Planetary Institute CD-ROM, #1644.
Stöffler, D., 2000. Maskelynite confirmed as diapelctic glass: indication for peak shock pressures below 45 Gpa in all martian meteorites (abstract). Lunar Planet. Sci. XXXI Lunar and Planetary Institute CD-ROM #1170.
Stöffler, D., Keil, K., Scott, E.R.D., 1991. Shock metamorphism of ordinary chondrites. Geochim. Cosmochim. Acta 55, 3845–3867.
Stopar, J.D., Lawrence, S.J., Lentz, R.C.F., Taylor, G.J., 2005. Preliminary analysis of nakhlite MIL 03346, with a focus on secondary alteration. Lunar Planet. Sci. XXXVI Lunar and Planetary Institute CD-ROM, #1137.
Sun, S.-S., McDonough, W.F., 1989. Chemical and isotopic systematics of ocean basalts: implications for mantle composition and processes. In: Saunders, A.D., Norry, M.J. (Eds.), Magmatism in the Ocean Basins, vol. 42. Geological Society of London, Special Publication, pp. 313–345.
Swindle, T.D., Olson, E.K., 2004. ^{40}Ar–^{39}Ar studies of whole rock nakhlites: evidence for the timing of formation and aqueous alteration on Mars. Meteorit. Planet. Sci. 39 (5), 755–766.
Swindle, T.D., Treiman, A.H., Lindstrom, D.J., Burkland, M.K., Cohen, B.A., Grier, J.A., Li, B., Olson, E.K., 2000. Noble gases in iddingsite from the Lafayette meteorite: evidence for liquid water on Mars in the last few hundred million years. Meteorit. Planet. Sci. 35, 107–116.
Szymanski, A., El Goresy, A., Brenker, F.E., Palme, H., 2003. Application of the Fe–Ti thermobarometer/oxybarometer to Nakhla and Y000593. NIPR Symposium 2003.
Terada, K., Monde, T., Sano, Y., 2002. Ion microprobe U–Pb dating and REE analyses of apatites in nakhlites (abstract). Meteorit. Planet. Sci. 37, A140 (#5078).

Terrebilini, D., Busemann, H., Eugster, O., 2000. Krypton-81 krypton cosmic ray exposure ages of martian meteorites including the new shergottite Los Angeles (abstract). Meteorit. Planet. Sci. 35, A155–A156.
Toporski, J., Steele, A., 2004. Evidence of biological activities in a depth profile through Martian meteorite Nakhla (abstract). Meteorit. Planet. Sci. 39 (Suppl.), A106 (#5197).
Toporski, J.K.W., Steele, A., Stapleton, D., Goddard, D.T., 1999. Contamination of Nakhla by terrestrial microorganisms (abstract). Lunar Planet. Sci. XXX Lunar and Planetary Institute CD-ROM, #1526.
Toporski, J.K.W., Steele, A., McKay, D.S., 2001. Electron microscopy studies and microbial culturing experiments on a depth profile thorugh martian meteorite Nakhla (abstract). Meteorit. Planet. Sci. 36, A207–A208 (#5442).
Treiman, A.H., 1985. Amphibole and hercynite spinel in Shergotty and Zagami: magmatic water, depth of crystallization, and metasomatism. Meteoritics 20, 229–243.
Treiman, A.H., 1986. The parental magma of the Nakhla achondrite: ultrabasic volcanism on the Shergottite Parent Body. Geochim. Cosmochim. Acta 50, 1061–1070.
Treiman, A.H., 1990. Complex petrogenesis of the Nakhla (SNC) meteorite: evidence from petrography and mineral chemistry. Proceedings of the 20th Lunar Planetary Science Conference, 273–280.
Treiman, A.H., 1993. The parental magma of the Nakhla (SNC) achondrite, inferred from magmatic inclusions. Geochim. Cosmochim. Acta 57, 4753–4767.
Treiman, A.H., 1995. S≠NC: multiple source areas for martian meteorites. J. Geophys. Res. 100, 5329–5340.
Treiman, A.H., 2003a. Chemical compositions of martian basalts (shergottites): some inferences on basalt formation, mantle metasomatism, and differentiation in Mars. Meteorit. Planet. Sci. 38, 1849–1864.
Treiman, A.H., 2003b. The Nakhla martian meteorite is a cumulate igneous rock: comment on Varela et al. (2001). Mineral. Petrol. 77, 271–277.
Treiman, A.H., Goodrich, C.A., 2001. A parent magma for the Nakhla martian meteorite: reconciliation of estimates from 1-bar experiments, magmatic inclusions in olivine, and magmatic inclusions in augite (abstract). Lunar Planet. Sci. XXXII Lunar and Planetary Institute CD-ROM, #1107.
Treiman, A.H., Goodrich, C.A., 2002. Pre-terrestrial aqueous alteration of the Y-000593 and Y-000749 nakhlite meteorites (abstract). NIPR Symposium Antarctic Meteorites, XXVII 166-167.
Treiman, A.H., Lindstrom, D.J., 1997. Trace element geochemistry of martian iddingsite in the Lafayette meteorite. J. Geophys. Res. 102, 1953–1963.
Treiman, A.H., Sutton, S.R., 1992. Petrogenesis of the Zagami meteorite: inferences from synchrotron X-ray (SXRF) microprobe and electron microprobe analyses of pyroxenes. Geochim. Cosmochim. Acta 56, 4059–4074.
Treiman, A.H., Drake, M.J., Janssens, M.-J., Wolf, R., Ebihara, M., 1986. Core formation in the Earth and Shergottite Parent Body (SPB): chemical evidence from basalts. Geochim. Cosmochim. Acta 50, 1071–1091.
Treiman, A.H., Barrett, R.A., Gooding, J.L., 1993. Preterrestrial aqueous alteration of the Lafayette (SNC) meteorite. Meteoritics 28, 86–97.
Treiman, A.H., Gleason, J.D., Bogard, D.D., 2000. The SNC meteorites are from Mars. Planet. Space Sci. 48, 1213–1230.
Treiman, A.H., Lanzirotti, A., Xirouchakis, D., 2004. Synchrotron X-ray diffraction analysis of meteorites in thin section: preliminary results (abstract). Lunar Planet. Sci. XXXV Lunar and Planetary Institute CD-ROM #1179.
Van Der Bogert, C.H., Schultz, P.H., Spray, J.G., 2004. Impact-induced frictional melting in ordinary chondrites: a mechanism for deformation, darkening and vein formation. Meteorit. Planet. Sci. 38 (10), 1521–1531.
Varela, M.E., Kurat, G., Clocchiatti, R., 2001. Glass-bearing inclusions in Nakhla (SNC meteorite) augite: heterogeneously trapped phases. Mineral. Petrol. 71, 155–172.
Varela, M.E., Kurat, G., Clocchiatti, R., 2003. Reply to comment: ''The Nakhla Martian meteorite is a cumulate igneous rock'' by A. Treiman. Mineral. Petrol. 77, 279–285.
Vicenzi, E.P., Fahey, A.J., 2001. Chemical imaging of nakhlite secondary mineralization at the sub-micrometer length scale: a TOF-SIMS study (abstract). Lunar Planet. Sci. XXXII Lunar and Planetary Institute CD-ROM, #2105.
Vicenzi, E.P., Heaney, P.J., 2000. Multiple martian fluids: the alteration sequence in the Lafayette SNC meteorite (abstract). Meteorit. Planet. Sci. 35, A164–A165.
Wager, L.R., Brown, G.M., 1967. Layered Igneous Rocks. W.H. Freeman & Co., San Francisco.
Wadhwa, M., Crozaz, G., 1995. Trace and minor elements in minerals of nakhlites and Chassigny: clues to their petrogenesis. Geochim. Cosmochim. Acta 59, 3629–3645.

Wadhwa, M., Crozaz, G., 2003. Trace element geochemistry of new nakhlites from the Antarctic and the Saharan desert: further constraints on nakhlite petrogenesis on Mars (abstract). Lunar Planet. Sci. XXXIV Lunar and Planetary Institute CD-ROM, #2075.

Walker, R.J., Brandon, A.D., Nazarov, M.A., Mittlefehldt, D., Jagoutz, E., Taylor, L.A., 2002. ^{187}Re-^{187}Os isotopic studies of SNC meteorites: an update (Abstract). Lunar Planet. Sci., XXXIII. Lunar and Planetary Institute, Abstr. 1042., CD-ROM.

Wänke, H., Dreibus, G., 1988. Chemical composition and accretion history of terrestrial planets. Philos. Trans. Roy. Soc. (London) A 235, 545–557.

Warren, P.H., 1998. Petrologic evidence for low-temperature, possibly flood evaporitic origin of carbonates in the ALH84001 meteorite. J. Geophys. Res. 103, 16,759–16,773.

Warren, P.H., 2002. Northwest Africa 1000: a new eucrite with maskelynite, unequilibrated pyroxene crisscrossed by fayalite-rich veins, and Stannern-like geochemistry (abstract). Lunar Planet. Sci. XXXIII Lunar and Planetary Institute CD-ROM, #1147.

Watson, L.L., Hutcheon, I.D., Epstein, S., Stolper, E.M., 1994. Water on Mars: clues from deuterium/hydrogen and water contents of hydrous phases in SNC meteorites. Science 265, 86–88.

Weiler, R., Baur, H., 1994. Krypton and xenon from the solar wind and solar energetic particles in two lunar ilmenites of different antiquity. Meteoritics 29, 570–580.

Weiler, R., Baur, H., 1995. Fractionation of Xe, Kr, and Ar in the solar corpuscular radiation deduced from closed system edtching of lunar soils. Astrophys. J. 453, 987–997.

Weincke, H.H., 1978. Chemical and mineralogical examination of the Nakhla achondrite. Meteoritics 13, 660–664.

Weins, R.C., Becker, R.H., Pepin, R.O., 1986. The case for Martian origin of the shergottites: trapped and indigenous gas components in EETA 79001 glass. Earth Planet. Sci. Lett. 77, 1439–1458.

Wimmer-Schweingruber, R.F., 2002. The composition of the solar wind. Adv. Space. Res. 30 (1), 23–32.

Wright, I.P., Grady, M.M., Pillinger, C.T., 1989. Organic material in a Martian meteorite. Nature 340, 220–222.

Wright, I.P., Grady, M.M., Pillinger, C.T., 1992. Chassigny and the nahklites: carbon-bearing components and their relationship to Martian environmental conditions. Geochim. Cosmochim. Acta 56, 817–826.

Wright, T.L., Okamura, R.T., 1977. Cooling and Crystallization of Tholeiitic Basalt, 1965 Makaopuhi Lava Lake, Hawaii. US Geological Surveyy Prof. Paper 1004. US Government Printing Office, Washington 78pp.

Wright, T.L., Peck, D.L., 1978. Crystallization and Differentiation of Alae Magma, Alae Lava Lake, Hawaii. US Geological Survey Prof. Paper 935-C. US Government Printing Office, Washington 20pp.